

Antigenicity of envelope protein complexes of *Mycobacterium avium* subsp. *paratuberculosis* and insights into T cell responses of infected animals

by

Fernando Lopes Leivas Leite

A thesis submitted to the graduate faculty

in partial fulfillment of the requirements for the degree of

MASTER OF SCIENCE

Co- Majors: Veterinary Microbiology and Immunobiology

Program of Study Committee:

Judith R. Stabel, Co-Major Professor

Michael Wannemuehler, Co-Major Professor

John Bannantine

Timothy Reinhardt

Iowa State University

Ames, Iowa

2014

Copyright © Fernando Lopes Leivas Leite, 2014. All rights reserved.

TABLE OF CONTENTS

	Page
ACKNOWLEDGEMENTS	iii
ABSTRACT	iv
CHAPTER 1. GENERAL INTRODUCTION	1
Introduction	1
Thesis organization	2
Literature review	2
Background	2
Infection and immune response to MAP	4
Evidence and possible correlation to T cell - anergy/hypofunction and T regulatory cells	7
T cell activation and roles of ZAP-70 and CTLA-4	9
Proteomics and antigens of MAP	14
Antigen preparations of MAP used in diagnostic applications	21
Studies to identify proteins relevant for diagnostic - and vaccine development	22
References	26
CHAPTER 2. ENVELOPE PROTEIN COMPLEXES OF MAP AND THEIR ANTIGENICITY	35
Abstract	35
Introduction	36
Materials and Methods	38
Results	47
Discussion	50
References	55
Figures and Tables	59
CHAPTER 3. ZAP-70 CTLA-4 AND PROXIMAL T CELL RECEPTOR SIGNALING IN ANIMALS INFECTED WITH MYCOBACTERIUM AVIUM SUBSP PARATUBERCULOSIS	70
Abstract	70
Introduction	71
Materials and Methods	73
Results	76
Discussion	78
References	85

Tables and figures	89
CHAPTER 4. GENERAL CONCLUSION	96
General Discussion	96
Recommendations for future research	99
APPENDIX	101

ACKNOWLEDGEMENTS

I would like to thank my major professors, Dr. Judy Stabel and Dr. Michael Wannemuehler, as well as my committee members, Dr. John Bannantine and Dr. Tim Reinhardt, for their guidance and mentorship throughout the course of this research.

In addition, I would also like to thank everyone from the Johne's research group; especially Margaret Walker and Janis Hansen who taught me very much as well as helped me in several experiments. From Dr. Tim Reinhardt's research group I would also like to thank Adrienne Staple and Tera Nyholm for always being willing to help and to have assisted a lot in the study of envelope proteins. All of the animal care takers and Paul Amundson made collecting animal samples very easy and to them I am also very thankful. I would also like to thank Bruce Pesch who was very patient and willing to explain the basics of flow cytometry.

Finally, thanks to my family for their support that was important in completing this degree.

ABSTRACT

Paratuberculosis is a disease caused by *Mycobacterium avium* subsp. *paratuberculosis* (MAP). This is a chronic enteric disease of ruminant animals with clinical signs taking from 2 to 5 years for manifestation. Current diagnostic tests are effective in identifying animals in later stages of infection; however, sensitivity among animals in the early stages of infection is low. In addition, currently available vaccines in the US fail to prevent infection of animals. Transitions in host immunity to MAP leading to clinical disease are poorly understood and their comprehension could lead to more targeted approaches for vaccine and diagnostic development. The objective of the first study was to identify protein complexes in the envelope of MAP to gain insight into pathogenic mechanisms as well as to identify antigenic proteins. Seven protein complexes were identified in the envelope of MAP and these complexes were fragmented into individual proteins with potential as diagnostic and vaccine targets. The second objective in this thesis was to study two crucial molecules in T cell signaling investigated in cows with subclinical and clinical disease. ZAP-70 (zeta-chain associated protein of 70 kDa) is involved in proximal T cell receptor signaling and its activation is necessary for T cell effector function. The second molecule studied was CTLA-4 (cytotoxic T-lymphocyte antigen-4), regarded as one of the major negative regulators of T cell function. All MAP infected animals demonstrated a significant reduction in expression of ZAP-70 among CD4⁺ T cells whereas only animals of subclinical status had a significant upregulation of CTLA-4 in the CD4⁺ T cell population. Both studies

contribute novel and important findings to the field of paratuberculosis. Protein interactions within the envelope of MAP were discovered along with the identification of several protein candidates for vaccine and diagnostic development. In addition, immune alterations that occur with infection and progression of disease were also demonstrated.

CHAPTER 1. GENERAL INTRODUCTION

Introduction

Paratuberculosis, also known as Johne's disease, is a major animal health burden to livestock worldwide. This is a chronic disease caused by *Mycobacterium avium* subsp. *paratuberculosis* (MAP) of which all ruminants are susceptible. The economic impact of the disease is highest among dairy cattle where it leads to decreased milk production, higher incidence of mastitis and lower fertility rates, contributing to premature culling of animals. The envelope of MAP is an important component of the bacterium, which contains the first antigens the host encounters upon infection. Therefore, this research project was focused upon understanding protein interactions among this compartment and in identifying proteins that have the potential to discriminate between non-infected and infected animals for the development of better diagnostic tools. The second research project addressed the immune response to MAP and possible alterations that occur within T cells during progression of the disease. T cells are a crucial part of the adaptive immune system and are necessary to effectively clear many infections, however little research has been done regarding T cell function or T cell signaling related to MAP infection. By analyzing ZAP-70 and CTLA-4, two crucial signaling molecules of T cells, differences in T cell phenotypes were investigated in animals of different disease states. In addition, by using phospho flow cytometry analysis, proximal T cell receptor signaling and ZAP-70 phosphorylation were also evaluated.

Thesis Organization

This thesis is organized into four chapters, two of which are papers intended for publication in peer-reviewed journals. The first chapter contains a general introduction to Johnes disease and a literature review describing what is known about the immune response to MAP. This includes a survey of some important antigens and proteomic studies performed with the bacterium. The second chapter contains the paper entitled “Envelope protein complexes of *Mycobacterium avium* subsp. *paratuberculosis* and their antigenicity” which has been prepared for submission to the Journal of Bacteriology. Chapter three contains the paper “ZAP-70, CTLA-4 and proximal T cell receptor signaling” and has been prepared for submission to the journal Infection and Immunity. Finally in chapter 4, the thesis finishes with a general conclusion and recommendations for future research.

Literature Review

Background

Paratuberculosis, also called Johnes’s disease, is a disease of ruminant animals caused by the bacterium *Mycobacterium avium* subsp. *paratuberculosis* (MAP). Paratuberculosis was described for the first time in 1895 by Dr. Heinrich Albert Johnes and Dr. Herman Markus, who examined the intestines of a cow with a history of decreased milk production and weight loss (Manning & Collins, 2010). Initially, a diagnosis of intestinal tuberculosis was made due to the similarity of lesions, however, a sample of infected tissue failed to cause disease in guinea pigs. Upon further histological

examination, acid-fast bacteria were observed throughout the intestine and a conclusion was made that the disease was caused by an etiologic agent other than *Mycobacterium tuberculosis* (Johne & Frothingham, 1895). The etiologic agent was later characterized as *Mycobacterium avium* subsp. *paratuberculosis* (Thorel et al., 1990).

Today, paratuberculosis has worldwide distribution, with varying prevalence among countries. In the US, it is estimated that a staggering 91% of dairy herds are infected with MAP (Lombard et al., 2013). The economic impact of Johne's disease is due mainly to reduced milk production, increased incidence of mastitis and early culling of animals (Lombard, 2011). Within an infected herd most animals would be in the subclinical stage of infection with decreased production parameters and no clinical signs of infection (Magombedze et al., 2013). As disease progresses, taking from 2-5 years, animals demonstrate clinical signs of disease which include emaciation and chronic or intermittent diarrhea, eventually leading to death (Stabel, 1998).

Although there are assays available to diagnose MAP infection as well as commercial vaccines, neither is completely effective (Patton, 2011; Facciolo et al., 2013). Current diagnostic tests, such as ELISAs, are ineffective in detection of animals in subclinical stage of infection (Facciolo et al., 2013). The vaccine currently licensed for use in the US lowers shedding of the organism and reduces clinical signs, however, prevention of infection is not achieved (Patton, 2011).

With this in mind, research is still needed to identify potential candidates for use in improving diagnostic assays and vaccines (Bannantine et al., 2010). Another major area of research that requires further work is the study of the host immune response to

MAP infection, in particular, those immunologic changes that occur as an animal progresses from subclinical to clinical disease states (Stabel, 2006). Research focused in these fields is required to achieve a better understanding of the disease and develop more targeted approaches for controlling and preventing paratuberculosis.

Infection and immune response to MAP

Infection by MAP occurs mainly by the fecal-oral route. This may occur by direct ingestion of MAP contaminated feces as well as by ingestion of milk and colostrum from infected dams, in addition to contaminated water and feed (Fecteau & Whitlock, 2010). Infection of the fetus has also been described in infected dams (Whittington & Windor, 2009). After entering the host, at the small intestine, MAP enters the submucosa aided by microfold cells (M cells) within the Peyer's patches (Momotani et al., 1988). MAP also has the ability to enter the host intestinal mucosa through enterocytes (Pott et al., 2009; Bermudez et al., 2010). It has been proposed that targeting and invasion of M cells is mediated by the formation of a fibronectin bridge between a fibronectin attachment protein of MAP and integrins on M cells (Secott et al., 2004). Other proteins that have also been implicated in invasion of the intestine by MAP include major membrane protein (Bannantine et al., 2003) as well as ModD, a fibronectin attachment protein, and proteins of the antigen 85 complex which are also fibronectin attachment proteins (Bannantine & Bermudez, 2013). Upon uptake by the M cells, MAP is transported to the submucosal side of the intestinal epithelium where it is taken up by macrophages.

MAP is an obligate intracellular pathogen and once in macrophages it can prevent maturation and acidification of the phagosome thus avoiding antimicrobial components of the lysosome (Hostetter et al., 2003). The expression of MHC molecules has also been shown to be downregulated in infected macrophages along with higher induced expression of IL-10 and TGF- β (Weiss & Souza, 2008). Khalifeh & Stabel (2004) demonstrated that macrophages exposed in culture to exogenous IL-10 and TGF- β significantly reduced their ability to kill MAP, suggesting these cytokines play an important role in infection, by limiting the bactericidal capabilities of macrophages. One of the virulence factors driving the increased survival of MAP has recently been described by Souza et al. (2013) who demonstrated that mannosylated lipoarabinomannan (Man-LAM), a glycolipid present in the envelope of MAP and other pathogenic mycobacteria, has the capacity to increase IL-10 production by macrophages as well as inhibit phagosome acidification, phagolysosome fusion, and reduce the killing of bacteria.

As Johne's disease progresses from subclinical to clinical stages the host makes an effort to contain infection by the formation of granulomas, similar to what occurs in other mycobacterial diseases (Gonzalez et al., 2005). In the early stages of disease and before the onset of clinical signs, granuloma formation leads to minimal lesions, localized in the intestine or lymph nodes. As the disease progresses, shedding of the bacteria occurs and intestinal lesions become more severe (Sweeney, 2011; Gonzalez et al., 2005). Due to cellular infiltration of macrophages and granulomatous inflammation in the intestine, malabsorption occurs leading to the clinical signs of diarrhea and

progressive weight loss (Sweeney, 2011). Animals can remain in a subclinical stage of infection for up to 2-5 years before the onset of clinical signs (Stabel, 1998). For unknown reasons, some animals never progress on to clinical disease.

In the early stages, the disease is controlled by a cell-mediated Th1 response where T cells activated by infected macrophages express Th1-associated cytokines, IFN- γ , IL-2 and TNF- α (Stabel, 2006). IFN- γ is a key molecule that helps in the activation of macrophages with the production of reactive oxygen and nitrogen species, activation of T cells, and maturation of DCs (He et al., 2007). Another important role for IFN- γ is the induction of IL-12 which further directs CD4⁺ cells to the Th1 subset. Studies have demonstrated that CD4⁺ cells are the primary source of IFN- γ in MAP infection (Stabel, 2010).

As the disease progresses and clinical manifestations begin to appear, there is a shift in the observed immune response. The Th1 response wanes as a Th2 type response rises that is characterized by the cytokines IL-4, IL-5 and IL-10 (Stabel, 2000; Stabel, 2006). The cause for this transition is unknown, and the Th2 response is not protective (Stabel 2000; Stabel, 2010). Khalifeh & Stabel (2004b) studied the dynamics of IL-10, TGF- β and IFN- γ gene expression in the ileum, ileocecal junction, ileocecal lymph node, and mesenteric lymph nodes of healthy cows as well as those in subclinical and clinical stages of infection. IL-10 levels were significantly higher in all tissues of cows with clinical disease and TGF- β mRNA was also higher among these animals. Healthy animals and those with subclinical disease expressed similar levels of these cytokines. In contrast, IFN- γ gene expression was significantly higher only among animals with

subclinical infection with no differences observed between healthy animals and those with clinical disease. This demonstrates clear immune differences among these three states and suggests that altered cytokine expression is related to advanced clinical disease. The importance of these cytokines as well as the consequences of changes in their expression have been demonstrated by studies finding that neutralization of IL-10 can increase the killing of MAP by bovine macrophages (Weiss et al., 2005) as well as lead to increased IFN- γ production by as much as 23-fold (Buza et al., 2004).

Evidence and possible correlation to T cell anergy/hypofunction and T regulatory cells.

One possible explanation for the loss of effectiveness toward controlling infection mediated by a Th1 response is the development of anergy and/or T regulatory (Treg) cells. One mechanism potentially leading to anergy or induced Treg (iTreg) development is a reduction in co-stimulation provided by macrophages or an environment rich in Treg-inducing cytokines such as TGF- β (Schwartz, 2003).

As mentioned earlier, IL-10 production is upregulated with the progression of disease (Khalifeh & Stabel, 2004b). There are few studies describing the involvement of Treg cells or anergy in relation to paratuberculosis. However, some recent evidence suggests a role for Tregs in progression of the disease (de Azevedo et al., 2008; Coussens et al., 2012). In one study, the removal of CD25⁺ CD4⁺ from a peripheral mononuclear cell preparation prior to stimulation with MAP antigen resulted in a decrease of IL-10 expression, suggesting an important role for these cells. Considering that Treg cells

would be induced in infected animals, the same study measured the percentage of Tregs in the peripheral blood mononuclear cells (PBMCs) of infected and control non-infected cattle. Results demonstrated CD4⁺ CD25⁺ cells were present in significantly greater proportion in infected animals (de Almeida et al., 2008).

Providing evidence towards anergy, Weiss et al. (2006) studied the phenotype and response of mononuclear leukocytes from the ileum of cows naturally infected with MAP. Lymphocytes isolated from the ileum of infected cows did not proliferate when incubated with MAP antigen, demonstrating a hyporesponsive state of these cells (Weiss et al., 2006). In a study to investigate the immune response to MAP in sheep, Begg et al. (2011) similarly observed that animals in more advanced stages of disease had non responsive T cells. Multibacillary sheep demonstrated decreased IFN- γ production among PBMCs and reduced ability to proliferate in response to MAP antigen and pokeweed mitogen. IL-12 was added to the cell culture in an attempt to aid their activation, however, addition of the cytokine had no significant effect on cellular responses, which may suggest a greater inhibition of these cells (Begg et al. 2011). More recently, Khare et al. (2012) studied the gene expression of ligated ileal loops in neonatal calves infected with MAP. This was in an effort to comprehend the early immune responses that lead to immune tolerance in subclinical animals. Some genes related to T cell signaling were not altered but others such as the transcription factors NFATC4 (nuclear factor of activated T-cells C4) and NFATC1 (nuclear factor of activated T-cells C1) were. These transcription factors are related to expression of IL-2 and other gene products important for activation, proliferation and differentiation of T-cells as well as

lymphoid and non-lymphoid cells. This demonstrates that alterations of the normal signaling events of the T cell during infection may occur, possibly contributing to the lesser function of these cells (Khare et al., 2012). Regarding B cells and possible anergy induction, Waters et al. (1999) studied the proliferative response of B cells to concanavalin A and MAP antigen in clinical and subclinical animals. It was demonstrated that B cells of animals in clinical stage of disease were unresponsive and did not proliferate upon antigen stimulation, in contrast to animals with subclinical disease which had proliferative responses to MAP antigen. This demonstrated that B cells of animals in clinical stage of disease are also altered and respond less to stimulation.

T cell activation and roles of ZAP-70 and CTLA-4

As mentioned earlier, T cells are an important component of the immune response to MAP infection, thus the study of these cells and especially their activation is important in identifying potential alterations that occur with the progression of disease, leading to clinical signs and eventual death of the animal.

Activation of the T cell occurs by the recognition of a presented antigen in conjunction with a major histocompatibility class (MHC) molecule. For CD4⁺ cells this is an MHC class II molecule while for CD8⁺ cells this is a MHC class I molecule. These MHC molecules once associated with a peptide, are recognized by the T cell receptor (TCR). Along with the TCR is the associated CD3 complex comprised of CD3 γ , CD3 δ , CD3 ϵ and CD3 ζ chains (Murphy, 2012). When presenting antigens to T cells, antigen presenting cells (APC) also engage a co-receptor in the T cell, CD28, with the ligands

B7.1 (CD80) and B7.2 (CD86) (Walker & Sansom, 2011). This engagement is necessary to prime naïve cells as well as inhibit anergy by stabilizing mRNA expression and induction of survival signals such as IL-2 production by AP-1 transcription factor activation (Rudd et al., 2009). Signaling leading to T cell activation is initiated by tyrosine phosphorylation within the cytoplasmic regions of the CD3 chains in regions called immuno-receptor tyrosine-based activation motifs (ITAMs). Specifically, ITAMs present in the CD3 ζ chains become phosphorylated by the tyrosine kinase Lck (lymphocyte-specific protein tyrosine kinase) that is constitutively associated with the cytoplasmic domains of the CD4 or CD8 co-receptor. When the co-receptor (CD4 or CD8) binds to the TCR:peptide:MHC complex, Lck is brought near the ITAMS and causes their phosphorylation. The molecule then responsible for carrying this signal forward for T cell activation is the ζ -chain associated protein of 70 kDa (ZAP-70) (Wang et al., 2010).

Upon activation, phosphorylated ITAMs in the TCR complex recruit ZAP-70 from the cytoplasm near the plasma membrane, where it is phosphorylated by Lck. ITAM binding and phosphorylation release ZAP-70 from an autoinhibited state in which it remains in inactivated cells (Wang et al., 2010). This enables ZAP-70 to phosphorylate two adaptor proteins, LAT (linker for the activation of T cells) and SLP-76 (Src homology 2 domain-containing leukocyte phosphoprotein of 76 kDa), leading to the recruitment of effector proteins that stimulate T cell activation (Murphy, 2012). The importance of ZAP-70 is evidenced by studies demonstrating that TCR signaling events are severely inhibited in Jurkat T cells lacking ZAP-70 (Williams et al., 1998). Also, loss

of ZAP-70 function results in severe combined immunodeficiency (SCID) in both humans and mice, which is characterized by a lack of functional peripheral T cells (Elder, 2001).

ZAP-70 is comprised of several tyrosine residues itself which need to be phosphorylated for its activation. Although critical, binding to ITAMs of the CD3 ζ chain and perturbation of the auto-inhibitory conformation alone is insufficient for complete ZAP-70 activation (Jin et al., 2004). Phosphorylation of tyrosine residues, by the action of Lck, and/or by ZAP-70 auto-phosphorylation, is also important. Requirements for full catalytic activity include phosphorylation of the tyrosine residue Y493, located in the kinase domain of ZAP-70. Another important tyrosine residue is Y319, which is a positive regulator of ZAP-70 function (Wang et al., 2010). Overexpression of Y319F (a tyrosine residue mutated to phenylalanine) in ZAP-70 in Jurkat cells resulted in a dominant-negative effect, with reduced TCR-triggered activation of downstream signaling events (Di Bartolo et al., 1999).

As there are molecules that lead to signaling that activate T cells there are also those that promote a down regulation of their functions. One such molecule is cytotoxic T-lymphocyte antigen-4 (CTLA-4). CTLA-4 has been implicated in termination of T cell activation as well as anergy induction and T regulatory cell function (Schneider et al., 2008; Walunas et al., 1994). There are many hypotheses on the manner in which CTLA-4 acts to dampen T cell responses. These include both intrinsic mechanisms causing alterations in cells that express the molecule as well as extrinsic mechanisms in which cells expressing CTLA-4 lead to decreased activity of other cells (Walker &

Sansom, 2011). The expression of CTLA-4 is constitutive in T regulatory cells whereas in conventional T cells the surface expression of CTLA-4 occurs following T cell activation. The function of CTLA-4 is controlled largely by regulation of its surface expression, as it is by its ligation on the cell surface that signaling is induced (Rudd et al., 2009).

One intrinsic mechanism of CTLA-4 inhibition is competition with CD28 for ligand binding to CD80 and CD86 on APCs. CTLA-4 has both higher affinity and avidity for CD80 and CD86 thereby limiting the access of CD28 to these molecules. CTLA-4 inhibits T-cell activation by reducing IL-2 production and IL-2 receptor expression, and by arresting T cells at the G1 phase of the cell cycle (Krummel & Allison, 1996; Sansom, 2000). This occurs by several mechanisms that involve inhibition of transcription factors such as AP-1 (activator protein 1), NF κ B (nuclear factor kappa-light-chain-enhancer of activated B cells) and NFAT (nuclear factor of activated T-cells). These are transcription factors central to lymphocyte activation that lead to diverse effector mechanisms such as proliferation and cytokine secretion (Murphy, 2012). CTLA-4 can also inhibit the formation of signaling platforms such as lipid rafts and microclusters in the T cell following TCR ligation. Specifically, microclusters that contain ZAP-70 induced that are formed following cell activation may be blocked following engagement of CTLA-4 (Rudd et al., 2009). An association between ZAP-70 and CTLA-4 has also been described by Guntermann and Alexander, (2002) demonstrating that ZAP-70 phosphorylation by Lck and proximal T cell receptor signaling can be impaired through the action of Src homology protein 2 domain-

containing tyrosine phosphatase 1 (SHP-1) protein due its enhanced activity upon CTLA-4 ligation in T cells.

Interestingly, Oosterwegel et al. (1999) demonstrated that CTLA-4 has a critical role in CD4⁺ T cell differentiation. T cells from CTLA-4 knockout mice carrying a class II restricted TCR specific for ovalbumin (ova) produced IL-4 even during primary stimulation and differentiated into almost pure populations of Th2 cells in contrast to wild type mice. In secondary stimulation with ova, CTLA-4 knockout mice expressed higher levels of IL-4 while the other group of mice expressed IFN- γ . Interestingly upon *in vivo* administration of anti-CD28 antibody, a Th2 differentiation was observed among CTLA-4 knockout mice, but not in wild-type mice. This study suggested that ligation of CTLA-4 blocks Th2 differentiation and that CD28 ligation alone may promote Th2 differentiation of T cells. Also regarding CD4⁺ T cell phenotypes, Knieke et al. 2009 demonstrated that CTLA-4 has a positive effect on Th1 cell migration. It was found that crosslinking of CTLA-4 together with CD3 and CD28 stimulation on activated Th1 cells increased expression of the chemokine receptors CCR5 and CCR7, which in turn enhanced cell migration. Interestingly Th1 lymphocytes expressing CTLA-4 increased their migration more than twice as compared to their negative counterparts showing that CTLA-4 can orchestrate specific migration of selected Th1 cells to sites of inflammation and antigenic challenge.

The specific role of CTLA-4 in Treg function is still debated. Studies have shown that activation of Tregs leads to an increased expression of CTLA-4 and that the molecule is responsible for augmenting Treg function, as blockade of the molecule can

abolish the suppression capabilities of Treg cells. One extrinsic mechanism of CTLA-4 is the secretion of TGF- β , a suppressive cytokine, by Treg cells upon their ligation on the cell surface (Walker & Sansom, 2011). Another described mechanism is the induction of indoleamine 2,3 dioxygenase (IDO) activity in APCs by Treg cells expressing CTLA-4. The induction of IDO leads to a localized tryptophan catabolism and causes its depletion. This leads other T cells to be inhibited from proliferating due to the lack of tryptophan (Fallarino et al., 2003). Interestingly there is also evidence that T cells expressing CTLA-4 can decrease the amount of CD80 and CD86 molecules on APCs by trans-endocytosis leading to impaired co-stimulation as well as suppression of T cell responses (Qureshi, 2011).

Proteomics and antigens of MAP

Along with the need to better understand the immune response to MAP there is also a demand for research to study and evaluate proteins of MAP for use in diagnostic and vaccine applications. In spite of the existence of several diagnostic assays for paratuberculosis involving protein preparations of MAP, especially ELISA assays, there is still a great need to improve the sensitivity and specificity of these platforms (Facciuolo et al., 2013). The major way to do so is to use proteins that can be shown to be both specific and highly antigenic. Proteomic research in MAP is also important to better comprehend the molecular mechanisms that are involved in virulence and host pathogen interactions.

Proteomics is the study of all proteins produced by an organism or a defined fraction thereof. In the case of MAP, sequence analysis has revealed that the organism encodes over 4,300 proteins (Li et al, 2005), a very large amount to be analyzed. Another challenge in proteomic research for MAP is the genetic similarity it shares with other mycobacterial species. This similarity has been reported to be greater than 97% with *Mycobacterium avium* subsp. *avium*, making unique DNA segments and proteins to MAP rare (Bannantine et al. 2003). When analyzing the proteins of a cell or bacterium including MAP, it is important to study proteins in the different compartments of the bacterium to facilitate analysis and later functional assignment of proteins (Reisinger & Eichacker, 2007).

One important compartment of MAP is the envelope, which like that of all mycobacteria is composed of a cytoplasmic membrane, a periplasmic space and outer membrane. The layered architecture of the mycobacterial cell envelope is more related to that of Gram-negative bacteria, despite the fact that MAP and other mycobacteria are considered to be Gram-positive (Zuber et al., 2008). Fatty acids account for 30% to 40% of the cell envelope mass. Of these fatty acids, mycolic acids are responsible for forming the outer membrane of the envelope (Niederweis et al., 2010). Between the outer membrane and cytoplasmic membrane is the periplasmic space which is composed mainly of an arabinogalactan and peptidoglycan polymer (Niederweis et al., 2010). The plasma membrane of mycobacteria does not appear to be different from that of other plasma biological membranes and has been reported to be homologous to those in other bacteria (Daffé & Draper, 1998). Also in the envelope are proteins that have both

physiologic roles such as porins for transporting of nutrients as well as roles involved in virulence such as fibronectin attachment proteins to facilitate infection of the host (Niederweis et al., 2010; Bannantine & Bermudez, 2013).

Envelope proteins of MAP have been studied by He and De Buck, (2010). A total of 309 proteins were identified, along with 38 proteins that were determined to be surface exposed. Analysis of proteins was performed by separating proteins in SDS-PAGE according to their molecular weight followed by in-gel digestion with trypsin resulting in a complex peptide mixture, which was then analyzed directly by mass spectrometry. To analyze surface exposed proteins, an enzymatic shaving technique was performed with trypsin on bacterial cells. Interestingly, very low correlation was observed between proteins found to be part of the cell envelope in comparison to those determined to be surface exposed. The authors suggest that this is likely due to the loose association of these proteins with the cell wall, making them less stable and more prone to detachment. As has been described, several surface proteins can be attached to the cell wall of bacteria in a non-covalent way and have been reported to be lost during mild standard manipulations (Kocincova et al., 2004). The study also identified one PPE protein in the cell wall fraction and four PPE proteins in the cell surfaced exposed proteome (He & De Buck, 2010). Yet protein interactions and potential antigenicity of proteins were not addressed in this study.

A technique that has been used to analyze proteins present in membranes as well as their interactions is blue native PAGE (polyacrylamide gel electrophoresis). This technique was originally described by Schagger and Jagow (1991) to study protein

complexes in mitochondria. Blue native PAGE is a technique that uses non-ionic detergents to solubilize hydrophobic proteins, often associated with membranes, yet allow protein interactions to remain intact and maintain proteins in their native state (Reisinger & Eichacker, 2007). Coomassie blue G-250 is added to solubilized proteins to give them a negative charge to allow for their migration in blue native-PAGE. The technique allows for the characterization of protein complexes within membrane fractions. To visualize subunits of complexes, it is necessary to breakdown inter-protein interactions. This can be done with the use of anionic detergents such as SDS (sodium dodecyl sulfate) which denatures proteins while giving them a negative charge (Reisinger & Eichacker, 2008). After treatment of complexes with SDS samples can be run on a polyacrylamide gel to visualize the subunits of each complex. After separation of proteins, mass spectrometry can be performed to identify individual proteins (Reisinger & Eichacker, 2007).

Blue native PAGE has been performed to analyze proteins present in membranes of bacterial pathogens. In *Borrelia burgdorferi*, 10 complexes were found within the outer membrane along with the subsequent finding that an adhesion protein involved in infection was part of one complex (Yang et al., 2011). Most complexes and protein interactions found were of unknown function, and interestingly many contained the same proteins as subunits. These identified protein subunits which were found in more than one complex are likely abundant and may have important roles within the membrane (Yang et al., 2011). A major discovery was made in *Helicobacter pylori* using blue native PAGE. The CagA (cytotoxin-associated gene A) protein is a major virulence

factor involved in the induction of gastric adenocarcinoma by the bacterium, and was found to be part of a complex with DNA gyrase subunit A (GyrA) protein (Hatakeyama & Higashi, 2005; Pyndiah et al., 2007). This led to the conclusion that the interaction of these two proteins is likely responsible for the higher growth rate of pathogenic isolates. This is due to the interaction of CagA with GyrA which likely facilitates normal DNA replication and leads to a better development of the bacterial cell (Pyndiah et al., 2007). Zheng et al. (2011) investigated complexes present within the envelope of *M. bovis* bacillus Calmette-Guérin (BCG). The study provided information in regards to bacterial physiology, finding several complexes and protein interactions involved in bacterial metabolism such as the Emb (Ethambutol) protein complex that is involved in synthesis of lipoarabinomannan and other cell envelope components (Alderwick et al., 2006; Zheng et al., 2011) .

The envelope of MAP needs to be further characterized for a better comprehension of its physiology and related virulence, as well as for the identification of potential antigens for diagnostic and vaccine development. Proteins associated with the cell envelope of MAP are likely to be the first to interact with the host and, therefore, the first proteins for immune recognition (Kleinnijenhuis et al., 2011). Identifying proteins present in the envelope, especially their interactions, would aid in comprehending the pathogenesis of MAP infection. Several proteins with roles in virulence have been found to be associated with the envelope of mycobacteria, including proteins of the PPE (proline-proline-glutamic acid) family as well as those of the antigen 85 complex (Forrellad et al., 2013). Both of these families of proteins have roles in virulence, and

proteins of the antigen 85 complex have been demonstrated to be highly immunogenic (Kathaperumal et al., 2008; Deng & Xie, 2012). Therefore, characterization of proteins and protein interactions present in the envelope become critical not only to the comprehension of the physiology and pathogenesis of the organism but also to identify potential antigenic proteins for use in vaccines and diagnostic assays.

Proteomic studies have also investigated other important factors that need to be considered in MAP research. Radosevich et al. (2006) studied the potential differences that may occur between different MAP isolates and changes that occur with laboratory adaptation of MAP strains. The proteomes of two isolates of MAP, a laboratory-adapted strain K-10 and a low passage clinical isolate were investigated. Proteins were extracted from both the envelope as well as the cytosol. The last step consisted of ultracentrifugation, resulting in a supernatant corresponding to the cytosolic protein fraction and a pellet corresponding to the bacterial envelope. Interestingly, there was 87% similarity between both strains analyzed over the 874 total proteins found. This study also described specific proteins that were up or down regulated in each strain in the envelope or cytosolic compartments. One of these proteins was MAP4336 which was upregulated 4.7-fold in the membrane fraction of isolate 187. This is an integral membrane protein from the MVIN family of proteins that have been found to be virulence factors. This study demonstrated that different low- and high-passage strains of MAP do have differences within their proteomes, and this must be considered when searching for virulence factors and antigens.

In an attempt to better understand the responses of MAP when infecting the host or when present in the environment, Gumber et al. (2009) analyzed the proteome of MAP under the stress of hypoxia and nutrient deprivation. After treating cultures with media containing either less oxygen or fewer nutrients, protein extraction was performed. This consisted of collecting bacterial cells and treating them with a lysis buffer containing urea, followed by centrifugation to remove cellular debris. Proteins were then run on two dimensional SDS-PAGE gels. The greatest number of differentially expressed proteins was categorized as hypothetical proteins with no functions found, however, some proteins were associated with the response of MAP to these stress conditions. Hypoxia induced the expression of heparin-binding haemagglutinin adhesion (HBHA)-like protein, which is required for extra pulmonary dissemination of *M. tuberculosis* (Pethe et al., 2001). The role of HBHA in MAP is not known, but is likely induced *in vivo* during infection, as revealed by this study.

To make use of proteins described as being differentially regulated during stress conditions, Gurung et al. (2012) analyzed differentially regulated proteins using bio-informatics software to predict both T cell and B cell epitopes within proteins. This analysis generated a list of 25 candidates, 8 of which were identified as potential candidates for study of antibody- and cell-mediated immune responses within infected hosts. The same research group evaluated the humoral response to these proteins in sheep (Kawaji et al., 2012). A recombinant antigen preparation was made and used in an ELISA platform to evaluate the responses among sheep with a wide range of disease states. The ELISA developed had similar sensitivity to a commercial ELISA and some

serum samples from uninfected sheep were also reactive. This demonstrates that finding improved antigens is not easy. There is still a need to find better antigens or antigen preparations that reliably distinguish infected animals from healthy on diagnostic tests.

Antigen preparations of MAP used in diagnostic applications

Several protein preparations of MAP have been used in different assay platforms to diagnose infection. A culture filtrate preparation, also known as johnin purified protein derivative (jPPD), has been used for cell-mediated immune tests, specifically the interferon-gamma release assay (Stabel & Whitlock, 2001). This is an antigen preparation made by filtering the culture of MAP after removal of bacterial cells. A problem with this preparation is the lack of standardized protocols for their production. Wynne et al. (2012) investigated differences in jPPDs and found that although broad proteomic composition of different jPPD preparations was similar, there were considerable differences in absolute abundance of specific proteins. These differences were attributed mainly to strain diversity as well as age of culture prior to antigen preparation.

Another antigen preparation that is widely used is the protoplasmic antigen (PPA). This preparation was described for mycobacteria by Beam et al. (1969) and early on demonstrated high reactivity and specificity when used to differentiate mycobacterial infections. This preparation consists of physical disruption of the bacterial culture followed by removal of bacterial debris and cell wall components (Beam et al., 1969). In MAP this preparation was used by Yokomizo et al. (1983) to develop an ELISA

platform for diagnosis of paratuberculosis. This assay identified 58% of cattle with positive fecal cultures. A problem with false positive results was resolved by the same author in 1985 by pre-absorption of sera with *Mycobacterium phlei* to remove cross-reactive antibodies (Yokomizo et al., 1985). Both the PPA preparation as well as the pre-absorption steps are used in commercial ELISAs today.

An improvement to ELISA sensitivity and specificity was achieved by using an ethanol extract preparation to isolate antigens of MAP (Eda et al., 2006). This assay was termed Ethanol Vortex ELISA (EVELISA) because the antigen preparation involved treating bacterial cells with 80% ethanol followed by agitation. The addition of a pre-absorption step to this assay resulted in a more robust and sensitive measure of MAP-specific antibodies (Scott et al., 2010). The estimated sensitivity of this assay also increased to 97.1% with a specificity of 100%. Because this preparation gently extracts the surface components of MAP, and these components appear to be useful antigens, we sought to further examine the envelope of MAP.

Studies to identify proteins relevant for diagnostic and vaccine development

Research has also focused on identifying specific proteins that could be used to diagnose MAP. One method that provides a platform to analyze as well as directly compare several proteins at once is the protein array (Bannantine et al., 2008). Upon analysis of 92 MAP proteins, Bannantine et al. (2008b) demonstrated the diagnostic potential of some proteins as these could detect antibodies in serum of animals soon after experimental infection. The protein encoded by MAP1087, a putative protein on the

surface of MAP, showed the highest antibody reactivity throughout the course of the study and antibodies to this protein were observed within 70 days after experimental infection.

More recently, Facciuolo et al. (2013), screened a culture filtrate preparation of MAP for reactivity among infected animals. Of the 162 total proteins identified, 4 proved to be antigenic by reacting to sera of subclinical and clinical animals. Nagata et al. (2013) discovered a very promising antigen, an enoyl coenzyme A hydratase encoded by MAP1197. In the ELISA format, this protein demonstrated the capacity to detect antibodies in subclinical animals 2–7 months earlier than by a commercially available ELISA kit. They also reported a 96.7% sensitivity and specificity of the ELISA.

Fewer studies have addressed the use of antigens in the IFN- γ release assay to detect cell-mediated immune responses. The advantages of this assay are that it could potentially have a greater sensitivity to diagnose subclinical animals, as it measures Th1 type responses which are characteristic of early stage infection. Hughes et al. (2013) investigated the potential of 30 proteins, previously identified as potentially MAP-specific in an IFN- γ release assay to diagnose subclinical infection in sheep. Of the candidates studied, all 30 recombinant proteins elicited an IFN- γ response in at least one of nine animals. Four proteins, encoded by MAP1297, MAP1365, MAP3651c and MAP0268c, were selected for further investigation based on the higher number of reactive animals as well as the magnitude of the response. Of these proteins, MAP3651c was the only one that demonstrated an increased response in infected animals in comparison to non-infected animals. Mikkelsen et al. (2011) investigated 14

recombinant proteins and compared them to jPPD in an IFN- γ release assay to detect paratuberculosis in cattle. jPPD proved to be unspecific while some proteins had the potential to differentiate among infected and non-infected animals. These included the hypothetical proteins LATP-2, MAP-1 and MAP-2 which do not share homology with any proteins from *Mycobacterium avium* subsp. *avium*. However it is still unknown whether these proteins are actually expressed by MAP, thus studies that investigate proteins that have been shown to be expressed by the bacterium are at an advantage for finding antigenic proteins.

Some recombinant proteins have also been evaluated as vaccine candidates. The current paratuberculosis vaccine available in the US (Mycopar, Boehringer Ingelheim) is a heat-killed whole cell antigen that has several disadvantages. These include: a potential health hazard to the veterinarian who administers the vaccine, granuloma formation at the injection site and possible interference with bovine tuberculosis skin testing as well as serologic detection of MAP infected animals (Patton, 2011). With this in mind the use of subunit vaccines may prove the most efficacious in developing a vaccine for paratuberculosis to reduce or eliminate these problems while maintaining the beneficial properties of the vaccine (Stabel et al., 2012). Koets et al. (2006), studied the use of a recombinant MAP protein, Hsp70, as a subunit vaccine in cattle experimentally infected with MAP. The results of the study demonstrated that recombinant MAP Hsp70 significantly reduced shedding of bacteria in feces during the first 2 years following experimental infection, demonstrating its potential as a vaccine candidate. Kathaperumal et al. (2008), studied three recombinant proteins of the antigen 85

complex as well as superoxide dismutase for their ability to protect calves after experimental challenge with MAP. Results from this study indicated that all four recombinant proteins induced a good Th1 response and conferred some protection against MAP infection in calves. Stabel et al. (2012) studied protein cocktails for their ability to protect mice to infection with MAP. The most promising cocktail contained the proteins MAP1087, MAP1204, MAP1272c; two of which had previously been shown to be antigenic in protein arrays blotted against sera from experimentally infected calves (Bannantine et al., 2008b). This cocktail of proteins elicited high IFN- γ responses as well as a reduction in MAP colonization of the liver, spleen, ileum and mesenteric lymph node of mice. Even with several attempts to improve and develop novel vaccines for paratuberculosis none have yielded an efficacious alternative. With this there is the need for new approaches such as the analysis of envelope protein complexes to identify novel promising antigens for vaccine development.

In conclusion, there have been several studies that have shed light in to MAP and mechanisms used by the bacterium to cause disease, however there is still a great need for a better understanding of Johne's disease and the development of improved control strategies. The research presented in this thesis investigated how T cells change in relation to infection status, by studying the signaling molecules ZAP-70 and CTLA-4, to investigate alterations among this cell population which is crucial for the control of paratuberculosis. Secondly, protein complexes in the envelope MAP were investigated to gain insight in to the physiology and pathogenesis of the organism as well as to identify novel antigens for diagnostic and vaccine development.

References

- Alderwick LJ, Seidel M, Sahm H, Besra GS, Eggeling L.** Identification of a novel arabinofuranosyltransferase (AftA) involved in cell wall arabinan biosynthesis in *Mycobacterium tuberculosis*. J Biol Chem. 2006. 281:15653-61.
- Bannantine JP, Bayles DO, Waters WR, Palmer MV, Stabel JR, Paustian ML.** Early antibody response against *Mycobacterium avium subspecies paratuberculosis* antigens in subclinical cattle. Proteome Sci. 2008b. 28;6:5.
- Bannantine JP, Bermudez LE.** No holes barred: invasion of the intestinal mucosa by *Mycobacterium avium subsp. paratuberculosis*. Infect Immun. 2013. 81:3960-5.
- Bannantine JP, Huntley JF, Miltner E, Stabel JR, Bermudez LE.** The *Mycobacterium avium subsp. paratuberculosis* 35 kDa protein plays a role in invasion of bovine epithelial cells. Microbiology. 2003. 149:2061-9.
- Bannantine JP, Paustian ML, Kapur V, Eda S.** Proteome and Antigens of *Mycobacterium avium subsp. paratuberculosis*. In: Paratuberculosis: organism, disease, control. 2010. CABI, Oxfordshire, UK.
- Bannantine JP, Waters WR, Stabel JR, Palmer MV, Li L, Kapur V, Paustian ML.** Development and use of a partial *Mycobacterium avium subspecies paratuberculosis* protein array. Proteomics. 2008. 8:463-74.
- Bannantine JP, Zhang Q, Li LL, Kapur V.** Genomic homogeneity between *Mycobacterium avium subsp. avium* and *Mycobacterium avium subsp. paratuberculosis* belies their divergent growth rates. BMC Microbiol. 2003. 9;3:10.
- Beam RE, Stottmeier KD, Kubica GP.** Purified protoplasmic peptides of mycobacteria: isolation of species-specific peptides from protoplasm of mycobacteria. J Bacteriol. 1969. 100:195-200.
- Begg DJ, de Silva K, Carter N, Plain KM, Purdie A, Whittington RJ.** Does a Th1 over Th2 dominance really exist in the early stages of *Mycobacterium avium subspecies paratuberculosis* infections? Immunobiology. 2011. 216:840-6.
- Bermudez LE, Petrofsky M, Sommer S, Barletta RG.** Peyer's patch-deficient mice demonstrate that *Mycobacterium avium subsp. paratuberculosis* translocates across the mucosal barrier via both M cells and enterocytes but has inefficient dissemination. Infect Immun. 2010. 78:3570-7.

Buza JJ, Hikono H, Mori Y, Nagata R, Hirayama S, Aodon-geril, Bari AM, Shu Y, Tsuji NM, Momotani E. Neutralization of interleukin-10 significantly enhances gamma interferon expression in peripheral blood by stimulation with Johnin purified protein derivative and by infection with *Mycobacterium avium subsp. paratuberculosis* in experimentally infected cattle with paratuberculosis. *Infect Immun.* 2004. 72:2425-8.

Coussens PM, Sipkovsky S, Murphy B, Roussey J, Colvin CJ. Regulatory T cells in cattle and their potential role in bovine paratuberculosis. *Comp Immunol Microbiol Infect Dis.* 2012. 35:233-9.

Daffé M, Draper P. The envelope layers of mycobacteria with reference to their pathogenicity. *Adv Microb Physiol.* 1998. 39:131-203.

de Almeida DE, Colvin CJ, Coussens PM. Antigen-specific regulatory T cells in bovine paratuberculosis. *Vet Immunol Immunopathol.* 2008. 125:234-45.

Deng W, Xie J. Ins and outs of *Mycobacterium tuberculosis* PPE family in pathogenesis and implications for novel measures against tuberculosis. *J Cell Biochem.* 2012 Apr;113(4):1087-95.

Di Bartolo V, Mege D, Germain V, Pelosi M, Dufour E, Michel F, Magistrelli G, Isacchi A, Acuto O. Tyrosine 319, a newly identified phosphorylation site of ZAP-70, plays a critical role in T cell antigen receptor signaling. *J Biol Chem.* 1999. 274: 6285–6294.

Eda S, Bannantine JP, Waters WR, Mori Y, Whitlock RH, Scott MC, Speer CA. A highly sensitive and subspecies-specific surface antigen enzyme-linked immunosorbent assay for diagnosis of Johne's disease. *Clin Vaccine Immunol.* 2006 Aug;13(8):837-44.

Elder ME, Skoda-Smith S, Kadlecsek TA, Wang F, Wu J, Weiss A. Distinct T cell developmental consequences in humans and mice expressing identical mutations in the DLAARN motif of ZAP-70. *J Immunol.* 2001. 166: 656–661.

Facciuolo A, Kelton DF, Mutharia LM. Novel Secreted Antigens of *Mycobacterium paratuberculosis* as Serodiagnostic Biomarkers for Johne's Disease in Cattle. *Clin Vaccine Immunol.* 2013. 20:1783-91.

Fallarino F, Grohmann U, Hwang KW, Orabona C, Vacca C, Bianchi R, Belladonna ML, Fioretti MC, Alegre ML, Puccetti P. Modulation of tryptophan catabolism by regulatory T cells. *Nat Immunol.* 2003. 4:1206-12.

Fecteau M, Whitlock R. Paratuberculosis in cattle. In: *Paratuberculosis: organism, disease, control.* 2010. CABI, Oxfordshire, UK.

Forrellad MA, Klepp LI, Gioffré A, Sabio y García J, Morbidoni HR, de la Paz Santangelo M, Cataldi AA, Bigi F. Virulence factors of the *Mycobacterium tuberculosis* complex. *Virulence*. 2013 Jan 1;4(1):3-66.

González J, Geijo MV, García-Pariente C, Verna A, Corpa JM, Reyes LE, Ferreras MC, Juste RA, García Marín JF, Pérez V. Histopathological classification of lesions associated with natural paratuberculosis infection in cattle. *J Comp Pathol*. 2005. 133:184-96.

Gumber S, Taylor DL, Marsh IB, Whittington RJ. Growth pattern and partial proteome of *Mycobacterium avium subsp. paratuberculosis* during the stress response to hypoxia and nutrient starvation. *Vet Microbiol*. 2009. 133:344-57.

Guntermann C, Alexander DR. CTLA-4 suppresses proximal TCR signaling in resting human CD4(+) T cells by inhibiting ZAP-70 Tyr(319) phosphorylation: a potential role for tyrosine phosphatases. *J Immunol*. 2002. 168:4420-9.

Gurung RB, Purdie AC, Begg DJ, Whittington RJ. In silico identification of epitopes in *Mycobacterium avium subsp. paratuberculosis* proteins that were upregulated under stress conditions. *Clin Vaccine Immunol*. 2012. 19:855-64.

Hatakeyama M, Higashi H. Helicobacter pylori CagA: a new paradigm for bacterial carcinogenesis. *Cancer Sci*. 2005. 96:835-43.

He T, Tang C, Xu S, Moyana T, Xiang J. Interferon gamma stimulates cellular maturation of dendritic cell line DC2.4 leading to induction of efficient cytotoxic T cell responses and antitumor immunity. *Cell Mol Immunol*. 2007. 4:105-11.

He Z, De Buck J. Localization of proteins in the cell wall of *Mycobacterium avium subsp. paratuberculosis* K10 by proteomic analysis. *Proteome Sci*. 2010. 8;8:21.

Hostetter J, Steadham E, Haynes J, Bailey T, Cheville N. Phagosomal maturation and intracellular survival of *Mycobacterium avium subspecies paratuberculosis* in J774 cells. *Comp Immunol Microbiol Infect Dis*. 2003. 26:269-83.

Hughes V, Denham S, Bannantine JP, Chianini F, Kerr K, May L, McLuckie J, Nath M, Stevenson K. Interferon gamma responses to proteome-determined specific recombinant proteins: potential as diagnostic markers for ovine Johne's disease. 2013. 155:197-204.

Jin L, Pluskey S, Petrella EC, Cantin SM, Gorga JC, Rynkiewicz MJ, Pandey P, Strickler JE, Babine RE, Weaver DT. The three-dimensional structure of the ZAP-70 kinase domain in complex with staurosporine: Implications for the design of selective inhibitors. *J Biol Chem* 2004. 279: 42818–42825.

Johne H.A., Frothingham L., 1895. Ein eigentuenlicher Fall von Tuberkulose beim Rind (A peculiar case of tuberculosis in a cow). Deutsch Zeitschrift fur Tiermedizin un Vergleich. Pathol., 21, 438-454.

Kathaperumal K, Park SU, McDonough S, Stehman S, Akey B, Huntley J, Wong S, Chang CF, Chang YF. Vaccination with recombinant *Mycobacterium avium* subsp. *paratuberculosis* proteins induces differential immune responses and protects calves against infection by oral challenge. Vaccine. 2008 Mar 26:1652-63.

Kawaji S, Nagata R, Whittington RJ, Mori Y. Detection of antibody responses against *Mycobacterium avium* subsp. *paratuberculosis* stress-associated proteins within 30 weeks after infection in cattle. Vet Immunol Immunopathol. 2012. 150:101-11.

Khalifeh MS, Stabel JR. Effects of gamma interferon, interleukin-10, and transforming growth factor beta on the survival of *Mycobacterium avium* subsp. *paratuberculosis* in monocyte-derived macrophages from naturally infected cattle. Infect Immun. 2004. 72:1974-82.

Khalifeh MS, Stabel JR. Upregulation of transforming growth factor-beta and interleukin-10 in cows with clinical Johne's disease. Vet Immunol Immunopathol. 2004b. 99:39-46.

Khare S, Lawhon SD, Drake KL, Nunes JE, Figueiredo JF, Rossetti CA, Gull T, Everts RE, Lewin HA, Galindo CL, Garner HR, Adams LG. Systems biology analysis of gene expression during in vivo *Mycobacterium avium paratuberculosis* enteric colonization reveals role for immune tolerance. PLoS One. 2012. 7:e42127. doi: 10.1371/journal.pone.0042127.

Kleinnijenhuis J, Oosting M, Joosten LA, Netea MG, Van Crevel R. Innate immune recognition of *Mycobacterium tuberculosis*. Clin Dev Immunol. 2011;2011:405310.

Knieke K, Hoff H, Maszyna F, Kolar P, Schrage A, Hamann A, Debes GF, Brunner-Weinzierl MC. CD152 (CTLA-4) determines CD4 T cell migration in vitro and in vivo. PLoS One. 2009 May 27;4(5):e5702. doi: 10.1371/journal.pone.0005702.

Kocíncová D, Sondén B, de Mendonça-Lima L, Gicquel B, Reytrat JM. The Erp protein is anchored at the surface by a carboxy-terminal hydrophobic domain and is important for cell-wall structure in *Mycobacterium smegmatis*. FEMS Microbiol Lett. 2004 Feb 16;231(2):191-6.

Koets A, Hoek A, Langelaar M, Overdijk M, Santema W, Franken P, Eden Wv, Rutten V. Mycobacterial 70 kD heat-shock protein is an effective subunit vaccine against bovine paratuberculosis. Vaccine. 2006.24:2550-9.

Krummel MF, Allison JP. CTLA-4 engagement inhibits IL-2 accumulation and cell cycle progression upon activation of resting T cells. *J Exp Med.* 1996. 183:2533-40.

Li L, Bannantine JP, Zhang Q, Amonsin A, May BJ, Alt D, Banerji N, Kanjilal S, Kapur V. The complete genome sequence of *Mycobacterium avium* subspecies *paratuberculosis*. *Proc Natl Acad Sci U S A.* 2005 102:12344-9.

Lombard JE, Gardner IA, Jafarzadeh SR, Fossler CP, Harris B, Capsel RT, Wagner BA, Johnson WO. Herd-level prevalence of *Mycobacterium avium* subsp. *paratuberculosis* infection in United States dairy herds in 2007. *Prev Vet Med.* 2013. 108:234-8.

Lombard JE. Epidemiology and economics of paratuberculosis. *Vet Clin North Am Food Anim Pract.* 2011. 27:525-35.

Magombedze G, Ngonghala CN, Lanzas C. Evaluation of the "Iceberg Phenomenon" in Johne's disease through mathematical modelling. *PLoS One.* 2013. 22;8(10):e76636. doi:10.1371/journal.pone.0076636.

Manning E.J.B., Collins M.T. History of paratuberculosis. In: *Paratuberculosis: organism, disease, control.* 2010. CABI, Oxfordshire, UK.

Mikkelsen H, Aagaard C, Nielsen SS, Jungersen G. Novel antigens for detection of cell mediated immune responses to *Mycobacterium avium* subsp. *paratuberculosis* infection in cattle. *Vet Immunol Immunopathol.* 2011. 143(1-2):46-54.

Momotani E, Whipple DL, Thiermann AB, Cheville NF. Role of M cells and macrophages in the entrance of *Mycobacterium paratuberculosis* into domes of ileal Peyer's patches in calves. *Vet Pathol.* 1988. 25:131-7.

Murphy K. Janeway's Immunobiology. 2012. Garland Science. New York, NY.

Nagata R, Kawaji S, Mori Y. Use of enoyl coenzyme A hydratase of *Mycobacterium avium* subsp. *paratuberculosis* for the serological diagnosis of Johne's disease. *Vet Immunol Immunopathol.* 2013. 155:253-8.

Niederweis M, Danilchanka O, Huff J, Hoffmann C, Engelhardt H. Mycobacterial outer membranes: in search of proteins. *Trends Microbiol.* 2010 Mar;18(3):109-16.

Oosterwegel MA, Mandelbrot DA, Boyd SD, Lorsbach RB, Jarrett DY, Abbas AK, Sharpe AH. The role of CTLA-4 in regulating Th2 differentiation. *J Immunol.* 1999 Sep 1;163(5):2634-9.

Patton EA. Paratuberculosis vaccination. *Vet Clin North Am Food Anim Pract.* 2011. 27:573-80.

Pethe K, Alonso S, Biet F, Delogu G, Brennan MJ, Locht C, Menozzi FD. The heparin-binding haemagglutinin of *M. tuberculosis* is required for extrapulmonary dissemination. *Nature.* 2001. 412:190-4.

Pott J, Basler T, Duerr CU, Rohde M, Goethe R, Hornef MW. Internalization-dependent recognition of *Mycobacterium avium* ssp. *paratuberculosis* by intestinal epithelial cells. *Cell Microbiol.* 2009. 11:1802-15.

Pyndiah S, Lasserre JP, Ménard A, Claverol S, Prouzet-Mauléon V, Mégraud F, Zerbib F, Bonneau M. Two-dimensional blue native/SDS gel electrophoresis of multiprotein complexes from *Helicobacter pylori*. *Mol Cell Proteomics.* 2007 Feb;6(2):193-206.

Qureshi OS, Zheng Y, Nakamura K, Attridge K, Manzotti C, Schmidt EM, Baker J, Jeffery LE, Kaur S, Briggs Z, Hou TZ, Futter CE, Anderson G, Walker LS, Sansom DM. Trans-endocytosis of CD80 and CD86: a molecular basis for the cell-extrinsic function of CTLA-4. *Science.* 2011. 332:600-3.

Radosevich TJ, Reinhardt TA, Lippolis JD, Bannantine JP, Stabel JR. Proteome and differential expression analysis of membrane and cytosolic proteins from *Mycobacterium avium* subsp. *paratuberculosis* strains K-10 and 187. *J Bacteriol.* 2007. 189:1109-17.

Reisinger V, Eichacker LA. How to analyze protein complexes by 2D blue native SDS-PAGE. *Proteomics.* 2007;7 Suppl 1:6-16.

Reisinger V, Eichacker LA. Solubilization of membrane protein complexes for blue native PAGE. *J Proteomics.* 2008. 71:277-83.

Rudd CE, Taylor A, Schneider H. CD28 and CTLA-4 coreceptor expression and signal transduction. *Immunol Rev.* 2009 May;229(1):12-26.

Sansom DM. CD28, CTLA-4 and their ligands: who does what and to whom? *Immunology.* 2000 Oct;101(2):169-77.

Schägger H, von Jagow G. Blue native electrophoresis for isolation of membrane protein complexes in enzymatically active form. *Anal Biochem.* 1991 Dec;199(2):223-31.

Schneider H, Valk E, Leung R, Rudd CE. CTLA-4 activation of phosphatidylinositol 3-kinase (PI 3-K) and protein kinase B (PKB/AKT) sustains T-cell anergy without cell death. *PLoS One*. 2008;3(12):e3842. doi: 10.1371/journal.pone.0003842.

Schwartz RH. T cell anergy. *Annu Rev Immunol*. 2003. 21:305-34.

Scott MC, Bannantine JP, Kaneko Y, Branscum AJ, Whitlock RH, Mori Y, Speer CA, Eda S. Absorbed EVELISA: a diagnostic test with improved specificity for Johne's disease in cattle. *Foodborne Pathog Dis*. 2010. 7:1291-6.

Secott TE, Lin TL, Wu CC. *Mycobacterium avium* subsp. *paratuberculosis* fibronectin attachment protein facilitates M-cell targeting and invasion through a fibronectin bridge with host integrins. *Infect Immun*. 2004. 72:3724-32.

Souza C, Davis WC, Eckstein TM, Sreevatsan S, Weiss DJ. Mannosylated lipoarabinomannans from *Mycobacterium avium* subsp. *paratuberculosis* alters the inflammatory response by bovine macrophages and suppresses killing of *Mycobacterium avium* subsp. *avium* organisms. *PLoS One*. 2013. 30;8(9):e75924. doi: 10.1371/journal.pone.0075924.

Stabel JR, Barnhill A, Bannantine JP, Chang YF, Osman MA. Evaluation of protection in a mouse model after vaccination with *Mycobacterium avium* subsp. *paratuberculosis* protein cocktails. *Vaccine*. 2012. 31:127-34.

Stabel JR, Whitlock RH. An evaluation of a modified interferon-gamma assay for the detection of paratuberculosis in dairy herds. *Vet Immunol Immunopathol*. 2001. 79:69-81.

Stabel JR. Transitions in immune responses to *Mycobacterium paratuberculosis*. *Vet Microbiol*. 2000. 77:465-73.

Stabel JR. Host responses to *Mycobacterium avium* subsp. *paratuberculosis*: a complex arsenal. *Anim Health Res Rev*. 2006 7:61-70.

Stabel JR. Immunology of Paratuberculosis Infection and Disease. In: *Paratuberculosis: organism, disease, control*. 2010. CABI, Oxfordshire, UK.

Stabel JR. Johne's disease: a hidden threat. *J Dairy Sci*. 1998. 81:283-8.

Sweeney RW. Pathogenesis of paratuberculosis. *Vet Clin North Am Food Anim Pract*. 2011. 27:537-46.

Thorel MF, Krichevsky M, Lévy-Frébault VV. Numerical taxonomy of mycobactin-dependent mycobacteria, emended description of *Mycobacterium avium*, and description

of *Mycobacterium avium* subsp. *avium* subsp. nov., *Mycobacterium avium* subsp. *paratuberculosis* subsp. nov., and *Mycobacterium avium* subsp. *silvaticum* subsp. nov. *Int J Syst Bacteriol.* 1990. 40:254-60.

Wadhwa A, Bannantine JP, Byrem TM, Stein TL, Saxton AM, Speer CA, Eda S. Optimization of serum EVELISA for milk testing of Johne's disease. *Foodborne Pathog Dis.* 2012 Aug;9(8):749-54.

Walker LS, Sansom DM. The emerging role of CTLA4 as a cell-extrinsic regulator of T cell responses. *Nat Rev Immunol.* 2011. 25:852-63.

Walunas TL, Lenschow DJ, Bakker CY, Linsley PS, Freeman GJ, Green JM, Thompson CB, Bluestone JA. CTLA-4 can function as a negative regulator of T cell activation. *Immunity.* 1994. Aug;1(5):405-13.

Wang H, Kadlecsek TA, Au-Yeung BB, Goodfellow HE, Hsu LY, Freedman TS, Weiss A. ZAP-70: an essential kinase in T-cell signaling. *Cold Spring Harb Perspect Biol.* 2010. 2:a002279. doi: 10.1101/cshperspect.a002279.

Waters WR, Stabel JR, Sacco RE, Harp JA, Pesch BA, Wannemuehler MJ. Antigen-specific B-cell unresponsiveness induced by chronic *Mycobacterium avium* subsp. *paratuberculosis* infection of cattle. *Infect Immun.* 1999. 67:1593-8.

Weiss DJ, Evanson OA, de Souza C, Abrahamsen MS. A critical role of interleukin-10 in the response of bovine macrophages to infection by *Mycobacterium avium* subsp. *paratuberculosis*. *Am J Vet Res.* 2005. 66:721-6.

Weiss DJ, Evanson OA, Souza CD. Mucosal immune response in cattle with subclinical Johne's disease. *Vet Pathol.* 2006. 43:127-35.

Weiss DJ, Souza CD. Review paper: modulation of mononuclear phagocyte function by *Mycobacterium avium* subsp. *paratuberculosis*. *Vet Pathol.* 2008. 45:829-41.

Whittington RJ, Windsor PA. In utero infection of cattle with *Mycobacterium avium* subsp. *paratuberculosis*: a critical review and meta-analysis. *Vet J.* 2009. 179:60-9.

Williams BL, Schreiber KL, Zhang W, Wange RL, Samelson LE, Leibson PJ, Abraham RT. Genetic evidence for differential coupling of Syk family kinases to the T-cell receptor: Reconstitution studies in a ZAP-70-deficient Jurkat T-cell line. *Mol Cell Biol.* 1998. 18: 1388–1399.

Wynne JW, Shiell BJ, Colgrave ML, Vaughan JA, Beddome G, Michalski WP. Production and proteomic characterisation of purified protein derivative from *Mycobacterium avium* subsp. *paratuberculosis*. *Proteome Sci.* 2012. 10:22.

Yang X, Promnares K, Qin J, He M, Shroder DY, Kariu T, Wang Y, Pal U. Characterization of multiprotein complexes of the *Borrelia burgdorferi* outer membrane vesicles. J Proteome Res. 2011. 10:4556-66

Yokomizo Y, Merkal RS, Lyle PA. Enzyme-linked immunosorbent assay for detection of bovine immunoglobulin G1 antibody to a protoplasmic antigen of *Mycobacterium paratuberculosis*. Am J Vet Res. 1983. 44:2205-7.

Yokomizo Y, Yugi H, Merkal RS. A method for avoiding false-positive reactions in an enzyme-linked immunosorbent assay (ELISA) for the diagnosis of bovine paratuberculosis. Nihon Juigaku Zasshi. 1985. 47:111-9.

Zheng J, Wei C, Zhao L, Liu L, Leng W, Li W, Jin Q. Combining blue native polyacrylamide gel electrophoresis with liquid chromatography tandem mass spectrometry as an effective strategy for analyzing potential membrane protein complexes of *Mycobacterium bovis* bacillus Calmette-Guérin. BMC Genomics. 2011. Jan 18;12:40.

Zuber B, Chami M, Houssin C, Dubochet J, Griffiths G, Daffé M. Direct visualization of the outer membrane of mycobacteria and corynebacteria in their native state. J Bacteriol. 2008. 190:5672-80.

CHAPTER 2. Envelope protein complexes of *Mycobacterium avium* subsp. *paratuberculosis* and their antigenicity

Modified from a paper to be submitted to *Journal of Bacteriology*

Fernando L. Leite¹, Timothy Reinhardt², John Bannantine², Judith R. Stabel²

¹Iowa State University, Department of Veterinary Microbiology and Preventive Medicine, ² U.S. Department of Agriculture, Agricultural Research Service, National Animal Disease Center, Ames, IA

Abstract

Mycobacterium avium subsp. *paratuberculosis* (MAP) is the causative agent of Johne's disease, a chronic enteric disease of ruminant animals. In the present study, blue native PAGE electrophoresis and 2D SDS-PAGE were used to separate MAP envelope protein complexes, followed by mass spectrometry (MS) to identify individual proteins within the complexes. Identity of individual proteins within complexes was further confirmed by MS upon excision of spots from 2D SDS-PAGE gels. Among the seven putative membrane complexes observed, major membrane protein (MAP2121c), a key MAP antigen involved in invasion of epithelial cells, was found to form a complex with cysteine desulfurase (MAP2120c). Other complexes found included those involved in energy metabolism (succinate dehydrogenase complex) as well as a complex formed by Cfp29, a characterized T cell antigen of *M. tuberculosis*. To determine antigenicity of proteins, Western blot was performed on replicate 2D SDS-PAGE gels with sera from

noninfected control cows (n=9) and naturally infected cows in the subclinical (n = 10) and clinical (n=13) stages of infection. Clinical animals recognized MAP2121c in greater proportion than subclinical and control cows, whereas cysteine desulfurase recognition was not differentiated by infection status. To further characterize antigenicity, recombinant proteins were expressed for 10 of the proteins identified and evaluated in an interferon-gamma (IFN- γ) release assay as well as immuno-blots. This study reveals the presence of protein complexes in the cell envelope of MAP, suggesting protein interactions in the envelope of this pathogen. Furthermore the identification of antigenic proteins with potential as diagnostic targets were characterized.

Introduction

Mycobacterium avium subsp. *paratuberculosis* (MAP) is the causative agent of paratuberculosis (Johne's disease), a chronic enteric wasting disease of ruminant animals with worldwide distribution (1). Paratuberculosis is predominantly a subclinical disease with economic impact mostly in dairy cattle in the US. As the disease progresses, there is a loss in milk production, as well as higher incidence of mastitis and infertility, leading to early culling of animals (2). Currently, the diagnostics of MAP is based mainly on the detection of the bacterium in feces by culture or PCR and by ELISA detection of MAP-specific antibodies. However, crude antigen preparations are used for antibody detection and these can limit the detection of asymptomatic animals. Detection of animals in the subclinical stage of infection can be difficult as these animals typically excrete MAP in low numbers and have not yet developed measurable antibody titers to

MAP (3,4). With this in mind, research to identify antigens that can be used to sensitively diagnose the disease is needed; in particular, antigens that are conducive for use in the IFN- γ assay, a measure of Th1-mediated immune response elicited by animals in the subclinical stage of infection (5).

MAP is a member of the avium complex of mycobacteria and has an envelope comprised of a cytoplasmic membrane and a cell wall consisting of peptidoglycan, arabinogalactan, mycolic acids and proteins (6,7). Proteins associated with the cell envelope of MAP are likely to be the first to interact with the host and, therefore, the first proteins for immune recognition (8). Several antigenic proteins as well as those with roles in virulence have been found to be associated with the envelope of mycobacteria, including proteins of the PPE family (9). Thus, characterization of proteins present in the envelope is critical not only to the comprehension of the physiology and pathogenesis of the organism but also to identify potential antigenic proteins for use in vaccines and diagnostic assays.

In the present study, blue native (BN) PAGE and 2D SDS-PAGE were used to characterize protein complexes in the envelope of MAP. BN PAGE is a technique that allows for the isolation of protein complexes with the use of non-ionic detergents allowing the solubilization of hydrophobic proteins which can be missed with other techniques such as iso-electric focusing (10). Mass spectrometry was performed on blue native gels as well as 2D SDS-PAGE gels to identify proteins within complexes. To determine antigenicity of proteins, Western blot was performed on replicate 2D SDS-

PAGE gels with sera from noninfected and naturally infected animals to identify novel antigens with potential as vaccine and diagnostic targets.

Materials and Methods

Bacteria.

A low passage clinical isolate of MAP, strain 509, was isolated from the jejunum of a cow manifesting clinical signs of paratuberculosis and was confirmed as MAP by IS900 and ISMAP02 PCR (data not shown). The bacterium was grown to log phase ($\text{Abs}_{540\text{nm}} = 0.2\text{-}0.4$) in Middlebrook 7H9 broth (pH 5.9) (Becton Dickinson) containing 0.05% Tween 80 (Sigma) and ferric mycobactin J (2 mg/liter; Allied Monitor), supplemented with oleic acid, albumin, dextrose, and catalase enrichment (OADC, BD). Cultures were pelleted by centrifugation at $10,000 \times g$ for 30 min at 4°C and washed twice with phosphate buffered saline (PBS). After the last centrifugation, pellets were stored at -80°C until used for envelope extraction.

Bacteria cell wall/membrane preparation.

Cell wall/membrane preparation was performed as described in Radosevich et al. (11) with some modifications. Sonication was performed in a hypotonic buffer (10 mM HEPES sodium salt, 1 mM EGTA, pH: 7.5, containing 1:100 protease inhibitor cocktail, Sigma). The sample was adjusted to 250 mM sucrose and centrifuged at $10,000 \times g$ for 30 min to remove unbroken cells and cellular debris. The supernatant was collected and centrifuged at $150,000 \times g$ for 1 h to isolate the cell wall/membrane. Protein quantification was performed using the Bio-Rad protein assay (Bio-Rad Laboratories) and all samples were stored at -20°C until use.

Blue Native PAGE.

Separation of the protein complexes present in the cell wall/membrane of MAP was performed by blue native PAGE (12). Samples were solubilized by adding 100 µg of protein to Native-PAGE sample buffer (Life technologies) with 0.5% digitonin (Life Technologies) for 1 h at 4°C in a rotating shaker. To remove insoluble protein, samples were centrifuged for 30 min at 14,000 x g at 4°C. The resulting supernatant was combined with G-250 coomassie in a final concentration corresponding to 25% of the detergent concentration. Extracts were loaded onto a 3-12% Native-PAGE gel (Life technologies). Electrophoresis was performed in Native-PAGE anode buffer (Life technologies,) and a cathode buffer containing 0.02% G-250 at 150 V. When the dye front migrated halfway into the gel the cathode buffer was replaced with cathode buffer containing 0.002% G-250 for the remainder of the 3hr run.

2D SDS-PAGE.

Second dimension SDS-PAGE was performed as described by Schamel, 2008 (13), with some modifications. Gel strips were excised from the blue native gel and stored at -20°C until use. To denature protein complexes the gel strips were incubated in a solution of 2x SDS sample buffer and 2x NuPAGE sample reducing agent (Life technologies) for 30 min at room temperature (RT) and incubated at 70°C for another 30 min. The strips were allowed to cool to RT for 30 min. Each strip was then inserted into a single well 1.0 mm 4-12% bis-tris gel (Life technologies). The strip was covered with 1x SDS sample buffer and 1 x NuPAGE sample reducing agent. Electrophoresis was

performed for 50 min at 200 V in MOPS buffer. Gels were stained using the SilverQuest silver stain kit (Life technologies).

Western-blot of 2D SDS-PAGE gels.

Electrophoretic transfer of proteins onto nitrocellulose was performed with a Trans Blot Cell (Bio-Rad Laboratories) with sodium phosphate buffer (25 mM) at 0.9 A for 90 min. After transfer, the membranes were blocked with PBS containing 0.1% Tween 20 (PBST) plus 2% bovine serum albumin (BSA) overnight at 4°C. Serum samples were diluted 1:200 in PBST with 2% BSA and incubated for two hours at RT. After the incubation, three washes were performed with PBST for 10 min each. Secondary antibody used was anti-goat IgG Horse radish peroxidase conjugate (Vector Labs) at a dilution of 1:20,000 for one hour of incubation. Following another three washes as described above, blots were incubated with SuperSignal West Pico Chemiluminescent Substrate (Thermo Fisher) for protein detection and exposed to X-ray film.

Preparation of trypsin digests.

2D-SDS-PAGE and native PAGE gels stained with the SilverQuest silver stain kit were imaged using the Gel Doc EZ imaging system (Bio-Rad Laboratories). Identified spots (2D SDS-PAGE gels) or bands (native page gels) were excised from the gels and placed in siliconized tubes containing destaining buffer (solution of 30% acetonitrile (ACN) and 70% triethylammonium bicarbonate (TEABB) and incubated at RT for 10 min. Destaining buffer was removed and this step was repeated 3 times. The gel pieces were then dried in a vacuum centrifuge without heat. Next the gel pieces were

rehydrated with a solution of 10 mM TCEP (Tris (2-carboxyethyl)-phosphine) for 5 min at 4°C then incubated in a 56°C water bath for 1 h. Alkylation was performed with a solution of 55 mM iodoacetamide for 1h at RT. Following incubation, the alkylation buffer was replaced with destaining buffer. For trypsin digestion, gel pieces were rehydrated with TEABB for 20 min at 4°C, followed by another incubation at 90°C for 20 min to heat denature proteins. After samples cooled to RT, one wash was performed with destaining buffer and the samples were dried in a vacuum centrifuge. A solution of proteomics grade trypsin (20 µg/ml; Sigma Aldrich) diluted in TEABB was added to cover the gel pieces and samples were incubated for 5 min at 4°C. A solution of 60% TEABB/40% ACN containing 25 µg/ml trypsin was used to cover the gel pieces and incubated overnight at 37°C in a shaking water bath. The next day the samples were cooled to RT. The digest solution was transferred to clean siliconized tubes. The gel slices were extracted 2x with 50:50 (vol/vol) ACN:5% formic acid, 1 x with 15:50:35 (vol/vol) isopropanol:ACN:5 % formic acid, and 2x with 80% ACN. All extracts were combined with the digest solution and dried in a vacuum centrifuge. The samples were stored dry at -20°C until used.

On line peptide chromatography and mass spectroscopy.

Samples were separated on a Proxeon Easy-nLC (Thermo Fisher Scientific), C18, 3 µm, 75 µm × 100 mm column in mobile phase A (95% H₂O: 5% acetonitrile and 0.1% formic acid) and mobile phase B (5% H₂O:95% acetonitrile and 0.1% formic acid) gradient, 0% B for 9 min, 6%–15% B from 10–80 min, 15–30% B from 80–88 min, 30–90% B from 88–90 min, at 300 nL/min. The analytical column was connected to a

Proxeon Nanospray Flex Ion Source (Thermo Fisher Scientific) on the front end of a LTQ OrbiTrap Velos (Thermo Fisher Scientific) mass spectrophotometer. The capillary temperature was set at 275°C and spray voltage optimized using the API stability evaluation software for the LTQ OrbiTrap Velos. Data dependent method settings were as follows: FTMS was 60,000 resolution from 300–2000 m/z followed by up to 10 ion trap MSMS scans. Activation was CID using normalized collision energy of 35. Minimal signal required was 5000 and repeat mass exclusion duration of 60 s (14).

Database Searches.

Tandem mass spectra were extracted by Protein Discoverer version 1.3.0.339. Charge state deconvolution and deisotoping were not performed. All MS/MS samples were analyzed Sequest (Thermo Fisher Scientific; version 1.3.0.339) and X! Tandem (The GPM, thegpm.org; version CYCLONE (2010.12.01.1) X! Tandem was set up to search the SP-MAP1770_120619.fasta (7368 entries) assuming trypsin cleavage. Sequest was set up to search SP-MAP1770_120619.fasta (7368 entries) also assuming trypsin cleavage. Sequest and X! Tandem were searched with a fragment ion mass tolerance of 0.08 Da and a parent ion tolerance of 10.0 PPM. Iodoacetamide derivative of cysteine were specified in Sequest and X! Tandem as fixed modifications. Oxidation of methionine was specified in Sequest and X! Tandem as a variable modification. Peptide and protein false discovery rates were 0.1% and 0.1% respectively with Scaffold probabilities set at 99% for protein and 95% for peptide identification.

Criteria for Protein Identification.

Scaffold (version Scaffold_3.6.5, Proteome Software Inc.) was used to validate MS/MS based peptide and protein identifications. Peptide identifications were accepted if they could be established at greater than 95.0% probability as specified by the Peptide Prophet algorithm (15). Protein identifications were accepted if they could be established at greater than 99.0% probability and contained at least 2 identified peptides. Protein probabilities were assigned by the Protein Prophet algorithm (16). Proteins that contained similar peptides and could not be differentiated based on MS/MS analysis alone were grouped to satisfy the principles of parsimony.

Bioinformatic analysis.

Predictions of trans-membrane topology were conducted using the TMHMM 2.0 program, publicly available from the Centre for Biological Sequence Analysis at the Technical University of Denmark <http://www.cbs.dtu.dk/services/TMHMM/>. Functional association prediction between identified proteins was analyzed using STRING version 9.05 interaction database <http://string-db.org/>.

Cloning of *Mycobacterium avium* subsp. *paratuberculosis* coding sequences.

Proteins that were identified by MS from 2D SDS PAGE gels and demonstrated antigenicity on Western blot analyses were cloned and expressed following protocols previously described (17). The pMAL protein fusion and purification system was used with the pMAL-c2x expression vector (New England Biolabs). After identification of the proteins of interest, the corresponding coding sequences were amplified from the annotated MAP genome (18). Primers were designed for the n-terminal and c-terminal portions of the proteins to span their whole coding sequence, XbaI and HindIII

restriction sites were added to the 5' and 3' primers respectively to allow digestion and insertion into the expression vector. The protein cysteine desulfurase (MAP2120c) had to be cloned in two fragments because its size was too large (2,013 kb) for full-length amplification and cloning. Amplification of the desired DNA sequences for insertion into the expression vector was performed using a master mix containing 20 µl GC Melt Buffer 2x Advantage (Clontech), 1 µl each of forward and reverse primers, 1 µl K-10 genome template, 0.2 µl polymerase, 20 µl distilled water and 2 µl dNTP nucleotide mix (Roche). PCR products were purified using the Gene Clean Turbo kit (Q-Biogene) and digested for one h at 37°C with XbaI and Hind III enzymes (New England Biolabs). Following purification with the Gene Clean Turbo kit, ligation was performed overnight at 16°C with T4 ligase and T4 ligase buffer (New England Biolabs). *E. coli* DH5- α was transformed by heat shock and incubated overnight in LB agar containing carbenicillin. To confirm transformation and ligation, 8 colonies from each agar plate were screened for the protein coding sequence of interest by PCR. One colony from each plate confirmed by PCR to have the cloned plasmid was further amplified by overnight culture in LB broth containing glucose (0.2%) and carbenicillin (100 mg/ml). Sequencing of cloned plasmids was performed to confirm in-frame insertion of the coding sequence to the 3' end of the *malE* gene in the vector, which encodes maltose binding protein (MBP) allowing for protein purification by affinity chromatography.

Protein expression and purification.

Protein expression and purification followed protocols previously described (17,19). Using the pMAL protein fusion and purification system (New England

Biolabs,), overnight cultures of cloned *E. coli* DH5- α were inoculated into 2 liter flasks containing 1 liter of LB broth supplemented with glucose (0.2%) and carbenicillin (100 μ g/ml) and cultured in a rotary shaker at 37°C. When an OD_{600nm} of 0.4-0.6 was reached, cells were induced with 360 μ l of 1M isopropyl-1-thio- β -D-galactoside (IPTG) solution for 2 h. After induction, cells were pelleted by centrifugation and resuspended in column buffer (20 mM TrisCl, 1 mM EDTA, pH: 7.4) and stored overnight at -20°C. Upon thawing of cells, sonication was performed for 4 min in an ice bath and the lysate was clarified by centrifugation. For purification of the fusion protein, affinity chromatography was performed using an amylose resin column. Protein was eluted with column buffer containing 10 mM maltose. Eluted protein was dialyzed in 1 liter PBS at 4°C with three exchanges using 10K Molecular weight cut off dialysis cassettes (Thermo Fisher). Final purified proteins were analyzed by SDS-PAGE gels stained with GelCode Blue (Thermo Fisher), and quantified by the Bio-Rad protein assay (Bio-Rad Laboratories) for use on immuno blots and interferon-gamma release assay.

Immunoblots.

For immunoblots, 12% SDS-polyacrylamide gels were cast with two lanes, one long lane across the top of the gel and another for loading protein size standard. A 100 μ l aliquot of recombinant protein (4.5 μ g total) was loaded to the long lane and the gel submitted to electrophoresis. The subsequent steps used for transfer to nitrocellulose are essentially those of the Western blot on 2D SDS-PAGE described above. The nitrocellulose blot was placed into a slot-blot device (Bio-Rad Laboratories) and individual serum samples were loaded into independent slots on the device. After 2 h,

the slots were washed in PBS-T, the device was disassembled and the nitrocellulose blot was placed in a tray containing PBS-T for additional washes. Blots were incubated with secondary antibody for 90 min and after washing with PBS-T were incubated with SuperSignal West Pico Chemiluminescent Substrate (Thermo Fisher) for protein detection and exposed to X-ray film. Band intensities were measured using ImageJ software by the National Institutes of Health <http://rsbweb.nih.gov/ij/>. In the case of a recombinant protein demonstrating more than one band of similar molecular weight, both were considered when calculating in band intensities.

Interferon-gamma release assay.

Whole heparinized blood was added in 300 µl volume to each well of a 96-well plate to evaluate the IFN- γ response to each recombinant protein. In addition, a whole-cell sonicate preparation and an envelope fraction of MAP were also added for comparison of protein reactivity in the assay and as controls to assess animal infection status. Concanavalin A (ConA; Sigma) and pokeweed mitogen (PWM; Sigma) were used as positive controls to validate cell reactivity. Each protein was tested in the concentrations of 10, 5 and 2.5 µg/ml and incubated for 18 h at 39°C in a humidified atmosphere with 5% CO₂. After incubation, plates were centrifuged for 5 min at 2500 x g and plasma samples were harvested to measure secreted IFN- γ . The Bovigam® (Prionics) ELISA assay was used to measure IFN- γ levels in antigen-stimulated plasma.

Statistical Analysis

Data analysis was performed using SAS 9.3 (SAS Institute Inc.). To analyze 2D western-blot data, Fisher's exact test was used. IFN- γ and slot blot results were analyzed with a one way ANOVA and linear combinations of means.

Results:

Protein Complexes found by Blue Native PAGE.

In this study, a total of seven putative protein complexes were observed in blue native PAGE gels, ranging from molecular weights of 119 to 996 kDa (Figure 1). Complexes I, II and V were most readily observed following Coomassie staining (Figure 1). To achieve these results, the detergents digitonin, Triton X-100 and *n*-dodecyl- β -D-maltoside (DDM) were compared as solubilizing agents at different concentrations. Digitonin at 0.5% was chosen as this was the lowest concentration where all complexes could be defined in blue native gels (data not shown) and because of its superior properties to disrupt annular lipids, which surround protein complexes (20). To identify the proteins present within each complex, complexes were denatured and run on 2D SDS-PAGE gels, but low resolution of proteins in 2D SDS-PAGE gels necessitated further optimization. Optimal results were obtained after samples were dialyzed and treated with benzonase to remove nucleic acids prior to running BN gels for subsequent 2D SDS-PAGE (data not shown). Several protocols were attempted to perform 2D SDS-PAGE, with the best protocol being a modification of that published by Schamel (13), requiring pre-incubation of samples in a 70°C water bath. Identification of proteins within complexes was performed by MS of excised bands from blue native gels (Figure

1, Table 1) and spots observed on 2D SDS-PAGE gels (Figure 2). A total of 29 spots were observed on 2D SDS-PAGE gels, 13 of which could be identified by MS (Table 2).

A summary of proteins found in each putative complex can be found in Table 1. Complex I was comprised of a cysteine desulfurase (MAP2120c) and major membrane protein (MAP2121c). This was confirmed by MS analysis of the representative band on the blue native gel (Table 1) as well as spots corresponding to the proteins found on the 2D SDS-PAGE gel (Figure 2, Table 2). Complex II was comprised of several proteins. Cfp29 (MAP0630c) was found in this complex along with a Dyp-type peroxidase family protein (MAP0631c). Other proteins found in complex 2 are involved in protein transport such as members of the Sec pathway (Sec D, Sec F) and members of the ABC transport system.

Members of the succinate dehydrogenase complex were found in complex III. Here the flavoprotein and iron-sulfur protein subunits of the complex, encoded by MAP3698c and MAP3967c respectively, were found. In complex VI, the protein glutamine synthetase (MAP1962) was observed to form a complex. Finally, complex VII was comprised of proteins involved in fatty acid synthesis, FadA2 (MAP3693), FadD15 (MAP1925) and FabG4 (MAP3692c).

Interactions of proteins within complexes were predicted by String 9.05 analyses. Among them were major membrane protein (MAP2121c) and cysteine desulfurase (MAP2120c) found in complex I (Figure 3). Others included Cfp29 (MAP0630c) and a dyp-type peroxidase family protein (MAP0631c) found in complex II and the proteins in

complex VII, FadA2 (MAP3693), FadD15 (MAP1925) and FabG4 (MAP3692c) (Figure 3).

Antigenicity of membrane complex proteins by 2D Western blot.

To identify antigenic proteins present within the envelope compartment of MAP, Western blots were performed using sera from 13 clinical, 9 subclinical and 10 control noninfected animals. Figure 4 contains immune blots representative of each infection stage of Johne's disease and serum reactivity for each protein is summarized in Table 3. Cysteine desulfurase (MAP2120c) garnered the most reactivity amongst all animals, reacting with sera from all clinical and control animals as well as 77.8% of subclinical animals. Several other proteins demonstrated antigenicity dependent upon the animal's stage of infection. Major membrane protein (MAP2121c) was recognized by 61.5% of animals with clinical paratuberculosis as opposed to 10% of control animals ($p < 0.05$) and 22.2% of subclinical animals. Interestingly, linocin/cfp29 (MAP0630c) had an opposite pattern of reactivity with 40% of control animals demonstrating antibodies to the protein in comparison to 7.6% of animals in the clinical stage of disease. Bacterioferritin (MAP1595c) was also found to be a strong, but not specific antigen showing reactivity in 92.3% of clinical, 55.6% of subclinical and 60% of control animals.

Cell mediated immune response to selected protein complex subunits.

Further evaluation of recombinant proteins in an IFN- γ assay demonstrated potential to discriminate animals in the early stage of infection. Most proteins demonstrated had significantly greater response in subclinical infected animals

compared to control noninfected animals and clinical cows (Figure 5). The proteins with the highest reactivity were cysteine desulfurase (MAP2120c) and phage shock protein A (MAP2855), followed by Cfp29/linocin (MAP0630c) and the 22kDa putative lipoprotein (MAP1138). Clinical animals in general had low reactivity to proteins, with the greatest reactivity being observed for phage shock protein A (MAP2855c). Control animals had low OD readings to most proteins, and the highest reactivity was observed for the 22kDa lipoprotein (MAP1138).

Humoral immune response to selected protein complex subunits.

Immuno-blot were performed with the recombinant proteins in an attempt to determine their antigenicity in the context of infection. In this analysis, several proteins demonstrated higher band intensities amongst the clinical group as compared to control animals and subclinical animals (Table 3). This is evident by the contrasting band intensities between these groups of proteins Acyl-CoA dehydrogenase (MAP0150) ($p < 0.05$) and 22 kDa lipoprotein (MAP1138c) ($p < 0.05$). Clinical animals had an average band intensity of 3,402 for Acyl-CoA dehydrogenase, while the corresponding values in the control and subclinical groups were 413 and 455, respectfully. For 22 kDa lipoprotein, the average among clinical animals was 708 in contrast to 2 found in the control group. In general, subclinical animals had low band intensity indicating negligible antibody to proteins. Two exceptions were phage shock protein A (MAP2855c), with an average band intensity of 1,706 and putative ATPase (MAP3844) with a band intensity of 1,506.

Discussion.

Using blue native PAGE and MS, putative membrane protein complexes of MAP were found and putative component proteins identified. This is the first study to characterize protein complexes in the envelope of MAP. Proteins that are co-located in a single protein complex can be reasonably thought of as interacting with each other at some level. Some interactions are fairly obvious, such as the MAP3698c and MAP3697c, which both encode subunits of the succinate dehydrogenase complex. Others need to be studied further to understand what the interaction means biologically (i.e. MAP2120c and MAP2121c). In this study, a total of seven putative protein complexes were identified. These results add another layer of detail to the organization of the mycobacterial cell wall.

Complex I was found to contain major membrane protein (MMP) encoded by MAP2121c, a characterized surface exposed protein of MAP. MMP has been shown to be involved in invasion of epithelial cells by MAP and to be recognized by sera of animals with paratuberculosis (21). Here we show that MMP forms a protein complex with a probable cysteine desulfurase (MAP2120c), an enzyme that removes elemental sulfur from cysteine for biosynthesis of a variety of co-factors (22). This enzyme is classified as a group II desulfurase based on the consensus sequence (RAGHHCA) around the conserved Cys625 (22). The Cys625 expressed from MAP2120c is the critical catalytic residue based on studies performed with other bacterial desulfurases (23). The inherent toxicity of free sulfide suggests the biogenesis of sulfur-containing co-factors is mediated by specific protein complexes (22) and perhaps complex I

containing the major membrane protein. Furthermore, both these genes are arranged in tandem on the MAP chromosome (18), and could be present in the same operon.

A protein homologous to MMP has also been found in *M. leprae*. Patients with leprosy were demonstrated to have both an antibody and an IFN- γ secreting T-cell proliferative response to this antigen (24). More recently, Shin et al. (25) observed high antibody titers to MAV2054, a protein with 100% sequence homology to MMP, in patients with *M. avium-M. intracellulare* complex (MAC) pulmonary disease and pulmonary tuberculosis. Data from the present study also suggests that MMP is a major antigen of MAP, having elicited both an antibody and an IFN- γ response in infected animals.

Cysteine desulfurase (MAP2120c) showed the highest antibody recognition among animals across all infection stages and was among the highest in IFN- γ response. Collectively, these data suggest that complex I may be important in the pathogenesis of MAP and contain immunodominant antigens of this pathogen.

A protein in Complex II was Cfp29 (MAP0630c), the mycobacterial homologue of linocin, a bacteriocin first identified in *Brevibacterium linens* (26). Cfp29 was found in the culture filtrate as well as membrane fractions of *M. tuberculosis* and was demonstrated to be a strong T cell antigen triggering the release of large quantities of IFN- γ from memory effector cells isolated during the recall of protective immunity in the mouse model of TB infection (27). In this study, Cfp29 also demonstrated strong T cell responses, eliciting high IFN- γ responses in subclinical animals. Also in complex II, a dye-decolorizing peroxidase (Dyp) type protein (MAP0631c) that is part of a novel

family of heme peroxidases was found. Although little research has been done regarding their function, this family of proteins appears to comprise bifunctional enzymes with hydrolase or oxygenase, as well as typical peroxidase activities (28). The interaction of these two proteins was predicted by String 9.05 due to co-occurrence in other organisms as well as tandem location of coding sequences within the genome. Considering the immune response to Cfp29 in animals infected with MAP characterized in this study, as well as the previous description of reactivity to this protein in tuberculosis infection (27), it is interesting to note that again an antigenic protein is found to be part of a complex. This provides clues as to the function of Cfp29 and how it may be structurally presented to the host during infection.

Proteins of the succinate dehydrogenase complex were identified in complex III. This 4-subunit complex contains proteins involved in the citric acid cycle and in oxidative phosphorylation. In this study, the flavoprotein (MAP3698c) and iron-sulfur (MAP3967c) subunits of the complex were found. Upon studying membrane complexes of *M. tuberculosis*, Zheng et al. (29) also found the flavoprotein and iron-sulfur subunits of this complex associated with the mycobacterial envelope. In the present study, another succinate dehydrogenase subunit was found encoded by MAP3443. Other subunits of the succinate dehydrogenase complex found in the genome have genes located in the same region and are encoded by MAP3442, MAP3441 and MAP3444. This suggests that MAP may contain two different succinate dehydrogenase complexes.

Glutamine synthetase (MAP1962) plays an essential role in the metabolism of nitrogen by catalyzing the reaction to convert glutamate and ammonia to form glutamine

and can form complexes of several identical subunits. In pathogenic mycobacteria, glutamine synthetase has been implicated as having a role in retarding phagosome acidification and phagosome–lysosome fusion (30). Additionally, it is believed to be involved in cell wall biosynthesis with the production of poly-L-glutamate–glutamine that is a major component of the cell wall in pathogenic mycobacteria (29), suggesting a major role in host-pathogen interactions during infection.

Several proteins had greater reactivity in the subclinical group as compared to clinical animals and control animals in the IFN- γ assay, suggesting they may be good diagnostic targets when used in this assay. Among these proteins was phage shock protein A (MAP2855). This protein is part of the phage-shock protein response (Psp), a conserved system of many bacteria to respond to extracellular stress. In some pathogens such as *Salmonella typhimurium*, phage shock protein A (PspA) has been demonstrated to be essential for virulence and survival of the bacterium inside the macrophage (30). This protein demonstrated high reactivity in subclinical animals even at the lowest concentration (data not shown).

MAP3290c encodes Mpt64, a protein characterized as an immune-dominant secreted antigen from *M. tuberculosis*. Several diagnostic assays for human tuberculosis have been developed using this protein, including immune-chromatographic assays to test for the protein in bacterial cultures, immunohistochemistry to identify the protein in tissues, and ELISA for detection of serum antibodies in infected patients (31). In the present study, Mpt64 was shown to be a strong T cell antigen with IFN- γ responses, as well as high reactivity in Western blots, demonstrating promise as a candidate for

diagnostic development. Chen et al. (32) investigated a mutant strain of MAP with a MAP3290c gene deletion as an attenuated vaccine for paratuberculosis. The deletion resulted in a more rapid elimination of the bacterium in mice in comparison to the wild-type strain, suggesting Mpt64 has an important role in pathogenesis.

The present study is the first to investigate protein complexes in the envelope of MAP. Seven putative protein complexes were found along with the identification of several novel antigenic proteins. The finding that some proteins such as MMP (MAP2121c) and Cfp29 (MAP0630c) are part of complexes provides some information as to their interactions with other proteins and possible associations with bacterial virulence. Some proteins, such as MMP (MAP2121c) demonstrated antigenicity dependent upon stage of infection, suggesting they are differentially regulated during the course of infection. This study illuminates an important compartment of MAP, the cell envelope, that is crucial for the pathogenesis of the bacterium and likely holds the initial antigens the host encounters upon infection.

References:

- 1. Stabel, J.** 1998. Johne's disease: a hidden threat. *J Dairy Sci.* 81:283-8.
- 2. Lombard J.E.** Epidemiology and economics of paratuberculosis. 2011. *Vet Clin North Am Food Anim Pract.* 27: 525-35.
- 3. Facciuolo A., Kelton D.F., Mutharia L.M.** 2013. Novel secreted antigens of *Mycobacterium paratuberculosis* as serodiagnostic biomarkers for Johne's disease in cattle. *Clin Vaccine Immunol.* 2013 Oct 2. [Epub ahead of print]
- 4. Scott M.C., Bannantine J.P., Kaneko Y., Branscum A.J., Whitlock R.H., Mori Y., Speer C.A., Eda S.** 2010. Absorbed EVELISA: a diagnostic test with improved specificity for Johne's disease in cattle. 7:1291-6.

5. **Stabel, J.R.** 2006. Host responses to *Mycobacterium avium* subsp. *paratuberculosis*: a complex arsenal. *Anim. Health Res. Rev.* 7:61-70.
6. **Niederweis M, Danilchanka O, Huff J, Hoffmann C, Engelhardt H.** 2010. *Mycobacterial outer membranes: in search of proteins.* *Trends Microbiol.* 18:109-16.
7. **He Z., De Buck J.** 2010. Localization of proteins in the cell wall of *Mycobacterium avium* subsp. *paratuberculosis* K10 by proteomic analysis. *Proteome Sci.* 8;8:21.
8. **Kleinnijenhuis J., Oosting M., Joosten L.A.B., Netea M.G., Van Crevel R.** 2011. Innate Immune Recognition of *Mycobacterium tuberculosis*. *Clin. and Dev. Immunol.* 2011 doi: 10.1155/2011/405310.
9. **Deng W., Xie J.** 2012. Ins and Outs of *Mycobacterium tuberculosis* PPE Family in Pathogenesis and Implications for Novel Measures Against Tuberculosis. *J Cell Biochem* 113: 1087–1095.
10. **Dresler J., Klimentova J., Stulik J.** 2011. Bacterial protein complexes investigation using blue native PAGE. *Microbiol. Res.* 166: 47-62.
11. **Radosevich T. J., Reinhardt T.A., Lippolis J.D., Bannantine J.P., Judith R. Stabel, J.R.** 2007. Proteome and Differential Expression Analysis of Membrane and Cytosolic Proteins from *Mycobacterium avium* subsp. *paratuberculosis* Strains K-10 and 187. *J Bacteriol.* 189: 1109–1117.
12. **Schägger H., Jagow G.** 1991. Blue native electrophoresis for isolation of membrane protein complexes in enzymatically active form. *Anal Biochem.* 199:223-31.
13. **Schamel W.W.** 2008. Two-dimensional blue native polyacrylamide gel electrophoresis. *Curr Protoc Cell Biol.* doi: 10.1002/0471143030.cb0610s38
14. **Reinhardt, T. A., Lippolis J.D., Nonnecke B.J., Sacco R.E.** 2012. Bovine milk exosome proteome. *J. Proteomics* 75: 1486-1492.
15. **Keller A, Nesvizhskii AI, Kolker E, Aebersold R.** 2002. Empirical statistical model to estimate the accuracy of peptide identifications made by MS/MS and database search. *Anal Chem.* 74: 5383-92.
16. **Nesvizhskii AI, Keller A, Kolker E, Aebersold R.** 2003. A statistical model for identifying proteins by tandem mass spectrometry. *Anal Chem.* 75: 4646-58.

- 17. Bannantine J.P., Stabel J.R., Bayles D.O., Geisbrecht B.V.** 2010. Characteristics of an extensive *Mycobacterium avium* subspecies *paratuberculosis* recombinant protein set. *Protein Expr Purif* 72: 223–233.
- 18. Li L., Bannantine J.P., Zhang Q., Amonsin A., May B., Alt D., Banerji N., Kanjilal S., Kapur V.** 2005. The complete genome sequence of *Mycobacterium avium* subspecies *paratuberculosis*. *Proc Natl Acad Sci U S A* 102: 12344–12349.
- 19. Bannantine J.P., Paustian M.L.** 2006. Identification of diagnostic proteins in *Mycobacterium avium* subspecies *paratuberculosis* by a whole genome analysis approach, *Methods Mol. Biol.* 345: 185–196.
- 20. Reisinger V., Eichacker L.A.** 2008. Solubilization of membrane protein complexes for blue native PAGE. *J Proteomics.* 71:277–83.
- 21. Bannantine J.P., Huntley J.F.J., Miltner E., Stabel J.R., Bermudez L.E.** 2003. The *Mycobacterium avium* subsp. *paratuberculosis* 35 kDa protein plays a role in invasion of bovine epithelial cells. *Microbiology* 149: 2061–2069.
- 22. Mihara H., Esaki N.** 2002. Bacterial cysteine desulfurases: their function and mechanisms. *Appl Microbiol Biotechnol.* 60:12–23.
- 23. Zheng L., White R.H., Cash V.L., Jack R.F., Dean D.R.** 1993. Cysteine desulfurase activity indicates a role for NIFS in metallocluster biosynthesis. *Proc. Natl. Acad. Sci. U S A.* 90:2754–8.
- 24. Triccas, J. A., Roche, P. W., Winter, N., Feng, C. G., Butlin, C. R. & Britton, W. J.** 1996. A 35-kilodalton protein is a major target of the human immune response to *Mycobacterium leprae*. *Infect Immun* 64 5171–5177.
- 25. Shin A., Lee K., Lee K.I., Shim T. S., Koh W., Jeon H.S., Son Y., Shin S., Kim H.** 2013. Serodiagnostic Potential of *Mycobacterium avium* MAV2054 and MAV5183 Proteins. *Clin Vaccine Immunol.* 20: 295–301.
- 26. Valdes-Stauber N, Scherer S.** 1996. Nucleotide sequence and taxonomical distribution of the bacteriocin gene *lin* cloned from *Brevibacterium linens* M18. *Appl Environ Microbiol.* 62: 1283–6.
- 27. Rosenkrands I, Rasmussen P. B., Carnio M., Jacobsen S., Theisen M., Andersen, P.** 1998. Identification and characterization of a 29-kilodalton protein from *Mycobacterium tuberculosis* culture filtrate recognized by mouse memory effector cells. *Infect Immun.* 66:2728–35.

28. **Sugano Y.** 2009. DyP-type peroxidases comprise a novel heme peroxidase family. *Cell Mol Life Sci.* 66 :1387-403.
29. **Zheng J., Wei C., Zhao L., Liu L., Leng W., Li W., Jin Q.** 2011. Combining blue native polyacrylamide gel electrophoresis with liquid chromatography tandem mass spectrometry as an effective strategy for analyzing potential membrane protein complexes of *Mycobacterium bovis* bacillus Calmette-Guérin. *BMC Genomics* , 12:40. doi: 10.1186/1471-2164-12-40.
30. **Harth G., Clemens D. L., Horwitz M.A.,** 1994. Glutamine synthetase of *Mycobacterium tuberculosis*: Extracellular release and characterization of its enzymatic activity. *Proc. Nat. Acad. Sci.* 91: 9342-9346.
31. **Chandra, H. Seemi Farhat Basir S.F., Gupta M., Banerjee N.** 2010. Glutamine synthetase encoded by *glnA-1* is necessary for cell wall resistance and pathogenicity of *Mycobacterium bovis*. *Microbiology* 156: 3669–3677.
32. **Darwin A.J.** 2013. Stress relief during host infection: the phage shock protein response supports bacterial virulence in various ways. *PLoS Pathogens* 9. doi: 10.1371/journal.ppat.1003388.
33. **Yin X, Zheng L, Lin L, Hu Y, Zheng F, Hu Y, Wang Q.** 2013. Commercial MPT64-based tests for rapid identification of *Mycobacterium tuberculosis* complex: A meta-analysis. *J Infect.* 67: 369-77.
34. **Chen J.W., Faisal S.M., Chandra S., McDonough S.P., Moreira M.A., Scaria J., Chang C.F., Bannantine J.P., Akey B., Chang Y.F.** 2012. Immunogenicity and protective efficacy of the *Mycobacterium avium* subsp. *paratuberculosis* attenuated mutants against challenge in a mouse model. *Vaccine* 30: 3015-25.

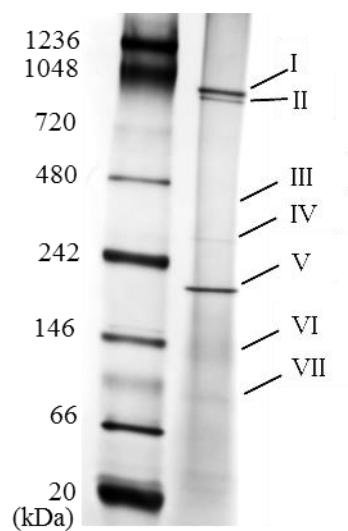


Figure 1. Blue native gel stained with Coomassie demonstrating the different complexes found.

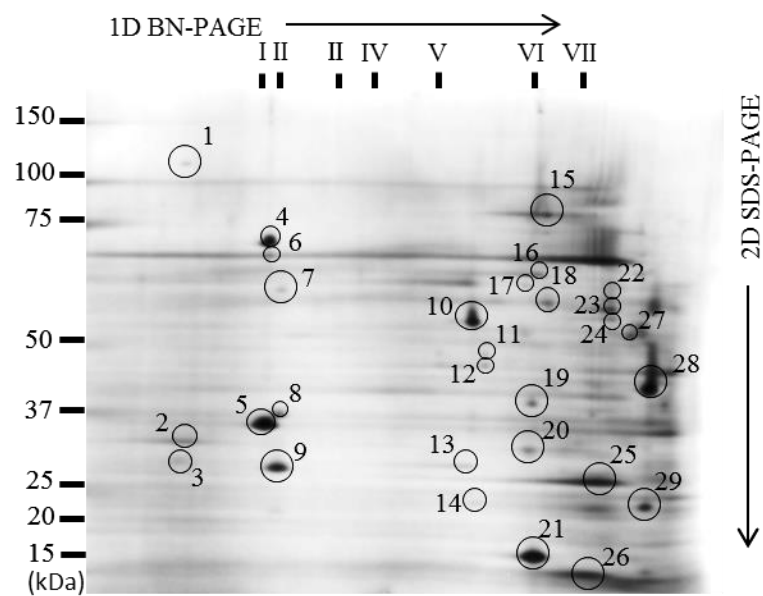


Figure 2. Second dimension SDS-PAGE gel with identified protein spots. Molecular weight ladder is marked on left. Roman numerals on top of gel indicate blue native gel bands.

Table 1. Summary of proteins identified by MS in each complex (band) of blue native gel.

Protein Description	Gene	Protein molecular weight (kDa)	Total number of spectra	Number of unique peptides	Percent sequence coverage	Predicted Trans-membrane Helices
Complex I						
Major membrane protein*	MAP_2121c	34	71	14	61.90	0
Probable cysteine desulfurase*	MAP_2120c	72	58	13	34.30	0
Complex II						
Linocin/Cfp 29*	MAP_0630c	29	110	17	76.20	0
Dyp-type peroxidase family	MAP_0631c	36	16	4	20.20	0
Putative RND superfamily drug exporter*	MAP_3641c	102	9	3	2.51	10
Putative exporter of polyketide antibiotics*	MAP_2561	56	5	2	6.03	12
Protein translocase subunit SecF*	MAP_1044	46	6	2	9.66	6
ABC-type multidrug transport system, ATPase component	MAP_3465	85	5	2	3.41	6
Daunorubicin resistance ABC transporter ATP-binding subunit	MAP_1238c	33	4	2	6.98	0
Arabinose efflux permease family protein	MAP_1596	72	3	2	4.70	13
Type VII secretion integral membrane protein EccD	MAP_1510	53	3	2	5.77	11

Table 1. continued

Transport protein	MAP_1240c	105	2	2	2.28	12
Complex III						
Succinate dehydrogenase/fumarate reductase flavoprotein subunit*	MAP_3698c	71	86	22	38.50	0
FadA2	MAP_3693	47	14	3	11.60	0
Succinate dehydrogenase and fumarate reductase iron-sulfur protein*	MAP_3697c	29	29	8	37.90	0
SppA*	MAP_4188	63	37	11	26.20	0
Putative uncharacterized protein	MAP_3699c	32	8	3	12.00	5
Complex IV						
Succinate dehydrogenase, flavoprotein subunit*	MAP_3443	64	15	4	7.02	0
Rieske Fe-S protein*	MAP_1934	44	11	3	11.70	3
3-oxoacyl-(Acyl-carrier protein) reductase*	MAP_2332c	328	4	2	0.84	0
Glycerol-3-phosphate dehydrogenase*	MAP_3423c	63	5	3	5.14	0
Preprotein translocase, SecE subunit*	MAP_4110	16	5	2	15.60	1
Complex V						
Bacterioferritin	MAP_1595	18	45	9	61.60	0
Isocitrate lyase*	MAP_1643	85	26	10	17.20	0
Fe-S oxidoreductase*	MAP_3831c	103	12	3	5.42	5

Table 1. continued

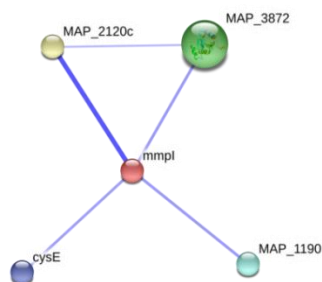
Putative uncharacterized protein*	MAP_0212	70	28	7	15.90	2
Pyridoxal biosynthesis lyase PdxS	MAP_2710c	32	17	5	23.10	0
Putative membrane protein	MAP_1016c	65	9	2	3.70	5
Putative uncharacterized protein	MAP_1689	44	6	3	9.98	0
Complex VI						
Glutamine synthetase*	MAP_1962	54	20	6	19.00	0
Complex VII						
FadA2*	MAP_3693	47	31	8	24.80	0
FadD15*	MAP_1925	65	13	3	7.33	0
FabG4	MAP_3692c	47	11	3	10.40	0
FadE25_2*	MAP_0150c	44	202	17	54.30	0
FadE3	MAP_3651c	41	4	2	8.38	0
Putative uncharacterized protein*	MAP_3972c	37	8	2	11.40	1
ATP synthase subunit alpha	MAP_2453c	60	9	3	9.03	0
Glycosidase	MAP_2433	77	18	6	12.50	0
22 kDa lipoprotein	MAP_1138c	24	17	4	21.80	0

Gel diffusion was observed with some proteins being found in more than one complex, when this occurred a * is marked next to the protein. Proteins were assigned to complexes based on presence on that band and higher number of spectra present within the assigned band. The full list of all identified proteins and three replicate MS runs can be found in supplemental file S1.

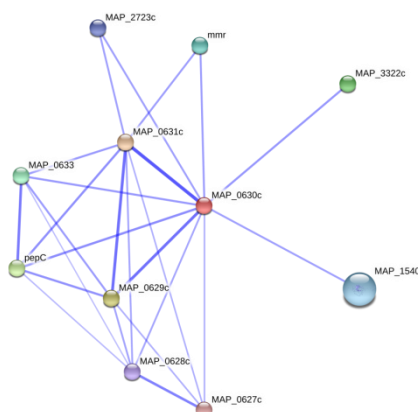
Table 2. Identified proteins by MS on 2D SDS-PAGE gels.

Spot ID	Protein Description	Gene	Protein molecular weight (kDa)	Number of unique peptides	Percent sequence coverage
2	Phage shock protein A	MAP_2855c	29	2	10.50
4	Probable cysteine desulfurase	MAP_2120c	71	3	7.60
5	Major membrane protein	MAP_2121c	33	8	38.10
9	Linocin/CFP29	MAP_0630c	28	4	16.60
10	Putative uncharacterized protein	MAP_3290c	21	2	13.20
15	Acyl-CoA dehydrogenase	MAP_4214c	41	2	16.30
17	Non-ribosomal peptide synthase	MAP_3482	73	2	3.65
18	grpE	MAP_3841	23	2	28.60
20	Putative ATPase	MAP_3844	154	2	2.44
21	Bacterioferritin	MAP_1595	18	7	58.50
23	Adenosine deaminase (Fragment)	MAP_2443	54	2	8.08
25	Methyltransferase, cyclopropane fatty acid synthase	MAP_3963	32	2	13.60%
28	Acyl-CoA dehydrogenase	MAP_0150c	43	3	8.44%

A)



B)



C)

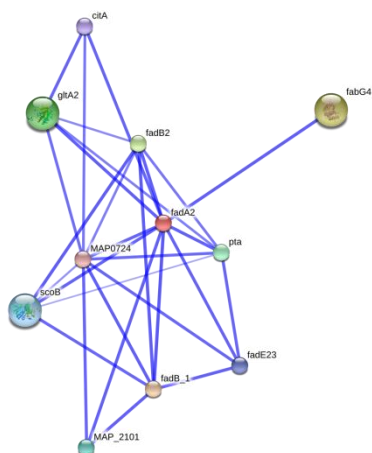


Figure 3. Confidence view generated by String 9.05 software of interaction between A) probable cysteine desulfurase (MAP2120c) and major membrane protein (mmpI), B) Cfp29 (MAP0630c) and Dyp-type peroxidase family protein (MAP0631c), C) FadA2 (MAP3693), FadD15 (MAP1925) and FabG4 (MAP3692c). The stronger predicted association between proteins is represented by thicker lines.

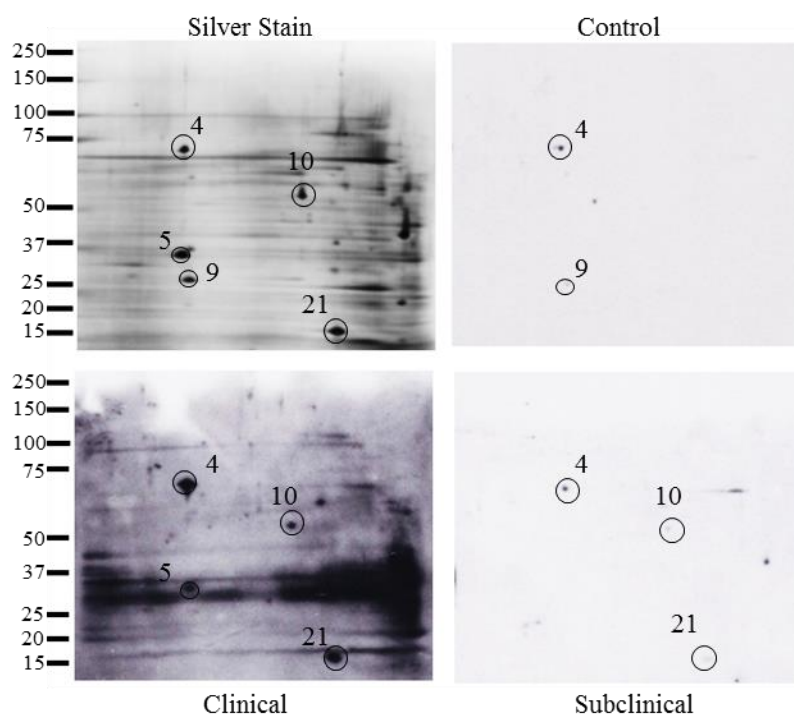


Figure 4. Representative western-blot of each group along with silver stain reference 2D gel. Main protein spots recognized are identified. Spot 4: Cysteine desulfurase (MAP2120c), 5: Major membrane protein (MAP2121c), 9: Cfp29 (MAP0630c), 10: Mpt64 (MAP3290c), 21: Bacterioferritin (MAP1595c).

Table 3. Protein spots reactive on 2D gels revealed by Western-blot with sera from control (n=10), subclinical (n=9) and clinical (n=13) non-infected animals.

Spot number, protein description and coding sequence	Control Cows % positive ^a	Sub Clinical Cows % positive ^a	Clinical cows % positive ^a
4, Probable Cysteine desulfurase, MAP2120c	100 (10/10)	77.8 (7/9)	100 (13/13)
21, Bacterioferritin, MAP1595c	60 (6/10)	55.6 (5/9)	92.3 (12/13)
10, Mpt64, MAP3290c	40 (4/10)	44.4 (4/9)	61.5 (8/13)
5, Major Membrane Protein, MAP2121c	10 (1/10)	22.2 (2/9)	61.5 (8/13)
33, No ID	20 (2/10)	22.2 (2/9)	15.4 (2/13)
1, No ID	20 (2/10)	33.3 (3/9)	38.5 (5/13)
28, Acyl-CoA dehydrogenase, MAP0150	20 (2/10)	33.3 (3/9)	7.6 (1/13)
6, No ID	0 (0/10)	11.1 (1/9)	7.6 (1/13)
20, Putative ATPase, MAP3844	0 (0/10)	0 (0/9)	15.4 (2/13)
9, Linocin/Cfp29, MAP0630c	40 (4/10)	33.3 (3/9)	7.6 (1/13)

^a % positive= number of serum samples that reacted positively on Western-blot of total serum samples in that infection group.

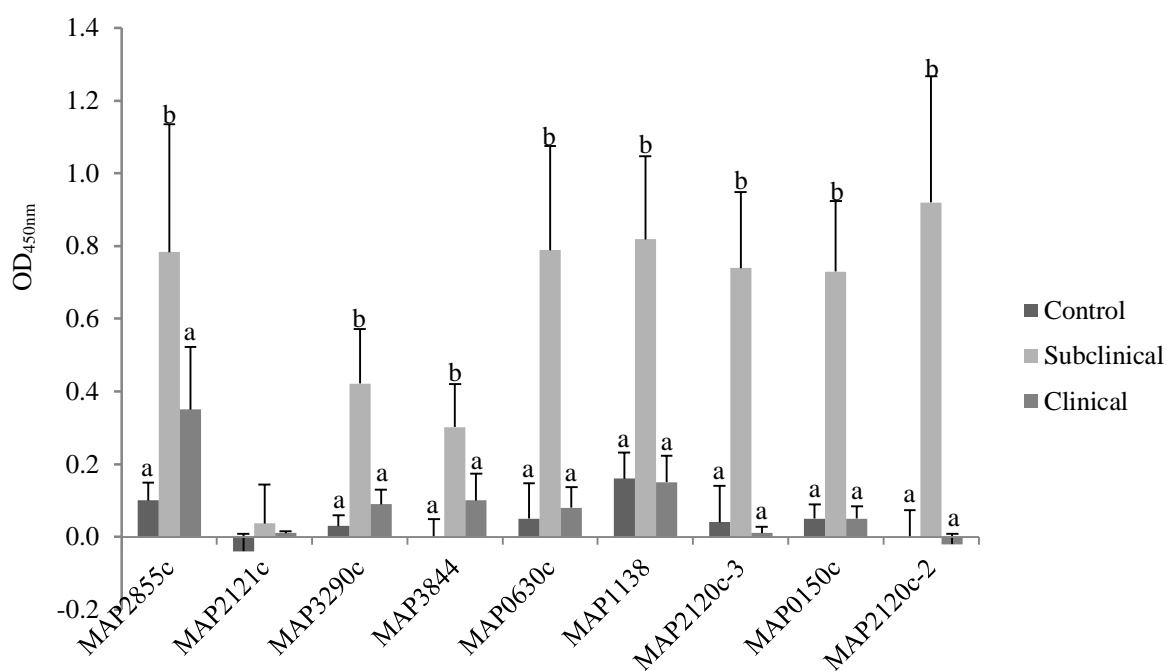


Figure 5. Interferon gamma release assay of recombinant proteins tested at 10µg/ml with animals of clinical (n=6), subclinical (n=5) and noninfected control (n=6). OD readings of responses to proteins with positive values after correcting for MBP and medium to the stimulation. Error bars represent standard error of the mean. Different letters indicate statistical significance ($p < 0.05$).

Table 4. Band intensity of proteins in slot blots with control (n=5), subclinical (n=7) and clinical (n=5) non-infected animals.

Protein ID	Control	Subclinical	Clinical
Cysteine desulfurase-2 (MAP2120c)	2,389 (\pm 711)a	330 (\pm 216)a	9,758 (\pm 3096)a
Cysteine desulfurase-3 (MAP2120c)	708 (\pm 343)a	181 (\pm 101)a	6,958 (\pm 2741)a
Linocin/Cpf59 (MAP0630c)	17 (\pm 16)b	398 (\pm 280)b	2,449 (\pm 914)a
Bacterioferritin (MAP1595)	2,379 (\pm 1032)a	196 (\pm 194)a	6,931 (\pm 3421)a
Major membrane protein (MAP2121c)	1,019 (\pm 571)a	413 (\pm 155)a	6,303 (\pm 3024)a
Acyl-CoA dehydrogenase (MAP0150)	413 (\pm 268)b	455 (\pm 448)b	3,402 (\pm 1403)a
Putative ATPase (MAP3844)	1,015 (\pm 920)a	1,506 (\pm 1197)a	3,573 (\pm 2487)a
Mpt64 (MAP3290c)	4,542 (\pm 4466)a	72 (\pm 48)a	944 (\pm 925)a
Phage shock protein A (MAP2855c)	121 (\pm 77)a	1,706 (\pm 846)a	5,116 (\pm 3768)a
22 kDa lipoprotein (MAP1138c)	2 (\pm 1.8)b	12 (\pm 7.2)b	708 (\pm 708)a
MAP complete homogenate	51 (\pm 23.84)b	1900 (\pm 1869)a	5356 (\pm 2201)a
MAP envelope preparation	999 (\pm 522)a	1274 (\pm 555)a	9066 (\pm 3365)a

Averages followed by standard error of the mean in parenthesis. Different letters indicate statistical significance ($p < 0.05$)

Band intensity of each animal was measured after subtracting background of maltose binding protein control reactivity, if a negative value was obtained it was substituted with the value of zero. Averages represent the band intensities of all animals in each infectious stage category.

CHAPTER 3. ZAP-70, CTLA-4 and proximal T cell receptor signaling in cows infected with *Mycobacterium avium* subsp. *paratuberculosis*

Modified from a paper to be submitted to Infection and Immunity

Fernando L. Leite^a, Bruce Pesch^b, John P. Bannantine^b, Timothy A. Reinhardt^b,
Judith R. Stabel^b

Department of Veterinary Microbiology and Preventive Medicine, Iowa State
University, Ames, IA 50011^a; USDA-ARS, National Animal Disease Center, Ames, IA
50010^b.

Abstract.

Paratuberculosis is a chronic intestinal disease of ruminant animals caused by *Mycobacterium avium* subsp. *paratuberculosis* (MAP). A hallmark of paratuberculosis is a transition from a cell-mediated Th1 type response to a humoral Th2 response with the progression of disease from a subclinical to clinical state. The objective of this study was to investigate the expression of two crucial molecules in T cell function, ZAP-70 (zeta-chain associated protein of 70 kDa) and CTLA-4 (cytotoxic T-lymphocyte antigen-4), in cows naturally infected with MAP. Peripheral blood mononuclear cells (PBMCs) isolated from control non-infected cows (n=5), and cows in clinical (n=6) and subclinical stages of paratuberculosis (n=6) were cultured alone (medium only), with concanavalin A, and a whole cell sonicate of MAP for 24, 72 and 144 hours to measure

the dynamic changes of ZAP-70 and CTLA-4 expression on CD4, CD8, and gamma delta ($\gamma\delta$) T cells. Flow cytometry was also performed to measure ZAP-70 phosphorylation to examine proximal T cell receptor signaling in animals of different disease status. It was found that the surface expression of CTLA-4 is dramatically increased in animals in subclinical stage of infection while levels of ZAP-70 are significantly decreased in CD4⁺ T cells of both subclinical and clinical animals, indicating a change in T cell phenotype with disease state. Interestingly, proximal T cell receptor signaling was not altered in infected animals. This study demonstrates changes in crucial signaling molecules in animals infected with MAP elucidating T cell alterations that are associated with disease progression.

Introduction.

Paratuberculosis, also called Johne's disease, is a disease of ruminant animals caused by the bacterium *Mycobacterium avium* subsp. *paratuberculosis* (MAP). Paratuberculosis is a chronic enteric disease with high economic impact in US dairy cattle, where it can cause decreased milk production, lead to early culling of animals, and reduce fertility rates (1). The disease is primarily subclinical, and clinical signs such as diarrhea and weight loss can take from 2 to 5 years to manifest (2). The disease has worldwide distribution in most ruminant species, and prevalence of paratuberculosis at the dairy herd level in the US is estimated to be 91.1% (3).

Infection of ruminant animals occurs primarily via exposure to contaminated feces or ingestion of colostrum/milk from infected dams (2). Upon infection, MAP

passes through the M cells in the small intestine where it is phagocytized by macrophages within the submucosa (4). Initially, animals control infection with a Th1 response predominated by secretion of cytokines such as IFN- γ that activate macrophages to allow killing of the intracellular bacterium (5). As disease progresses and clinical manifestations begin to occur, there is a shift from a cell-mediated Th1 to a non-protective Th2 response characterized by antibody titers to MAP. The molecular mechanisms underlying this transition are poorly understood (6). Previous research has also found that cells isolated from animals with clinical disease neither secrete IFN- γ when stimulated with MAP antigen, nor proliferate or respond to T cell mitogens such as concanavalin A (7,8). This suggests that there are other mechanisms involved in T cell function during the progression of disease other than simply the shift to a Th2 response, and these may include the induction of tolerance and anergy/hypofunction of T cells.

ZAP-70 (zeta-chain associated protein of 70 kDa) and CTLA-4 (cytotoxic T-lymphocyte antigen-4) are two critical components of the T cell that are involved in modulation of host immune responses (9,10). Upon engagement of the T cell receptor with an antigen presented by a MHC molecule of an antigen presenting cell, ZAP-70 is directed to ITAMS (immuno-receptor tyrosine-based activation motifs) of the zeta chain of the CD3 receptor, after which it is activated by phosphorylation and invokes downstream signaling molecules of the T cell leading to its full activation (9). Depletion studies have demonstrated that in the absence of ZAP-70 a functional immune synapse cannot occur, resulting in retardation of cell activation with subsequent impacts on ability of the cell to secrete cytokines or carry out effector functions (11). CTLA-4 is

regarded as a major negative regulator of T cell responses and its co-ligation with the T cell receptor (TCR) can induce anergy (12). Its inhibitory function occurs by engagement of B7 ligands (CD80/CD86) expressed on antigen presenting cells, resulting in inhibition of cytokine production and T cell proliferation (13). These two molecules work together to either allow T cell activation (ZAP-70) or to abrogate T cell responses (CTLA-4).

The present study was designed to measure signaling molecules of T cell activation, ZAP70 and CTLA-4, through flow cytometry in cows in different stages of disease. Mechanisms of cellular activation were further explored by quantifying the phosphorylation of ZAP70 following activation of cells to determine if the signaling cascade was compromised. This is the first study to examine these positive and negative T cell regulators in Johne's disease. Our findings suggest these molecules may be responsible for the immune shift that occurs in progression from subclinical to clinical Johne's disease.

Materials and Methods.

Animals.

Holstein dairy cows used in this study were placed in three groups based on stage of disease. This consisted of noninfected healthy cows (n = 5), cows naturally infected with *M. avium* subsp. *paratuberculosis* but asymptomatic (n = 6) (i.e., subclinical stage), and cows with clinical signs of paratuberculosis (n = 6). Animals were classified as clinical or subclinical based upon results from interferon gamma release assay, serum antibody, and fecal culture. On average, cows in the study were 6 years of age with 3-4

lactation periods. All animals were housed at the National Animal Disease Center (Ames, IA). Cows infected with MAP were housed separately from healthy control cows to prevent cross-contamination between groups. All animal-related procedures were approved by the IACUC of the National Animal Disease Center (Ames, IA).

Blood collection, culture conditions, and sample collection.

Blood was collected from the jugular vein in 2X acid citrate-dextrose solution (1:10) and used for isolation of peripheral blood mononuclear cells (PBMCs) from the buffy coat as previously described (14). These cells were resuspended to 2×10^6 cells/ml in complete RPMI-1640 medium (Life technologies, Carlsbad, CA) supplemented with 100 units/mL of penicillin, 100 μ g/mL of streptomycin, and 0.25 μ g/mL of Fungizone® (Gibco, Carlsbad, CA). Cell culture was performed in 6 well flat-bottomed plates at 39°C in 5% CO₂ in a humidified atmosphere. In vitro treatments consisted of no stimulation (NS; medium only), concanavalin A (ConA) (10 μ g/ml; Sigma St. Luis, MO), and whole-cell sonicate of MAP prepared as previously described (15) (MPS; 10 μ g /ml). Plates were incubated for 24, 72 and 144 hours and cells were harvested for flow cytometric analyses. During the last 5 hours of incubation a cocktail of 10 μ g/ml brefeldin A (Sigma), 1 μ g/ml ionomycin (Sigma) and 50 ng/ml PMA (Sigma) was added to enable intracellular measurement of IFN- γ .

Flow cytometric measurement of ZAP, pZAP70, CTLA-4, and IFN- γ .

Cells were gently removed from culture plates by pipetting and resuspending cultures in phosphate buffered saline (PBS). These were then counted on a Z2 Coulter Particle Count and Size Analyzer (Beckman Coulter). One million cells were added per

well in a 96 well round bottom plate (Corning Incorporated) followed by 50 μ l cocktail of primary antibodies to T cell surface markers CD4, CD8, gamma delta T cell receptor ($\gamma\delta$ TCR) (WSU Monoclonal Antibody Center) and CTLA-4 (Ancell) (Table 1). After a 15 min incubation at room temperature (RT), plates were centrifuged for 2 min at 400 x g, the supernatant was decanted, and 50 μ l of a secondary antibody cocktail was added, including PE-Cy7 anti-mouse IgM (5 μ l/ml; Southern Biotech), APC Cy7 anti-mouse IgG2b (7 μ l/ml; Southern Biotech), Alexa Fluor 350 anti-mouse IgG1 (25 μ l/ml; Life Technologies). After incubation for 15 min at RT, plates were centrifuged as described above then fixed and permeabilized following manufacturer's instructions with the Cytotfix/Cytoperm solution (BD Biosciences). Cells were washed twice with Perm/Wash buffer (BD Biosciences), followed by intracellular staining for 30 min at 4°C for the molecules ZAP-70, phosphorylated ZAP-70 (pZAP-70), and IFN- γ . After another two washes with Perm/Wash buffer (BD Biosciences) cells were resuspended in PBS with 0.4% sodium azide for flow cytometric analysis. Samples were evaluated using 10,000 events per sample, using a FACScan flow cytometer (CellQuest software; Becton, Dickinson). Analyses were conducted by gating on live cells based upon forward and side scatter characteristics (FlowJo; Tree Star). Due to the low level of live cells in the ConA treatment at 144 hr culture this treatment was not considered for analysis.

Phospho flow cytometric analysis of pZAP-70.

To measure ZAP-70 phosphorylation during T cell activation, the technique of phospho flow cytometry was used following a modified protocol (16). Isolated PBMCs were plated at 2×10^6 /ml in 96 well round bottom plates in RPMI 1640 medium (Life

technologies) and allowed to rest for one hour at 39°C in 5% CO₂. No fetal bovine serum was present in the medium in order to reduce baseline ZAP-70 phosphorylation. T cell activation was performed with anti-CD3 (10 µg/ml; MM1A), MAP whole-cell sonicate (MPS; 10 µg/ml), and the inclusion of 11 mM hydrogen peroxide as a positive control to induce non-specific tyrosine phosphorylation. After addition of different treatments, cells were incubated for 15 min at 39°C in 5% CO₂ in a humidified atmosphere. This was followed by fixation of the cells to halt phosphorylation events with Cytofix/Cytoperm solution (BD Biosciences). After cells were fixed and permeabilized, cell staining followed the protocol of cultured cells for staining of pZAP-70 and ZAP-70 within CD4, CD8 and $\gamma\delta$ TCR T cells (Table 1). A substitution of CD8 clone MCA837 (Serotec) was made as the clone CACT80C (WSU Monoclonal Antibody Center) does not stain cells that have been previously fixed. A time trial determined that at 15 min the maximum cell activation as measured by ZAP-70 phosphorylation was achieved (data not shown), thus this was the time allowed for cell activation used for the experiments.

Statistical Analysis.

Data were analyzed using the PROC Mixed function of SAS 9.02 (SAS Institute, Cary, NC) 144hr culture was analyzed in a separate model because of the lacking ConA treatment and higher variance within samples. Two-sided $P < 0.05$ values were considered significant.

Results

T cell expression of Zap-70 after stimulation for 24, 72 and 144 hr.

After 24 h culture, both clinical and subclinical animals had significantly ($P < 0.05$) fewer ZAP-70 + CD4 T cells regardless of the in vitro treatment. This trend was also true for CD8 and $\gamma\delta$ T cells, although with less marked difference and without statistical significance (Figure 1). Expanding PBMC culture time to 72 and 144 hr resulted in increased percentages of CD4+ T cells expressing ZAP-70 for the clinical and subclinical groups to a level similar to non-infected animals after stimulation of cells with MPS (Figure 2a). However, this effect was not observed for pZAP-70 expression (Figure 2b). Further, differences in pZAP70 expression were not observed for CD8+ and $\gamma\delta$ TCR+ T cells regardless of animal treatment group (data not shown).

Analysis of CTLA-4 and IFN- γ expression in T cells of 24, 72 and 144 hr cultures.

Surface expression of CTLA-4 was measured in CD4, CD8, and $\gamma\delta$ T cell subsets throughout the different time points. In 24 hr cultures, the subclinical group had more CD4+ and CD8+ T cells expressing CTLA-4 than the clinical and control group (Figure 3). The marked difference observed in CTLA-4 expression between infection groups observed in CD4+ T cells is also demonstrated in flow cytometry density plots of Figure 5. The surface expression of CTLA-4 was negligible among $\gamma\delta$ T cells (Figure 3). In cultures of 72 and 144 hrs, the subclinical group maintained the trend of being the group with the highest CTLA-4 expression and the number of cells expressing CTLA-4 went down (Figure 3). Because this negative regulator of T cells is expressed at a higher level in subclinical cows, this could suggest that MAP utilizes this as an escape mechanism for survival in the host. Trends were harder to identify within intracellular IFN- γ

expression, although levels of this cytokine did increase over time within CD4⁺ T cells isolated from clinical and subclinical animals and stimulated with MPS (Figure 4).

Phospho flow cytometry and measurement of ZAP-70 phosphorylation.

To address proximal T cell receptor signaling and T cell activation, phospho flow cytometry was performed to measure phosphorylation of ZAP-70 following TCR (T Cell Receptor) engagement. This is one of the first events in the signaling cascade of T cells, and is necessary to promote cell activation and effector functions. Hydrogen peroxide was used as positive control and anti-CD3 antibody to measure the activation capacity of the cell in an antigen independent manner. Within the CD4⁺ cell subset, hydrogen peroxide was the treatment with the highest phosphorylation, followed by the anti-CD3 treatment; and both were statistically significant ($p < 0.05$) in relation to the NS treatment for the clinical and control groups (Figure 6). No statistical significance was observed between the MPS and NS treatments. In $\gamma\delta$ TCR + T cells, all animal groups responded to anti-CD3 and hydrogen peroxide treatments, with statistical significance to both in relation to the NS control. CD8⁺ cells were the only subset of the three T cell populations to have responded more to anti-CD3 antibody than hydrogen peroxide (Figure 6). And this treatment had statistically higher responses ($p < 0.05$) in relation to all treatments for control, subclinical and clinical animals.

Discussion

Studies in paratuberculosis have provided evidence towards anergy or T cell hypofunction with disease. Weiss et al. (7) studied the phenotype and response of mononuclear leukocytes from the ileum of cows naturally infected with MAP.

Lymphocytes isolated from the ileum of infected cows did not proliferate when incubated with MAP antigen, demonstrating a hyporesponsive state of these cells correlating with anergy (7). In a study to investigate the immune response to MAP in naturally and experimentally infected sheep, Begg et al. (8) found similar hyporesponsiveness in animals in more advanced stages of disease. Animals had decreased IFN- γ production and reduced ability to proliferate in response to MAP antigen and pokeweed mitogen (PWM). Interleukin-12 was also added to the cell cultures in an attempt to aid their stimulation; however, addition of the cytokine had no significant effects on the cellular responses (8). In paratuberculosis there are a limited number of studies that have addressed potential alterations within T cells and the events leading to clinical disease. Yet this information is critical to providing a better understanding of the disease as well as the possibility of more targeted approaches for vaccine and therapeutic development.

Leprosy is a mycobacterial disease that shares an analogous transitory immune response similar to paratuberculosis. Patients with early stage infection and tuberculoid leprosy possess a cell-mediated immunity (CMI) that is considered to be effective in controlling disease. While there is a transition to a Th2 type response with decreased CMI responses in patients as bacterial load increases and patients evolve to the more severe lepromatous leprosy phase in which clinical signs of disease become evident and T cell hypofunction has been observed (17). Kumar et al. (18) demonstrated that patients with advanced forms of leprosy had significantly less pZAP-70 and ZAP-70 present in their T cells. Along with this finding, Cbl-b was also shown to be upregulated

in diseased patients. Cbl-b is an ubiquitin ligase and potent negative regulator of T cell function that is present in most anergic T cells (19). By immunoprecipitation it was shown that ZAP-70 was associated with this molecule in T cells of diseased patients (18). Considering the importance of ZAP-70 in T cell signaling, it would be expected that the T cells identified as being ZAP-70 negative have a decreased potential for activation and effector function potentially being rendered anergic.

In the present study, the finding that cows infected with MAP had fewer ZAP-70 + T cells, especially CD4+ cells, is indicative of an immunological change in the cells of these animals. Several different mechanisms could be involved including protein interactions such as ubiquitination. With longer times in culture both subclinical and clinical animals had increased percentages of ZAP-70 + CD4+ T cells. This increase may be due to the death of cells that lacked ZAP-70 in culture or the loss of an inhibition factor leading to decreased expression of the molecule. Interestingly, the baseline levels of ZAP-70 phosphorylation remained lower among infected animals as compared to control non-infected animals throughout the different culture periods.

Expression of CTLA-4 on T cells was markedly increased in animals with subclinical paratuberculosis. The difference observed between subclinical and clinical animals as well as control non-infected animals was more prominent within the CD4+ population. Expression of CTLA-4 in $\gamma\delta$ T cells has been investigated in cattle, however with varied results. Howard et al. (20) did not find expression of CTLA-4 or the related CD28 molecule among bovine $\gamma\delta$ T cells, similar to the results of Hanrahan et al. (21) who found negligible expression of these molecules in sheep $\gamma\delta$ T cells. Blumerman et

al. (22) reported that the co-stimulation requirements of bovine $\gamma\delta$ T cells differ from CD4⁺ and CD8⁺ cells, and also did not find CD28 within bovine $\gamma\delta$ T cells, which is suggestive that a potential role of CTLA-4 among these cells could be different. This study however did find CTLA-4 mRNA within bovine $\gamma\delta$ T as did Fikri et al. (23).

Together this indicates that the expression of CTLA-4 within bovine $\gamma\delta$ T cells is likely variable, a probable reason why in this study very low expression of the molecule was found. Another aspect that needs to be considered is that previous studies did not measure CTLA-4 on the surface of cells as performed in this study, rather mRNA levels were measured, most of CTLA-4 is contained within the cell as surface expression is tightly regulated because of its impacts on T cell function (24). The decreased expression of the molecule over time observed in the different T cell subsets was expected. Previous studies in mice and human cells have demonstrated that upon T cell activation the maximal surface expression of CTLA-4 occurs following 48-72 hrs of cell activation, followed by reduced expression with longer incubation periods (25, 26). In this study, maximal expression was found at 24 hrs possibly due to a difference of the bovine species in comparison to mouse and human and/or stimulation conditions. It is interesting to note that the expression of IFN- γ followed a reciprocal pattern compared to CTLA-4 expression, with higher levels of intracellular IFN- γ attained as time in culture increased. This may be due to the negative effects CTLA-4 has on cytokine production. Specifically, blocking of the CTLA-4 receptor has been shown to increase IFN- γ production in T cells (27). CTLA-4 could induce lower levels of IFN- γ expression in animals with paratuberculosis, as may be suggested from the results of this study.

Perhaps it is not a coincidence that the CD4⁺ T cells were the subset with the highest CTLA-4 expression. This is the same population (T helper cell) that would be expected to play a bigger role in directing a Th1 type response through macrophage activation. Considering the effects that CTLA-4 has on T cell function, MAP may induce a higher expression of CTLA-4 in T cells of infected animals as an evasion strategy from the immune system to promote chronic infection. Interestingly, in patients with leprosy similar observations were made. Palermo et al. (28) found the same pattern of CTLA-4 expression in which patients with tuberculoid leprosy expressed significantly more CTLA-4 compared to lepromatous patients (28). As suggested in that study and in corroboration with data from this study, CTLA-4 expression may be involved in the induction of T cell hypofunction during early and mid-stages of infection, while likely other molecules could be involved in the maintenance of an anergic T cell state in the later stages of chronic infection. Programmed death-1 (PD-1) is a cell surface molecule that regulates adaptive immune response and is related to T cell exhaustion, a state that, contrary to anergy, is progressive, with dysfunction worsening overtime (29).

Also pertinent to paratuberculosis infection are other roles that CTLA-4 has been demonstrated to have in T cells, especially those of the Th1 phenotype. Oosterwegel et al. (30) demonstrated that CTLA-4 has a critical role in CD4⁺ T cell differentiation. In contrast to wild type mice, T cells from CTLA-4 knockout mice produced IL-4 during primary stimulation with cells differentiating into almost pure populations of Th2 cells (30). This study suggested that B7 binding to CTLA-4 blocks Th2 differentiation. Thus the expression of this molecule among the subclinical group may serve the purpose of

inhibiting a Th2 differentiation bias of these cells. Also regarding CD4⁺ T cell phenotypes, Knieke et al. (31) demonstrated that CTLA-4 has a positive effect on Th1 cell migration. It was found that crosslinking of CTLA-4 together with CD3 and CD28 stimulation on activated Th1 cells increased expression of the chemokine receptors CCR5 and CCR7, which in turn enhanced cell migration sites of inflammation two-fold over CTLA-4 negative counterparts. These results suggest that CTLA-4 can orchestrate specific migration of selected Th1 cells to sites of inflammation and antigenic challenge. This may provide an explanation of how animals in the subclinical stage can control infection if T cells expressing high levels of CTLA-4 are efficiently migrating to target sites of infection.

In addition, cells that express CTLA-4 have been shown to have extrinsic functions causing downregulation in other cells. This includes the induction of indoleamine 2,3 dioxygenase (IDO) activity in APCs, which leads to tryptophan catabolism that can inhibit other T cells from proliferating (32). This may also be an immune alteration caused by the increased CTLA-4⁺ T cells in animals infected with MAP as increased IDO activity has been described in animals with paratuberculosis (33).

The lack of changes in proximal T cell receptor signaling as measured by TCR activation and ZAP-70 phosphorylation between infected and control animals in this study is not necessarily surprising. Hanschen et al. (34) also used phospho flow cytometry to compare T cell receptor signaling among regulatory T cells (Treg) and non-Treg CD4⁺ cells. Interestingly, they found that T cell activation by anti-CD3 antibody

induced a response in ZAP-70 phosphorylation with higher magnitude in Tregs compared to non-Treg cells. Also, it was found that antigen-specific TCR stimulation did not significantly activate these signaling pathways, similar to what is reported here. Coussens et al. (35) reported an elevated number of Treg cells in PBMCs of animals infected with MAP but failed to discriminate between cows in subclinical or clinical stages of infection. The elevated number of Tregs present in infected animals may explain why there was no alteration in proximal T cell signaling in this study, with the clinical group yielding the highest phosphorylated ZAP-70 response in CD4⁺ T cells following anti-CD3 activation. Although not statistically significant, it was interesting to note differences between control and clinical animals in CD4⁺ cells, when comparing the anti-CD3 treatment to the hydrogen peroxide treatment. The hydrogen peroxide treatment, as a positive control, may represent the full potential of cells for ZAP-70 phosphorylation. When comparing the anti-CD3 to the hydrogen peroxide treatment, control animals had similar stimulation values for both treatments while in clinical animals the hydrogen peroxide treatment was markedly higher. This demonstrates that potentially clinical animals may have a decreased capacity of proximal T cell receptor signaling as the full potential of activation was not achieved with the anti-CD3 treatment. A subject for future investigation is if MAP has the ability to directly inhibit ZAP-70 phosphorylation as has been described in *M. tuberculosis*. Mahon et al. (36) demonstrated that pre-incubation of T cells with *M. tuberculosis* mannosylated lipoarabinomannan (Man-LAM) inhibits ZAP-70 phosphorylation, a mechanism likely due to insertion of Man-LAM into the membrane of target T cells. This may be a

possible mechanism of MAP as well, considering Man-LAM from this organism has also been shown to invoke cellular immunity (37).

This study investigated crucial molecules involved in T cell function in the context of paratuberculosis. Very few studies have addressed T cell function in paratuberculosis, especially T cell signaling events. Surprisingly, findings from this study correlate very well with findings from other studies in leprosy, suggesting the etiological agents of both diseases share similar mechanisms of immune evasion to cause chronic infection. This study for the first time discovered alterations in two crucial signaling molecules of the T cell in animals infected with MAP, shedding light into immune alterations that occur and possible triggers that lead to clinical paratuberculosis.

References

1. **Lombard JE.** 2011. Epidemiology and economics of paratuberculosis. *Vet. Clin. North Am. Food Anim. Pract.* 27:525-535.
2. **Stabel, JR.** 1998. Johne's disease: a hidden threat. *J. Dairy Sci.* 81:283-288.
3. **Lombard JE, Gardner IA, Jafarzadeh SR, Fossler CP, Harris B, Capsel RT, Wagner BA, Johnson WO.** 2013. Herd-level prevalence of *Mycobacterium avium* subsp. *paratuberculosis* infection in United States dairy herds in 2007. *Prev. Vet. Med.* 108:234-238.
4. **Bannantine JP, Bermudez LE.** 2013. No holes barred: invasion of the intestinal mucosa by *Mycobacterium avium* subsp. *paratuberculosis*. *Infect. Immun.* 81:3960-3965.
5. **Sweeney, RW.** 2011. Pathogenesis of Paratuberculosis. *Vet. Clin. North Am. Food Anim. Pract.* 27:537-546.
6. **Stabel, JR.** 2006. Host responses to *Mycobacterium avium* subsp. *paratuberculosis*: a complex arsenal. *Anim. Health Res. Rev.* 7:61-70.

7. **Weiss, DJ, Evanson OA, Souza CD.** 2006. Mucosal Immune Response in Cattle with Subclinical Johne's Disease. *Vet. Pathol.* 43:127-135.
8. **Begg DJ, de Silva K, Carter N, Plain KM, Purdie A, Whittington RJ.** 2011. Does a Th1 over Th2 dominance really exist in the early stages of *Mycobacterium avium* subspecies *paratuberculosis* infections? *Immunobiology* 216:840-846.
9. **Wang H, Kadlec TA, Au-Yeung BB, Goodfellow HE, Hsu LY, Freedman TS, Weiss A.** 2010. ZAP-70: an essential kinase in T-cell signaling. *Cold Spring Harb. Perspect. Biol.* 2:a002279. doi: 10.1101/cshperspect.a002279.
10. **Walker LS, Sansom DM.** 2011. The emerging role of CTLA4 as a cell-extrinsic regulator of T cell responses. *Nat. Rev. Immunol.* 25:852-863.
11. **Blanchard N, Di Bartolo V, Hivroz C.** 2002. In the immune synapse, ZAP-70 controls T cell polarization and recruitment of signaling proteins but not formation of the synaptic pattern. *Immunity.* 17:389-399.
12. **Schneider H, Valk E, Leung R, Rudd CE.** 2008. CTLA-4 activation of phosphatidylinositol 3-kinase (PI 3-K) and protein kinase B (PKB/AKT) sustains T-cell anergy without cell death. *PLoS One* 3(12):e3842. doi: 10.1371/journal.pone.0003842.
13. **Rudd CE, Taylor A, Schneider H.** 2009. CD28 and CTLA-4 coreceptor expression and signal transduction. *Immunol. Rev.* 229:12-26.
14. **Khalifeh MS, Stabel JR.** 2013. Clinical disease upregulates expression of CD40 and CD40 ligand on peripheral blood mononuclear cells from cattle naturally infected with *Mycobacterium avium* subsp. *paratuberculosis*. *Clin. Vaccine Immunol.* 20:1274-1282.
15. **Stabel JR, Waters WR, Bannantine JP, Lyashchenko K.** 2011. Mediation of host immune responses after immunization of neonatal calves with a heat-killed *Mycobacterium avium* subsp. *paratuberculosis* vaccine. *Clin. Vaccine Immunol.* 18:2079-2089.
16. **Haas A, Weckbecker G, Welzenbach K.** 2008. Intracellular Phospho-Flow cytometry reveals novel insights into TCR proximal signaling events. A comparison with Western blot. *Cytometry A* 73:799-807.
17. **Walker SL, Lockwood DN.** 2006. The clinical and immunological features of leprosy. *Br. Med. Bull.* 77-78:103-121.

18. **Kumar S, Naqvi RA, Khanna N, Rao DN.** 2011. Disruption of HLA-DR raft, deregulations of Lck-ZAP-70-Cbl-b cross-talk and miR181a towards T cell hyporesponsiveness in leprosy. *Mol. Immunol.* 48: 1178-1190.
19. **Venuprasad K.** 2010. Cbl-b and itch: key regulators of peripheral T-cell tolerance. *Cancer Res.* 8:3009-3012.
20. **Howard CJ, Sopp P, Brownlie J, Parsons KR, Kwong LS, Collins RA.** 1996. Afferent lymph veiled cells stimulate proliferative responses in allogeneic CD4+ and CD8+ T cells but not gamma delta TCR+ T cells. *Immunology* 88:558-564.
21. **Hanrahan CF, Kimpton WG, Howard CJ, Parsons KR, Brandon MR, Andrews AE, Nash AD.** 1997. Cellular requirements for the activation and proliferation of ruminant gammadelta T cells. *J. Immunol.* 159:4287-4294.
22. **Blumerman SL, Herzig CT, Wang F, Coussens PM, Baldwin CL.** 2007. Comparison of gene expression by co-cultured WC1+ gammadelta and CD4+ alphabeta T cells exhibiting a recall response to bacterial antigen. *Mol Immunol.* 44:2023-35.
23. **Fikri Y, Nyabenda J, Denis M, Pastoret PP.** 2000. Purification and characterization of bovine WC1+ gammadelta T lymphocytes from peripheral blood. *Vet. Res.* 31:229-239.
24. **Valk E, Rudd CE, Schneider H.** 2008. CTLA-4 trafficking and surface expression. *Trends Immunol.* 29:272-279.
25. **Walunas TL, Lenschow DJ, Bakker CY, Linsley PS, Freeman GJ, Green JM, Thompson CB, Bluestone JA.** 1994. CTLA-4 can function as a negative regulator of T cell activation. *Immunity.* 1:405-413.
26. **Wang XB, Zheng CY, Giscombe R, Lefvert AK.** 2001. Regulation of surface and intracellular expression of CTLA-4 on human peripheral T cells. *Scand. J. Immunol.* 54:453-458.
27. **Alegre ML, Shiels H, Thompson CB, Gajewski TF.** 1998. Expression and function of CTLA-4 in Th1 and Th2 cells. *J. Immunol.* 161: 3347–3356.
28. **Palermo Mde L, Trindade MÂ, Duarte AJ, Cacere CR, Benard G.** 2012. Differential expression of the costimulatory molecules CD86, CD28, CD152 and PD-1 correlates with the host-parasite outcome in leprosy. *Mem. Inst. Oswaldo Cruz* 107:167-173.

29. **Wherry EJ.** 2011. T cell exhaustion. *Nat. Immunol.* 12:492-499.
30. **Oosterwegel MA, Mandelbrot DA, Boyd SD, Lorscheid RB, Jarrett DY, Abbas AK, Sharpe AH.** 1999. The role of CTLA-4 in regulating Th2 differentiation. *J. Immunol.* 163:2634-2639.
31. **Knäuper K, Hoff H, Maszyńska F, Kolar P, Schrage A, Hamann A, Debes GF, Brunner-Weinzierl MC.** 2009. CD152 (CTLA-4) determines CD4 T cell migration *in vitro* and *in vivo*. *PLoS One* 4(5):e5702. doi: 10.1371/journal.pone.0005702.
32. **Walker LS, Sansom DM.** 2011. The emerging role of CTLA-4 as a cell-extrinsic regulator of T cell responses. *Nat. Rev. Immunol.* 11:852-863.
33. **Plain KM, de Silva K, Earl J, Begg DJ, Purdie AC, Whittington RJ.** 2011. Indoleamine 2,4-dioxygenase, tryptophan catabolism, and *Mycobacterium avium* subsp. *paratuberculosis*: a model for chronic mycobacterial infections. *Infect. Immun.* 79:3821-3832.
34. **Hanschen M, Tajima G, O'Leary F, Hoang K, Ikeda K, Lederer JA.** 2012. Phospho-flow cytometry based analysis of differences in T cell receptor signaling between regulatory T cells and CD4+ T cells. *J. Immunol. Methods* 376:1-12.
35. **Coussens PM, Sipkovsky S, Murphy B, Roussey J, Colvin CJ.** 2012. Regulatory T cells in cattle and their potential role in bovine paratuberculosis. *Comp. Immunol. Microbiol. Infect. Dis.* 35:233-239.
36. **Mahon RN, Sande OJ, Rojas RE, Levine AD, Harding CV, Boom WH.** 2012. *Mycobacterium tuberculosis* ManLAM inhibits T-cell-receptor signaling by interference with ZAP-70, Lck and LAT phosphorylation. *Cell Immunol.* 275:98-105.
37. **Souza C, Davis WC, Eckstein TM, Sreevatsan S, Weiss DJ.** 2013. Mannosylated lipoarabinomannans from *Mycobacterium avium* subsp. *paratuberculosis* alters the inflammatory response by bovine macrophages and suppresses killing of *Mycobacterium avium* subsp. *avium* organisms. *PLoS One* 8(9):e75924. doi: 10.1371/journal.pone.0075924.

Table 1. Primary antibodies used in study.

Target	IgG type	Working conc.	Clone	Fluorochrome used
CD4	IgM	10 µl/ml	CATC83B	PE-Cy7
CD8	IgG ₁	10 µl/ml	CACT80C	Alexa 350
CD8	IgG _{2a}	20 µl/ml	MCA837	Alexa 350
γδTCR	IgG _{2b}	10 µl/ml	GB21A	APC Cy7
CTLA-4*	IgG ₁	8 µl/ml	ANC152.2/8H5	PerCp
ZAP-70*	IgG ₁	10 µl/ml	1E7.2	Pacific Blue
IFN-γ*	IgG ₁	20 µl/ml	MCA1783PE	PE
pZAP-70*	Rabbit polyclonal	10 µl/ml	Polyclonal to Y319	Alexa488

* Directly conjugated. Surface marker antibodies were diluted in PBS with 0.4% sodium azide, intracellular markers ZAP-70, phosphorylated ZAP-70 (pZAP-70) and IFN-γ were diluted in BD Perm Wash Buffer. CTLA-4 conjugated to PerCp with the Easy link PerCP conjugation kit (Abcam, Cambridge, ENG). pZAP-70 conjugated to Alexa Fluor® 488 with the Alexa Fluor® 488 Antibody Labeling Kit (Life technologies, Carlsbad,CA).

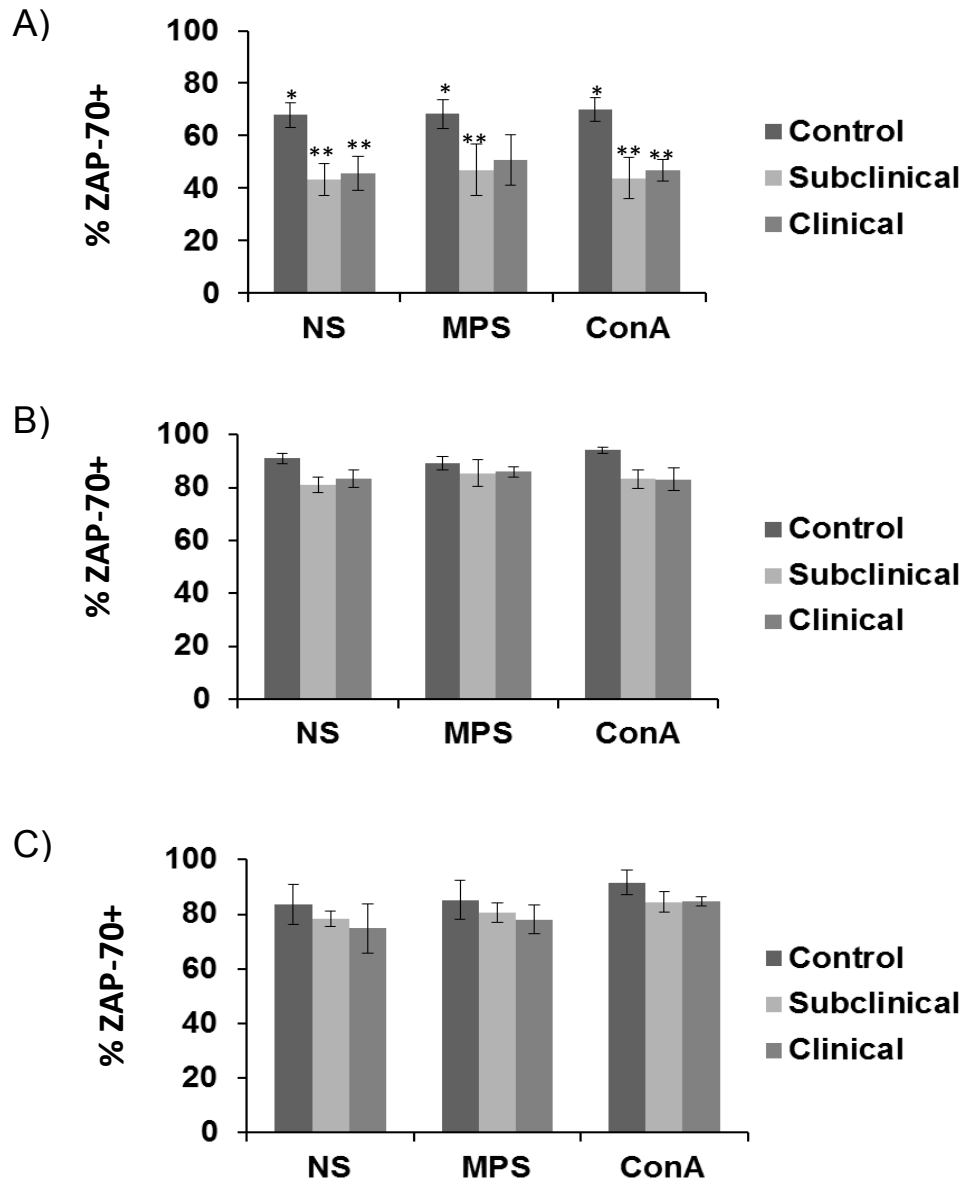


Figure 1. Expression of ZAP-70 studied in 24 hours cell culture obtained from healthy control cows and cows naturally infected with MAP in the subclinical and clinical stages of infection. A) CD4+ T cells. B) CD8+ T cells. C) $\gamma\delta$ TCR+ T cells. Data are presented as percentage of ZAP70+ T cells (mean \pm SEM). Significant differences between treatment groups are designated by asterisk *, ** ($P < 0.05$).

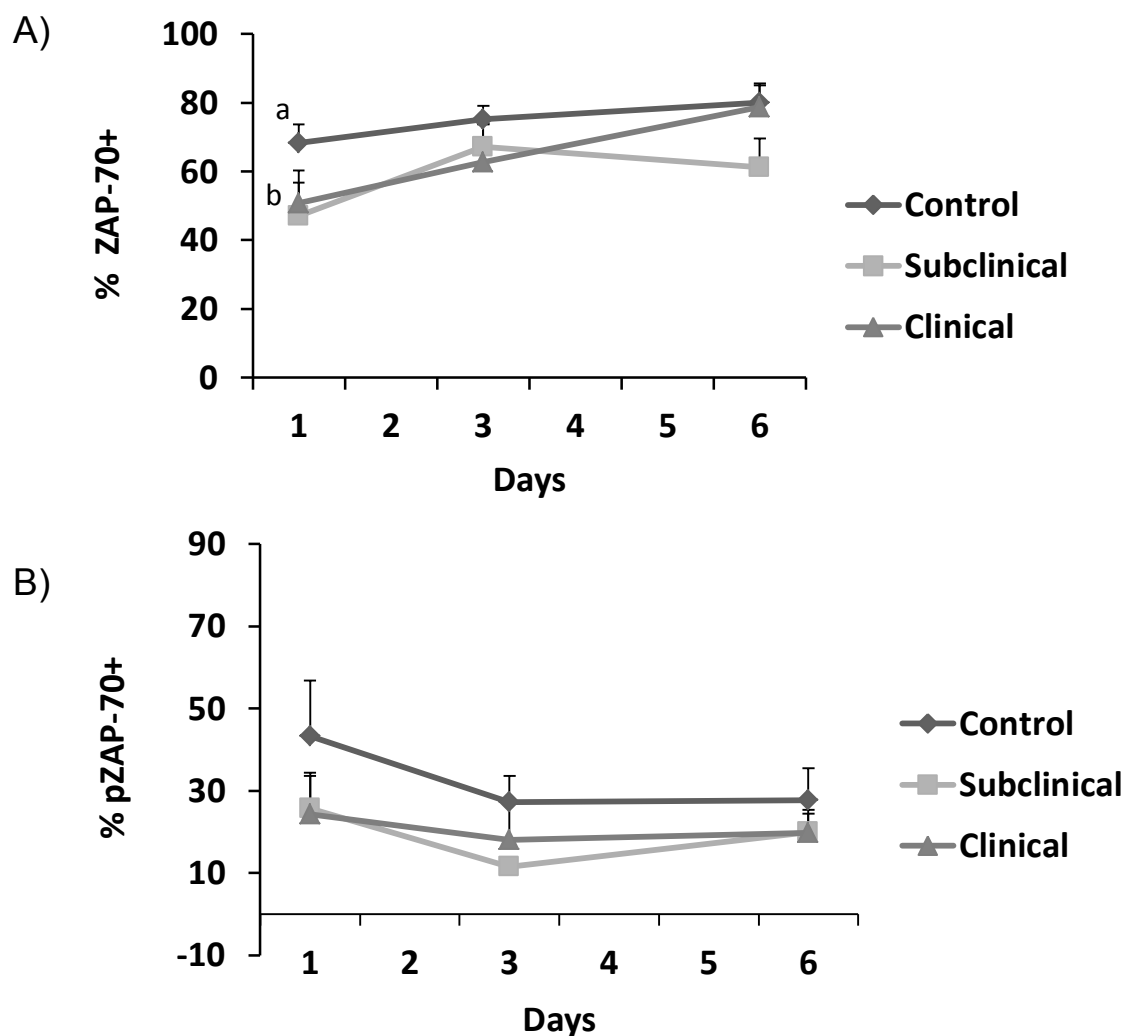


Figure 2. Expression of ZAP-70 (A) and pZAP-70 (B) on CD4⁺ T cells isolated from healthy control cows and cows naturally infected with *M. avium* subsp. *paratuberculosis* in the subclinical and clinical stages of infection. Peripheral blood mononuclear cells were cultured with a whole cell sonicate of MAP (10 µg/ml) for 24, 72, and 144 hr prior to flow cytometric measurement of ZAP70 and pZAP70. Data are presented as percentage of cells (mean ± SEM). Significant differences between infection group within a time point are designated by different letters ($P < 0.05$).

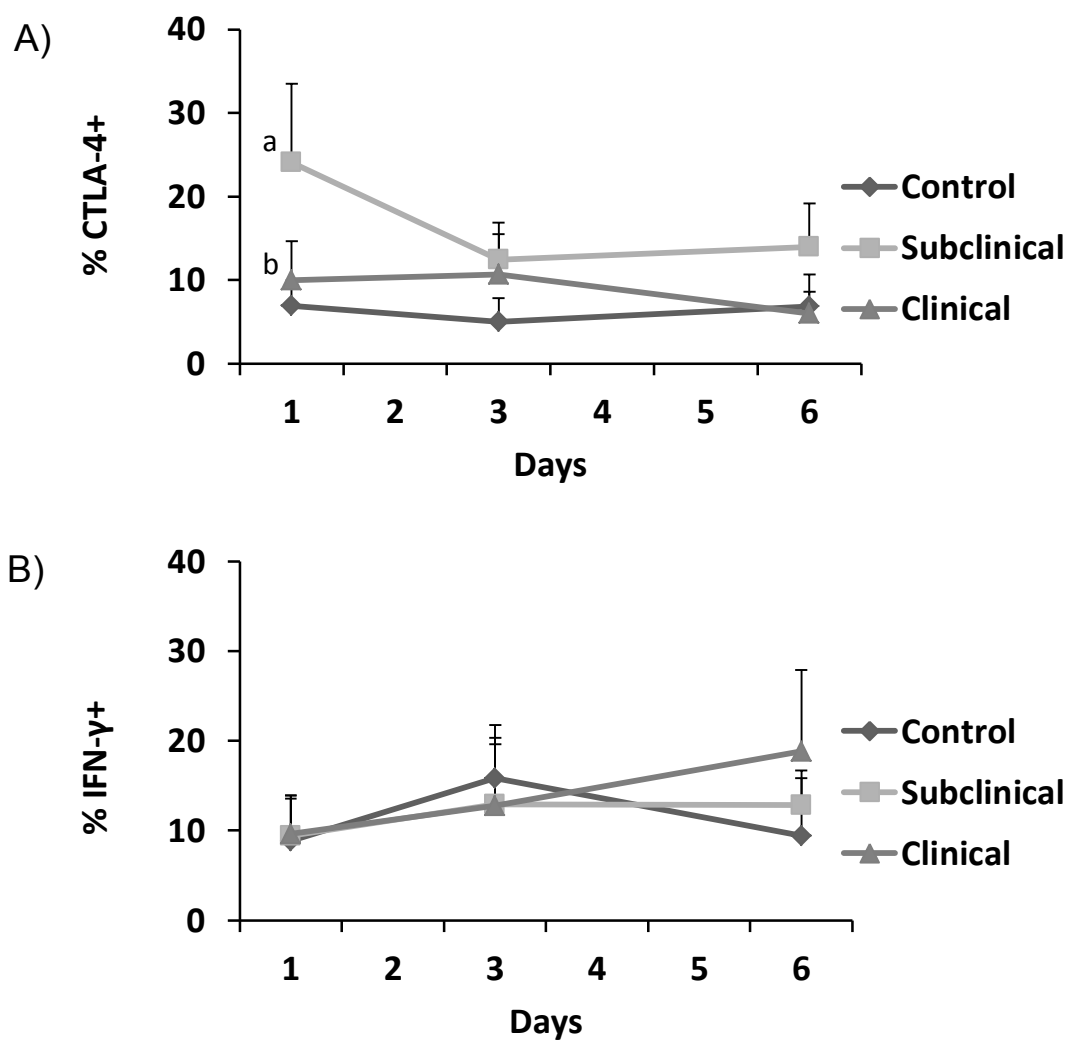


Figure 3. Expression of CTLA-4+ (A) and IFN- γ + (B) on CD4+ T cells isolated from healthy control cows and cows naturally infected with *M. avium* subsp. *paratuberculosis* in the subclinical and clinical stages of infection. Peripheral blood mononuclear cells were cultured with a whole cell sonicate of MAP (10 μ g/ml) for 24, 72, and 144 hr prior to flow cytometric measurement of ZAP70 and pZAP70. Data are presented as percentage of cells (mean \pm SEM). Significant differences between stage groups within a time point are designated by different letters ($p < 0.05$).

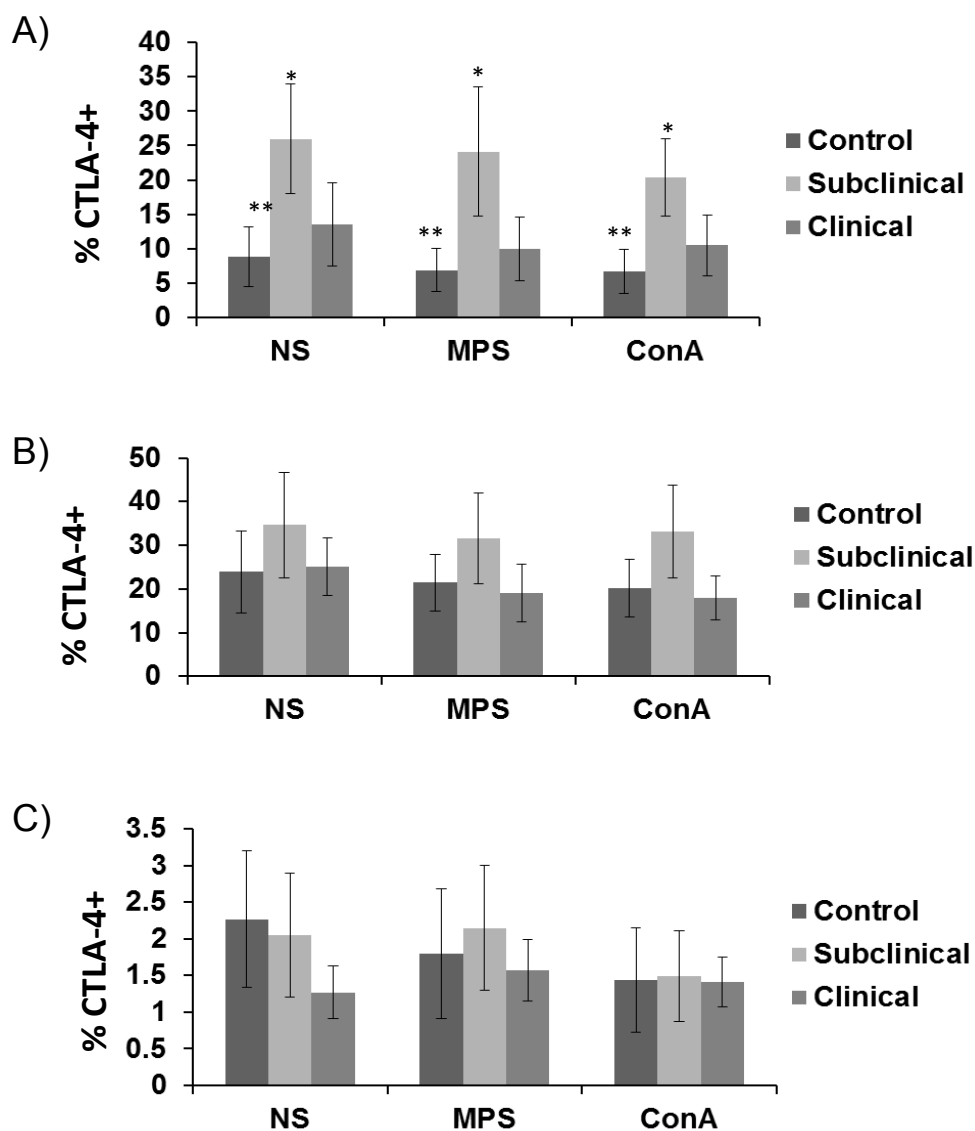


Figure 4. Expression of CTLA-4+ on A) CD4+ T cells. B) CD8+ T cells. C) $\gamma\delta$ TCR+ T cells after 24 hr culture of peripheral blood mononuclear cells obtained from healthy control cows and cows naturally infected with *M. avium* subsp. *paratuberculosis* in the subclinical and clinical stages of infection. Data are presented as percentage of CTLA-4+ cells (mean \pm SEM). Significant differences between treatment groups are designated by asterisks *, ** ($P < 0.05$).

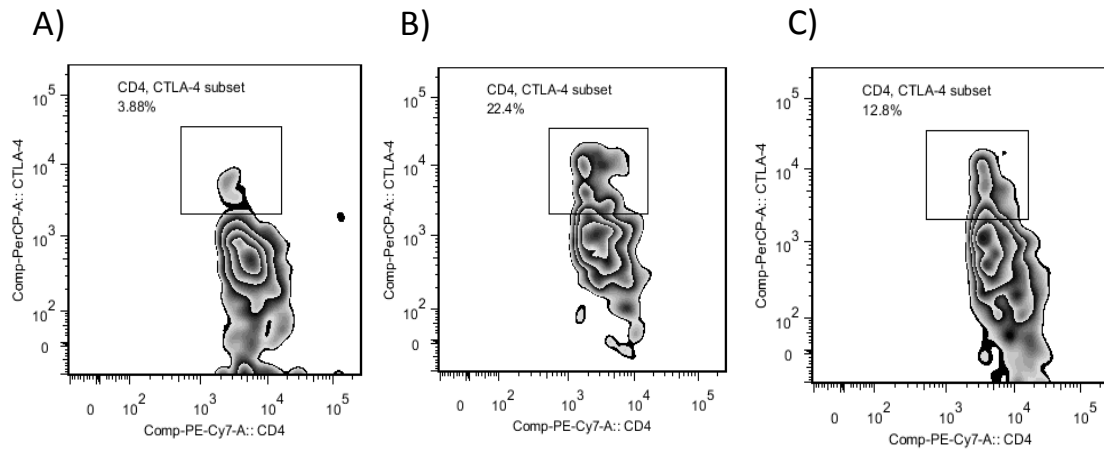


Figure 5. Histogram demonstrating representative flow cytometric staining for surface expression of CTLA-4 on CD4 cells cultured with a whole cell sonicate of MAP (10 $\mu\text{g/ml}$) for 24hr from a control non-infected cow (A), a subclinical cow (B), and a clinical cow (C).

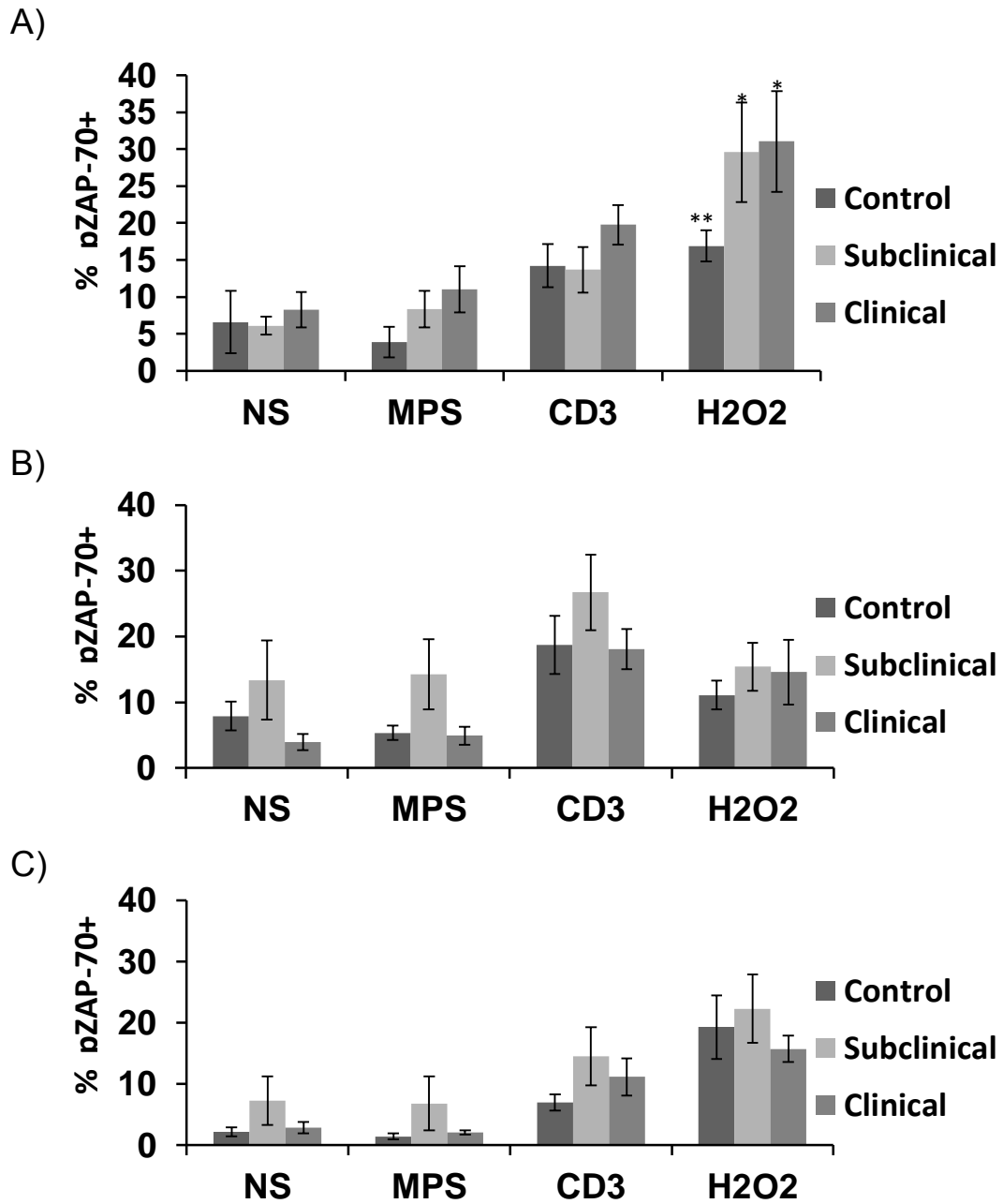


Figure 6. Phospho flow analysis of ZAP-70 phosphorylation following T cell activation in CD4+, CD8+ and $\gamma\delta$ TCR+ cells. Significant differences between treatment groups are designated by different numbers of asterisks ($p < 0.05$).

CHAPTER 4: GENERAL CONCLUSION

General Discussion

The study of protein complexes within the envelope of MAP yielded several interesting findings. This was the first study to characterize protein complexes in the envelope of MAP. A total of seven protein complexes were found within the envelope. Some complexes such as the succinate dehydrogenase complex were expected to be found as they have described physiological functions within the membrane, however, the composition of other protein complexes provided novel information.

Major membrane protein (MAP2121c), a described antigen of MAP and other pathogenic mycobacterial species, was found to form a complex with a cysteine desulfurase protein (MAP2120c), demonstrating that these two proteins are interacting with each other at some level. When analyzing the antigenicity of these proteins, it was shown that both were highly antigenic. Major membrane protein was recognized mainly by clinical animals, while cysteine desulfurase was reactive to most animal sera as studied by Western blot. Recombinant proteins were made of both proteins, and cysteine desulfurase demonstrated a very high reactivity among subclinical animals, demonstrating potential for diagnostic development. This indicates that complex I may be important in the pathogenesis of MAP and contains immunodominant antigens of this pathogen.

Another very interesting complex discovered was one formed with the protein Cfp 29 (MAP0630c). This protein was first characterized as linocin, a bacteriocin of *Brevibacterium linens* and later described to be a protein with high T cell reactivity

among memory effector cells isolated during the recall of protective immunity in the mouse model of tuberculosis infection. This protein was also found to be a T cell antigen of MAP with high IFN- γ response in subclinical animals. In the same complex was a protein of the Dyp-type peroxidase family (MAP0631c) as well as others involved in protein export.

Several novel antigens were found when evaluating proteins that were identified by mass spectrometry in the interferon gamma release assay. These included phage shock protein A (MAP2855c), a putative ATPase (MAP3844) as well as Mpt64 (MAP3290c), a major target for human tuberculosis diagnostics and previously not investigated for this purpose in paratuberculosis.

The second study performed addressed the immune response of animals to MAP, especially differences observed in animals in clinical and subclinical stages of disease. It was found that ZAP-70, a molecule crucial for T cell activation, was down-regulated in both clinical and subclinical animals, demonstrating an alteration that occurs in T cells with MAP infection. This down-regulation was more pronounced among CD4⁺ T cells, but was also observed in CD8⁺ and $\gamma\delta$ TCR + T cells. Considering the importance of this molecule to T cells, it is very likely that the T cells which have less or negligible ZAP-70 are hypofunctional and less responsive to stimulus.

Another very interesting finding was that CD4⁺ T cells of subclinical animals expressed significantly more CTLA-4 than control non-infected cows and cows of clinical status. CTLA-4 is regarded as one of the major negative regulators of T cells and has a broad range of mechanisms to dampen immune response. However, this molecule

has also been shown to have a positive role in inhibiting a Th2 bias of T cells, as well as facilitating migration of Th1 cells to sites of infection. Both of these are possible functions of this molecule among subclinical animals.

Also regarding T cells, proximal T cell receptor signaling as measured by phosphorylation of ZAP-70 was investigated in animals of subclinical and clinical status and compared to non-infected control animals. Antigen specific as well as non-specific stimulation was studied. Interestingly there was no change in signaling with disease state and animals of clinical as well as subclinical status responded well to non-specific TCR stimulation. This was not expected as previous research has shown that T cells animals in clinical stages of disease can be hypofunctional. These results, however, could be a function of a higher number of Treg cells within these animals, cells that have been demonstrated to have greater proximal T cell receptor signals in response to stimulus in comparison to non-Treg cells.

Studying changes in T cells of animals infected with MAP leads to the conclusion that there are clear differences in T cell phenotype of infected animals (i.e. down-regulation of ZAP-70). Although not known exactly at this time, these alterations more than likely have significant impacts on the immune response of these animals. It was also interesting to observe clear differences between subclinical and clinical stages of infection (i.e. changes in CTLA-4 expression), demonstrating that these two stages do have some distinct immune characteristics which once better understood can lead to more directed approaches for vaccine and diagnostic development.

Recommendations for future research

Along with several discoveries, this research also leads to more questions and direction for future research. Regarding envelope protein complexes it would be interesting to investigate the exact interaction of major membrane protein (MAP2121c) and cysteine desulfurase (MAP2120c), and if this is in fact a complex that would participate in the biosynthesis of sulfur containing co-factors as literature suggests. The same goes for other complexes with antigenic proteins that may be related to virulence such as the complex formed with Cfp 29 (MAP0630c). One possible way to address the complex's function as well as its role in pathogenesis may be to delete the proteins of the complex and evaluate the resulting mutant. The mutant strain could be evaluated in relation to survival in macrophages, invasion of epithelial cells and survival in an animal model such as the mouse. Another possibility would be to study the mutants as a potential live attenuated vaccine candidate.

Several different antigenic proteins were found within the envelope of MAP. This suggests potential for use of these proteins in diagnostic tests for paratuberculosis. Considering their antigenicity, as evidenced by results of the interferon gamma release assay and Western-blot, these proteins are likely also good candidates for development of a subunit vaccine or a vaccine with a vector such as a strain of salmonella expressing these proteins.

Regarding studies of T cell responses in animals infected with MAP, several questions also arise. It would be very interesting to investigate the mechanism involved in down-regulation of ZAP-70 and if this finding is representative of a more broad

alteration of these cells. It would be interesting to investigate the consequence of the lack of ZAP-70 in these cells and measure their cytokine and proliferative responses in comparison to other cells.

Also regarding ZAP-70, it was not expected that animals with clinical paratuberculosis would have similar and higher responses to antigen non-specific TCR stimulation than those of control non-infected status. This may be due to a higher percentage of Treg cells within these animals. This possibility could be studied by analyzing the responsive subset of cells and measuring markers of Treg cells such as Foxp3. Regarding this research it would also be interesting to investigate if MAP has the ability to directly inactivate ZAP-70 phosphorylation, as has been demonstrated with *M. tuberculosis*.

It was interesting to observe such a high expression of CTLA-4 within subclinical animals. As was discussed before, CTLA-4 can have inhibitory functions to T cells, however, it could also promote a Th1 bias and enhanced migration of T cells to sites of infection having a positive role in subclinical animals. These are interesting topics to address to better understand the role of CTLA-4 in paratuberculosis.

This further research would aid in both understanding more of the dynamics of the immune response to MAP as well as the role of specific proteins and protein complexes in the virulence of this pathogen. Hopefully coming closer to providing improved tools to control and prevent paratuberculosis.

APPENDIX

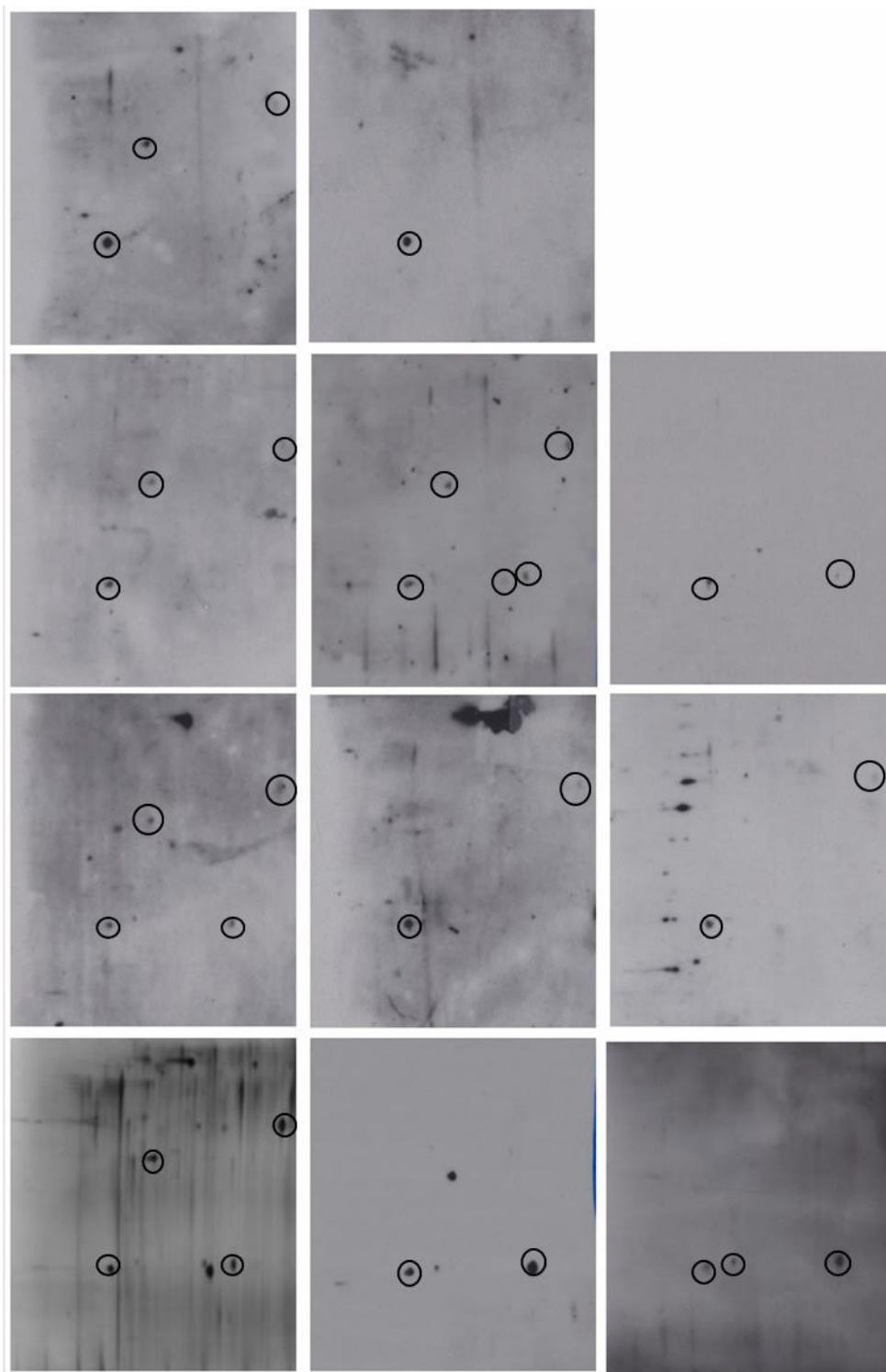


Figure A.1 Western-blots performed on 2D-SDS-PAGE gels with serum from control non-infected cows. Circles represent reactive proteins that were identified by mass spectrometry. Uppermost left picture is a Silver Stained 2D-SDS-PAGE reference gel.

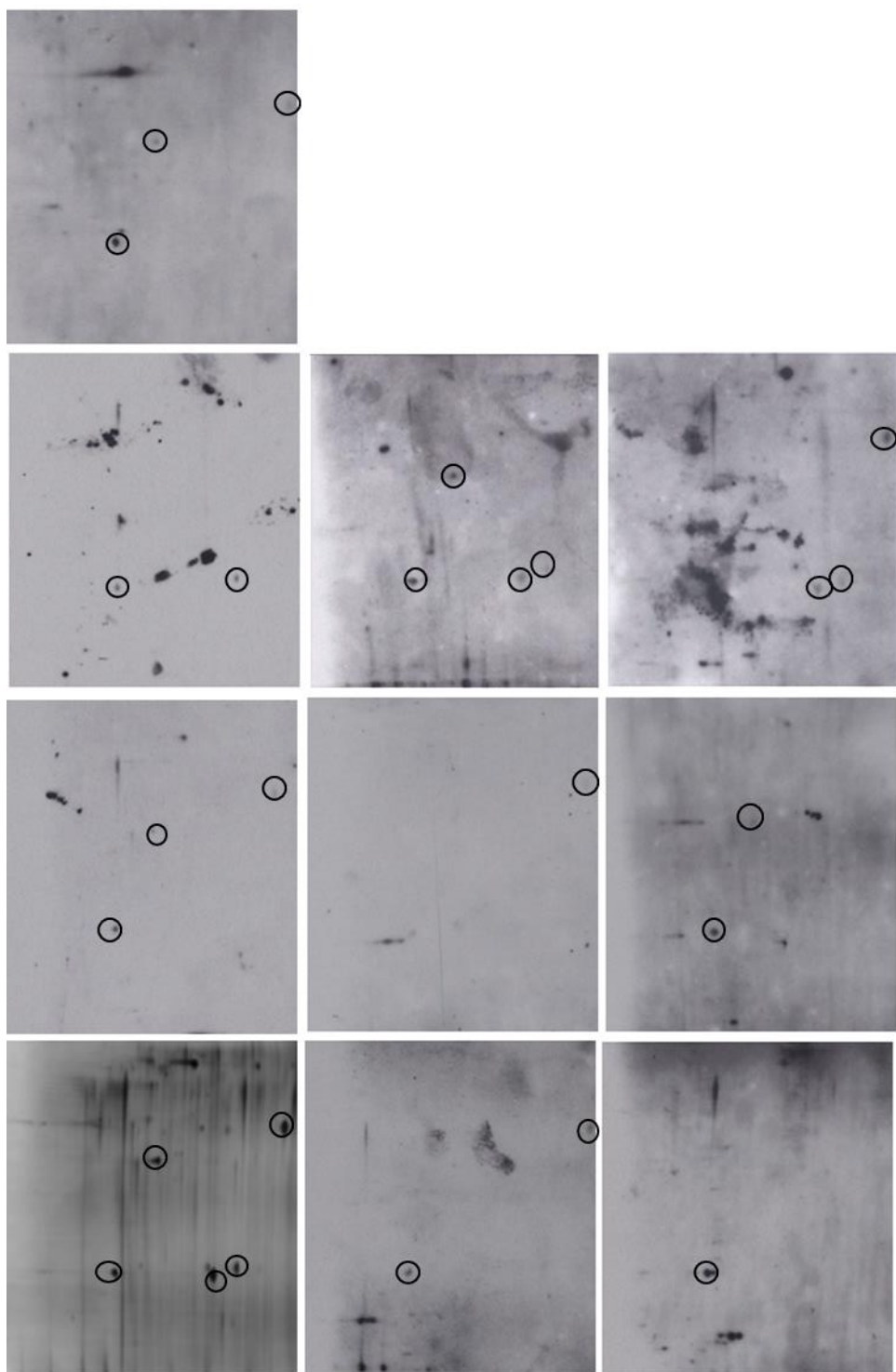


Figure A.2 Western-blot performed on 2D-SDS-PAGE gels with serum from subclinical cows. Circles represent reactive proteins that were identified by mass spectrometry. Uppermost left picture is a Silver Stained 2D-SDS-PAGE reference gel.

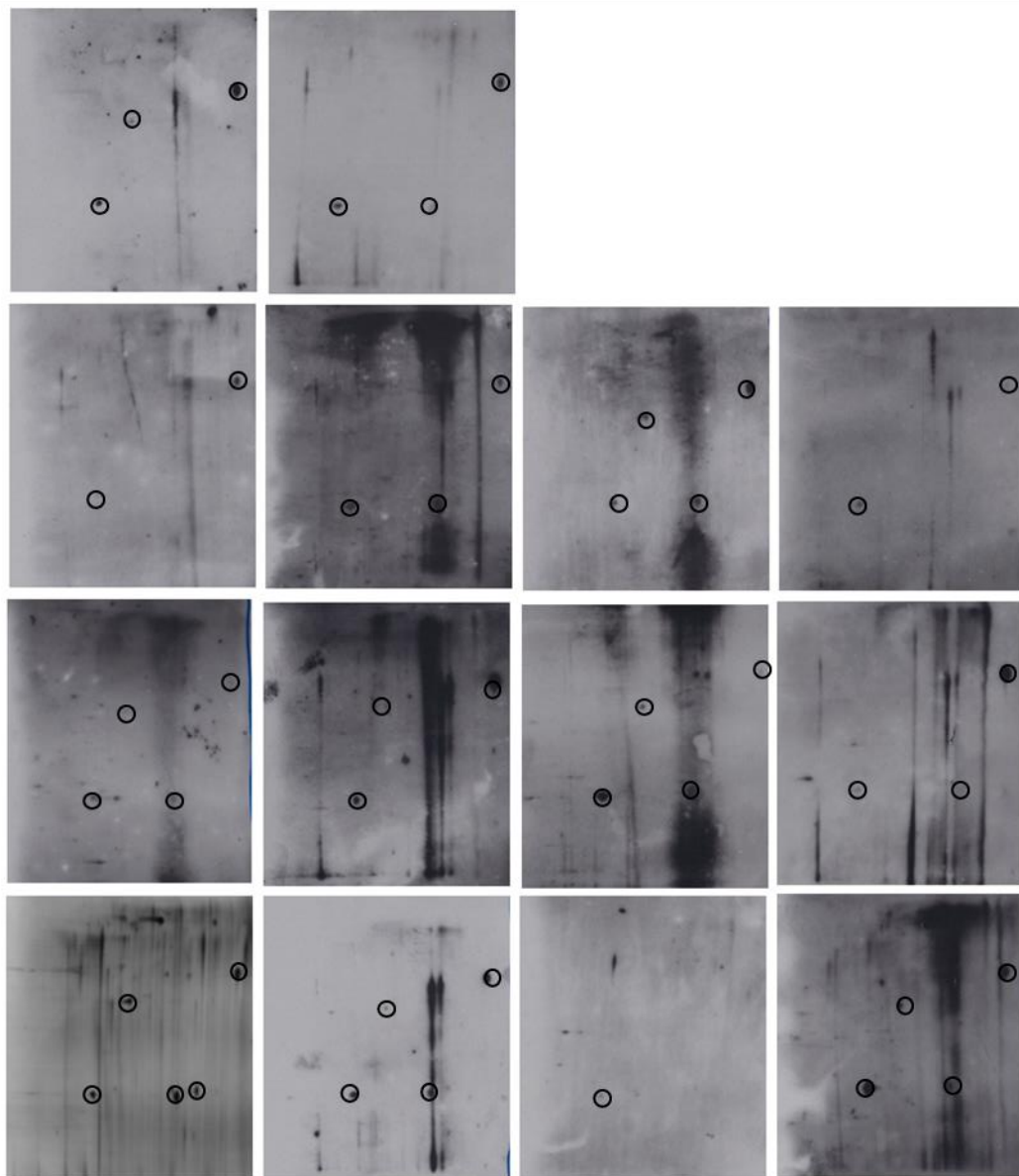


Figure A.3 Western-blot images performed on 2D-SDS-PAGE gels with serum from clinical cows. Circles represent reactive proteins that were identified by mass spectrometry. Uppermost left picture is a Silver Stained 2D-SDS-PAGE reference gel.

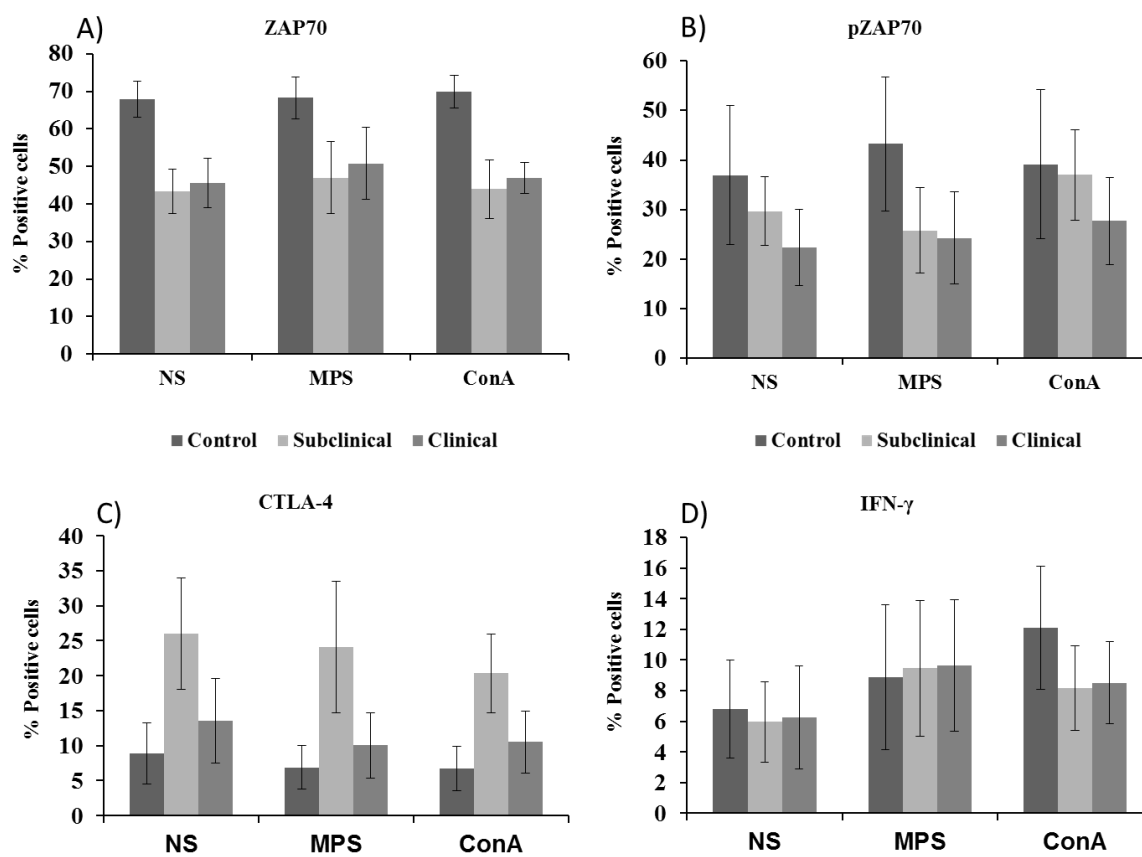


Figure A.4 CD4+ cells cultured for 24hr and analysis of A) ZAP-70, B) pZAP-70, C) CTLA-4, D) IFN- γ

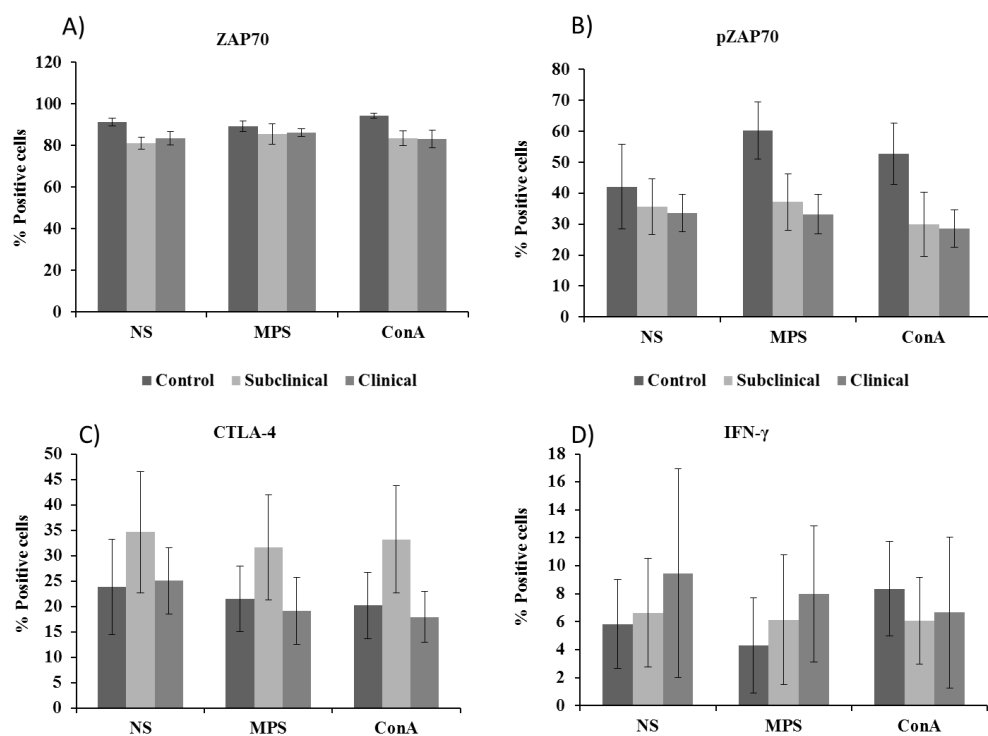


Figure A.5 CD8+ cells cultured for 24hr and analysis of A) ZAP-70, B) pZAP-70, C) CTLA-4, D) IFN- γ

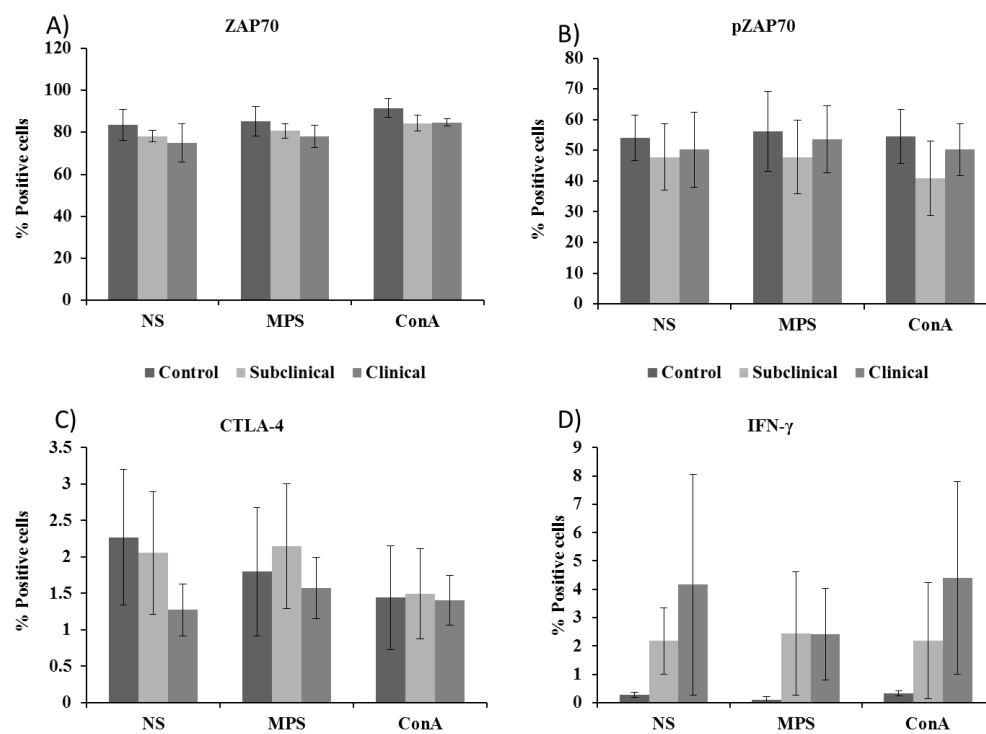


Figure A.6 $\gamma\delta$ TCR+ cells cultured for 24hr and analysis of A) ZAP-70, B) pZAP-70, C) CTLA-4, D) IFN- γ

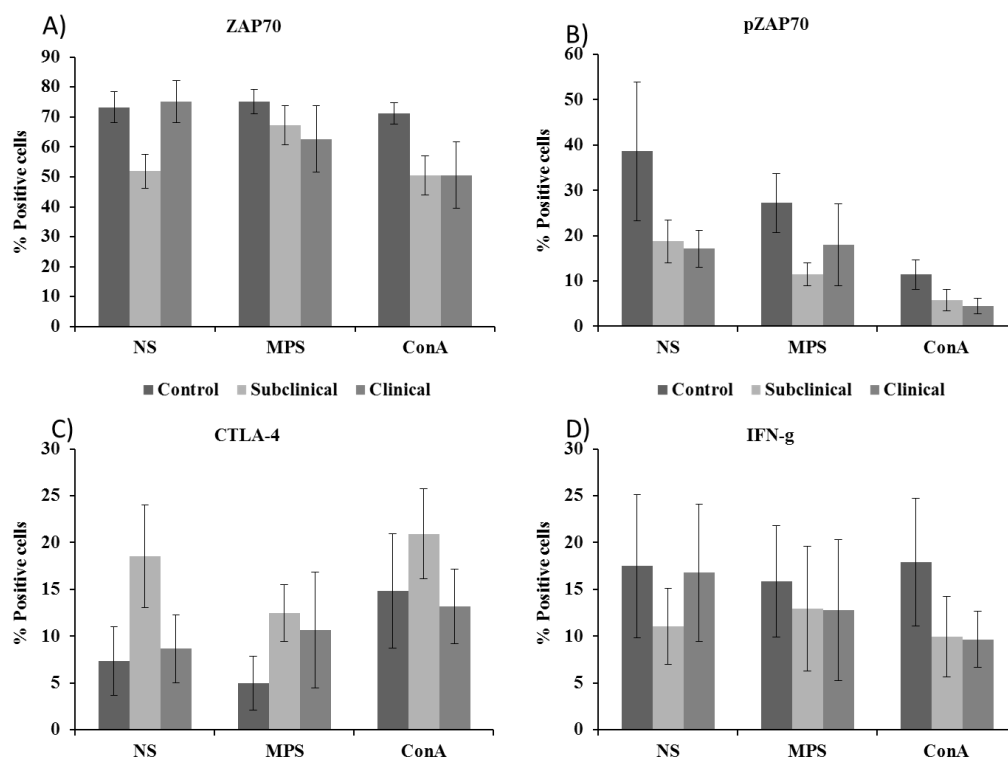


Figure A.7 CD4⁺ cells cultured for 72hr and analysis of A) ZAP-70, B) pZAP-70, C) CTLA-4, D) IFN- γ

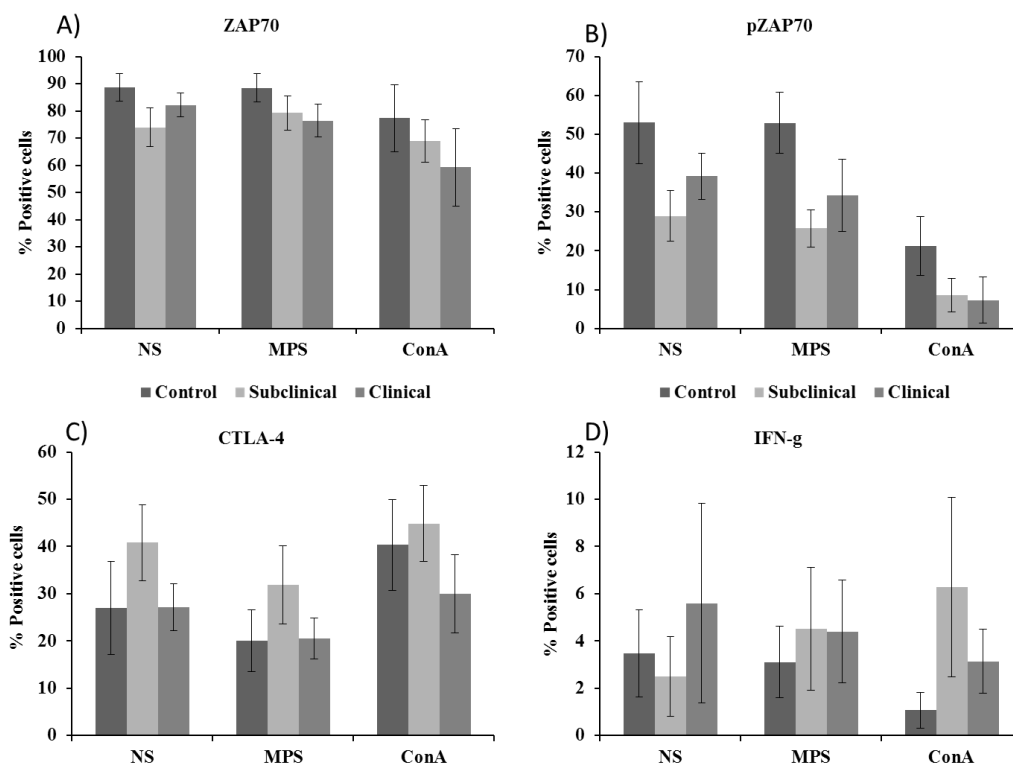


Figure A.8 CD8 + cells cultured for 72hr and analysis of A) ZAP-70, B) pZAP-70, C) CTLA-4, D) IFN- γ

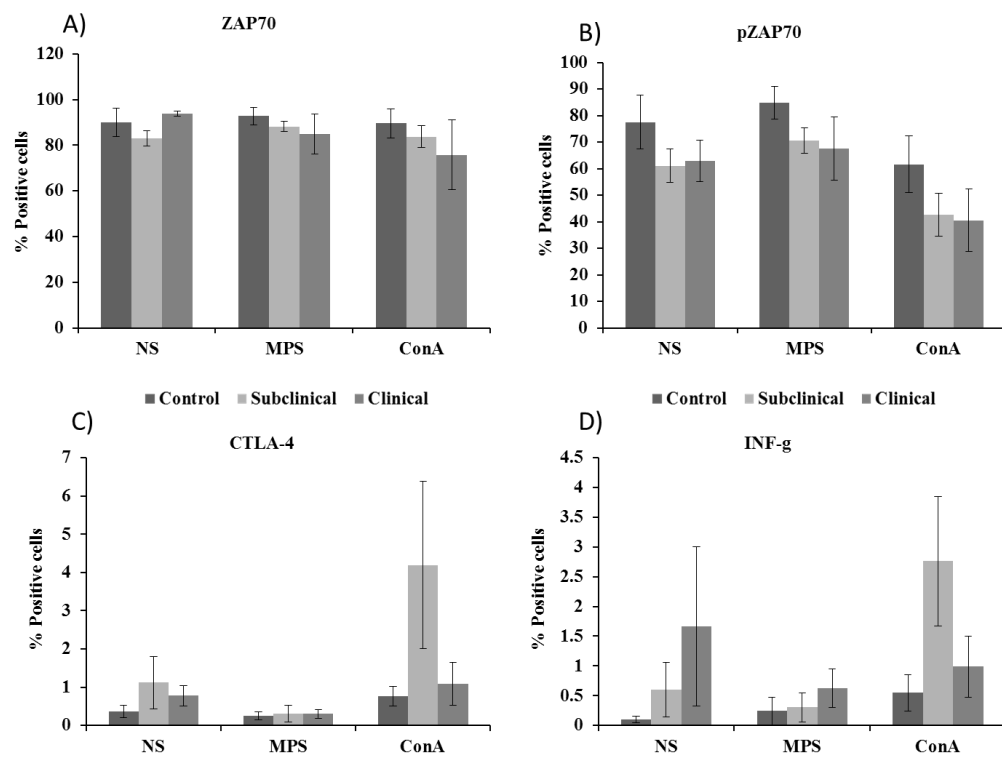


Figure A.9 $\gamma\delta$ TCR⁺ cells cultured for 72hr and analysis of A) ZAP-70, B) pZAP-70, C) CTLA-4, D) IFN- γ

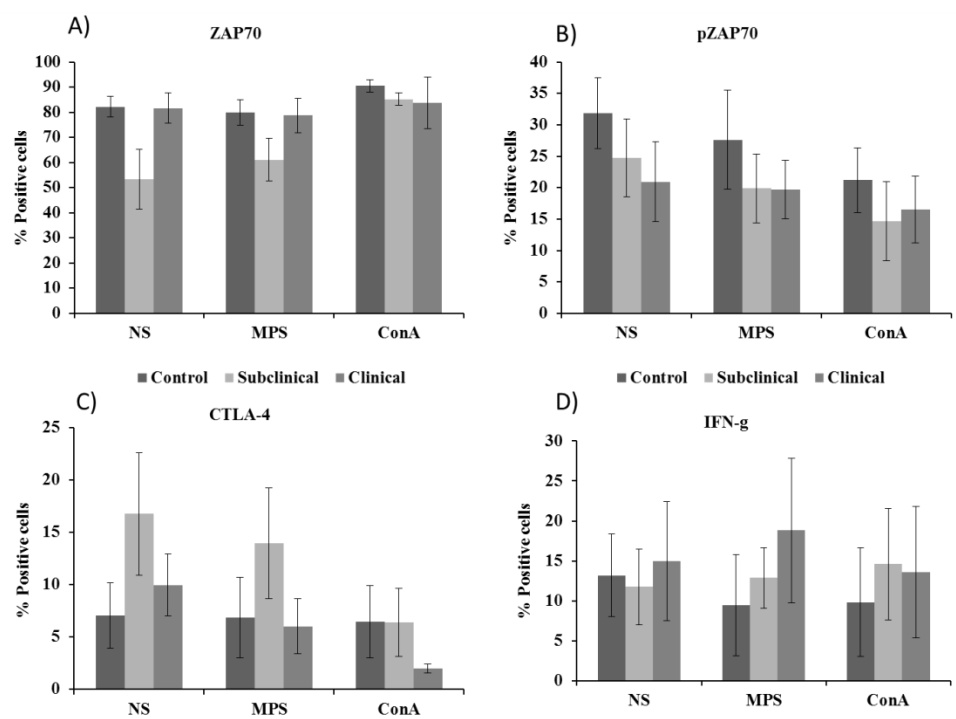


Figure A.10 CD4+ cells cultured for 144hr and analysis of A) ZAP-70, B) pZAP-70, C) CTLA-4, D) IFN- γ

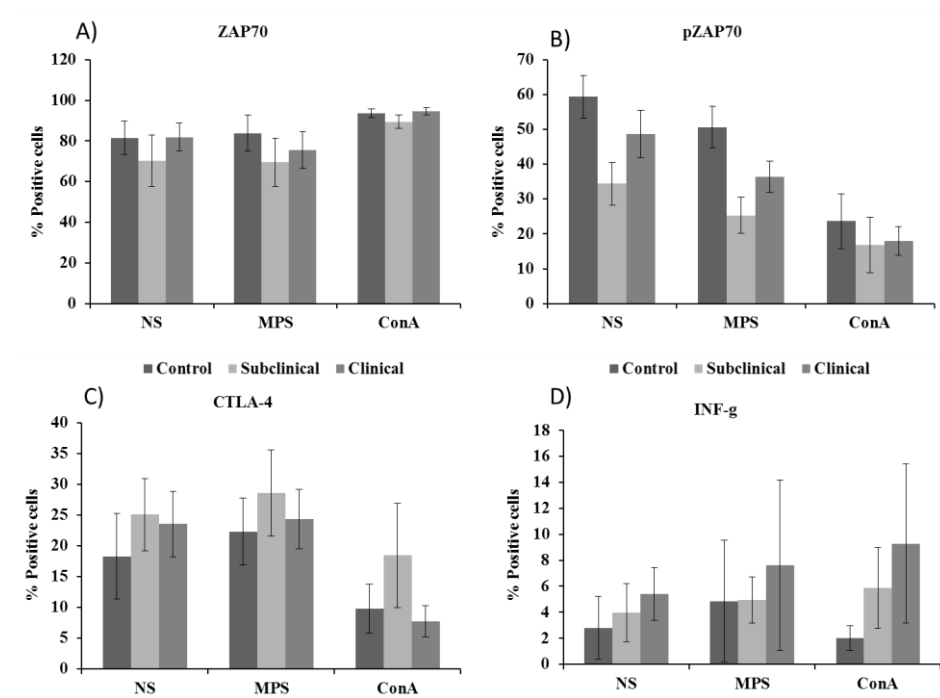


Figure A.11 CD8+ cells cultured for 144hr and analysis of A) ZAP-70, B) pZAP-70, C) CTLA-4, D) IFN- γ

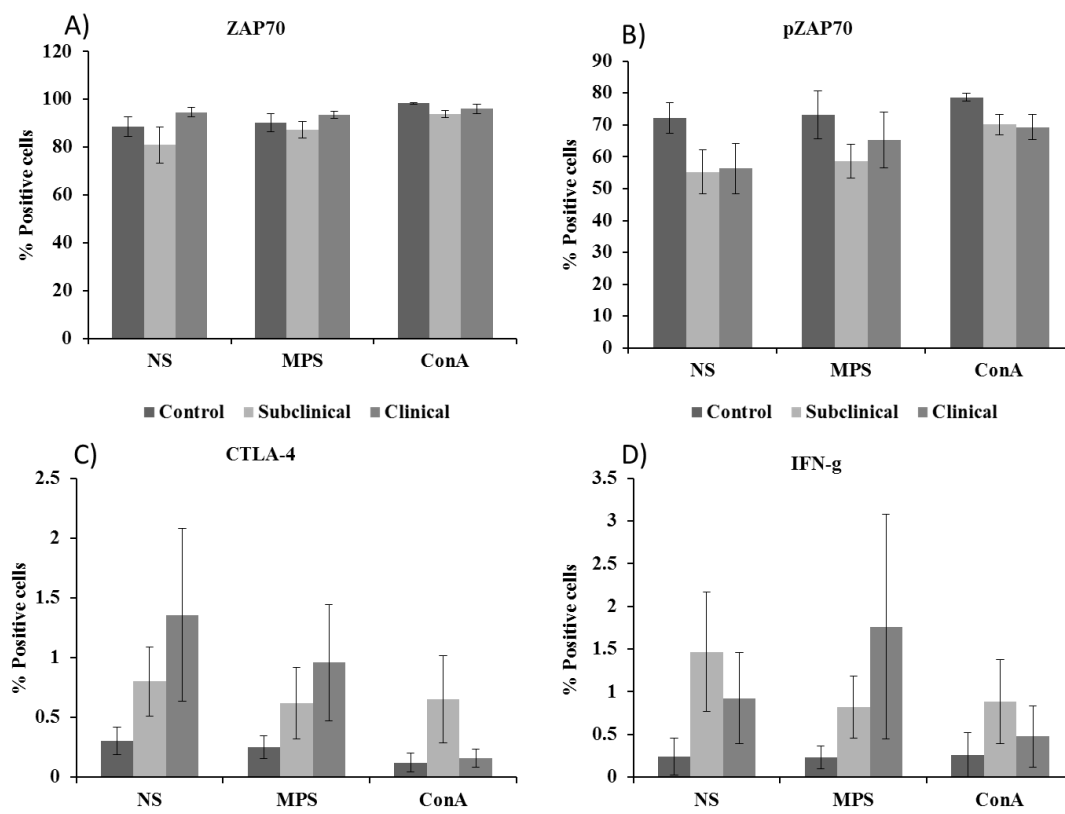


Figure A.12 $\gamma\delta$ TCR⁺ cells cultured for 144hr and analysis of A) ZAP-70, B) pZAP-70, C) CTLA-4, D) IFN- γ